T.C.

DOKUZ EYLUL UNIVERSITY
IZMIR INTERNATIONAL
BIOMEDICINE AND GENOME
INSTITUTE

CHARACTERIZATION OF THE EFFECTS OF IDH1 MUTATION ON MONOCYTE DIFFERENTIATION AT TRANSCRIPTOME LEVEL IN EARLY STAGES OF GLIOMA FORMATION

EBRU DİLER

MOLECULAR BIOLOGY AND GENETICS

MASTER THESIS

IZMIR-2019

THESIS CODE: DEU.HSI.MSc/2016850022

T.C.
DOKUZ EYLUL UNIVERSITY
IZMIR INTERNATIONAL
BIOMEDICINE AND GENOME
INSTITUTE

CHARACTERIZATION OF THE EFFECTS OF IDH1 MUTATION ON MONOCYTE DIFFERENTIATION AT TRANSCRIPTOME LEVEL IN EARLY STAGES OF GLIOMA FORMATION

MOLECULAR BIOLOGY AND GENETICS

MASTER THESIS

EBRU DİLER

Assist. Prof. Yavuz OKTAY

THESIS CODE: DEU.HSI.MSc/2016850022

TABLE OF CONTENTS

LIST OF TABLES

LIST OF FIGURES

ABBREVIATIONS

CNS : Central Nervous System

GBM : Glioblastoma

LGG : Low Grade Glioma

HGG : High Grade Glioma

IDH : Isocitrate dehydrogenase

2-HG : 2-Hydroxyglutarate

G-CIMP: Glioma CpG island methylator phenotype

RTKs : Receptor Tyrosine Kinases

TME : Tumor microenvironment

GAM : Glioma-associated microglia / macrophage

TIL : Tumor-infiltrating lymphocytes

BMDM : Bone marrow-derived macrophage

MDSC : Myeloid-derived suppressive cells

HLA : Human leukocyte antigen

PRR : Pattern-recognition receptor

TLR : Toll-like receptor

CTL : C-type lectin

NLR : NOD-like receptors

PAMP : Pathogen-associated molecular pattern

DAMP : Damage-associated molecular pattern

APC : Antigen Presenting Cell

MPS : Mononuclear phagocyte system

M-CSF : Macrophage colony stimulating factor

IHA : Immortal Human Astrocyte

CM : Conditioned Media

RNA-seq : RNA sequencing

TP1 : 1st Time Point CM

TP2 : 2nd Time Point CM

TP3 : 3rd Time Point CM

EC : Empty Control CM

C : Control

ACKNOWLEDGMENTS

The scientific studies in the context of this master thesis has been taken place in Izmir Biomedicine and Genome Institute, at Dokuz Eylul University. I would be thankful to all the people who stand by me with their precious contributions to this study.

First and foremost, I would like to say how much l am grateful and l appreciate to my mentor and my supervisor Assist. Prof. Yavuz OKTAY for providing me with a chance to be a member in his laboratory, for his unbroken support, leading and extensive knowledge that helped me throughout this study.

I would like to say my special thanks to Assoc. Prof. Gökhan KARAKÜLAH and his team who helped me a lot with the bioinfomatics parts of my thesis as well as Assoc. Prof. Duygu SAĞ and her team. I appreciate their contributions and advices to my studies.

I also would like to thank to my lab members, Aykut KURUOĞLU, Burcu EKİNCİ, Fadime ÖZTOPRAK, Ece SÖNMEZLER, Kaan OKAY and Tutku YARAŞ, who were there during my tough times and gave me all their support, assistance, sincere help and kindness during the thesis project. I also would like to thank to Dr. Vanesa Segovia BUCHELI for being my side like a sister and mentor during the thesis project. I am also thankful to the jury members Assist. Prof. Yavuz OKTAY, Assoc. Prof. Duygu SAĞ and Assoc. Prof. Özden YALÇIN ÖZUYSAL for evaluating my thesis and giving their precious advices and opinions for me being a better scientist in the future.

Last but not least, I want to thank to my dearest sister Emine ÖZBİÇER, who always supported me in my whole life not only as a sister but also as a friend. In this point, I should thank to my parents, Ayşegül DİLER and Vahit DİLER, twice for all they did.

I also would like to thank to my my friends Fırat BAKIR, Nurselin ATEŞ, Ezgi Gül ERDEM, and Melis Dilara ARSLANHAN for being by my side during all my toughest and happiest times.

CHARACTERIZATION OF THE EFFECTS OF IDH1 MUTATION ON MONOCYTE DIFFERENTIATION AT TRANSCRIPTOME LEVEL IN EARLY STAGES OF GLIOMA FORMATION

Ebru Diler, Dokuz Eylul University Izmir International Biomedicine and Genome Institute, ebru.diler@msfr.ibg.edu.tr

ABSTRACT

Gliomas are the most common primary brain tumors with a distinct histological and genomic background. IDH mutations are the most common genetic alteration in lower grade gliomas and almost always effect the same residue (R132H) that confer new function to the IDH enzyme. IDH1 R132H produces an oncometabolite namely 2-hydroxygluterate (2-HG) and its accumulation leads to genome wide epigenetic changes. In addition to its cell intrinsic roles in tumor initiation, 2-HG have been proposed to effect the tumor microenvironment acting in a paracrine manner. In this study, we aimed to investigate the effects of secreted factors from astrocytes that mimic the early stages of IDH1 R132H gliomas on monocyte differentiation. To this end immortal human astrocytes that express IDH1 R132H in a dox-inducible manner were used to mimic tumor initiation and conditioned media (CM) were collected in different time points and primary monocytes were exposed to it during differentiation to macrophages. Transcriptome wide analysis of differentiated macrophages by RNA sequencing reveal that 124 genes are differentially expressed in response to IDH1 mutation. Gene ontology analysis indicating that IDH1 mutation may interfere with p53 signaling pathway. In consistent with the literature, negative regulation of complement activation signatures elevated in IDH1 R132H exposed time point cases. Th1 and Th2 cell differentiation, cytotoxic T cell homeostasis are the other significantly enriched pathways in given genes of interest. It has been speculated that secreted factors from astrocytes in early stages of glioma formation may affect the macrophages resulting transcriptomic changes to shape tumor microenvironment.

IDH1 MUTASYONUNUN GLİOM OLUŞUMUNUN ERKEN AŞAMALARINDA MONOSİT FARKLILAŞMASINA ETKİLERİNİN TRANSKRİPTOM DÜZEYİNDE KARAKTERİZASYONU

Ebru Diler, Dokuz Eylül Üniversitesi İzmir Uluslararası Biyotıp ve Genom Enstitüsü, ebru.diler@msfr.ibg.edu.tr

ÖZET

Gliomalar, farklı histolojik ve genom kökenli olan en yaygın primer beyin tümörleridir. IDH mutasyonları, düşük dereceli gliomalarda en yaygın genetik değişimdir ve hemen hemen her zaman IDH enzimine yeni işlevler veren aynı bölgeyi (R132H) etkiler. IDH1 R132H, 2-hidroksilütre (2-HG) adlı bir onkometabolit üretir ve bu onkometabolitin birikimi, genom genelinde epigenetik değişikliklere yol açar. Tümör başlangıcındaki hücre içi rollerine ek olarak, 2-HG, parakrin şekilde etki ederek tümör mikro ortamını etkileyebilmektedir. Bu çalışmada, IDH1 R132H gliomaların erken evrelerini taklit eden astrositlerden salgılanan faktörlerin monosit farklılaşması üzerindeki etkilerini araştırmayı amaçladık. Bu amaçla, doksisiklin ile indüklenebilir bir şekilde IDH1R132H'yi eksprese eden ölümsüz insan astrositleri, tümör başlangıcını taklit etmek için kullanılmış ve farklı zaman noktalarında koşullu ortam (CM) toplanmış ve primer monositler makrofajlara farklılaşma sırasında toplanan koşullu ortama maruz bırakılmıştır. RNA sekanslama sonucunda elde edilen verilere göre, farklılaştırılmış makrofajların transkriptom analizi, 124 genin IDH1 mutasyonuna cevap olarak farklı şekilde eksprese edildiğini ortaya koymaktadır. Gen ontoloji analizi ile IDH1 mutasyonunun p53 sinyal yolunu etkileyebileceği gösterilmiştir. Literatür ile uyumlu olarak, IDH1 R132H astrosit hücrelerinden toplanan koşullu ortama maruz kalan farklılaşmış monosit hücrelerinde komplement sistemin negatif regule edildiği transkriptom düzeyinde ortaya konmuştur. Gen ontoloji analizinde, Thl ve Th2 hücre farklılaşması, sitotoksik T hücresi homeostazı, belirgin olarak etkilenen diğer yollaklardır. Glioma oluşumunun erken evrelerinde astrositlerden salgılanan faktörlerin, tümör mikro ortamını şekillendirmek için transkriptomik değişikliklere neden olarak monositlerin makrofaj hücrelerine farklılaşmasını etkileyebileceği düşünülmektedir.

1 INTRODUCTION AND AIM

Gliomas are the most common brain and central nervous system (CNS) tumors. Gliomas account for ~30 % of all brain tumors, and ~80% of malignant tumors. It is a heterogeneous disease with a distinct histological and genomic background. The most common type is glioblastoma (GBM) (~56%) followed by the low-grade glioma (~30%) seen in adults (Goodenberger & Jenkins, 2012). Recent genomic studies revealed important molecular marks to classify the glioma subtypes. The growing knowledge about the genomic background of the glioma, allow nowadays to a specific glioma subtype diagnostic enabling the use of more suitable therapies to a given patient. Nevertheless, the survival of the patients is still around the ~35% (Ostrom et al., 2018). The understanding of molecular mechanisms promoting tumor progression and formation it is critical to establish new therapeutic targets for glioma and reduce the lethality of the disease.

1.1 Aim of the study

IDH mutation is thought to be one of the driver mutation seen in early stages of glioma formation. The idea that tumor formation is the result of some modifications in sequential order; in turn, the IDH mutations are the initial mutations changing the course of tumor differentiation. Somatic mutations on IDH let again of function on the enzyme associated with the formation of cancer. However, inhibited function of IDH enzyme resulting in production of an oncometabolite namely 2-hydroxygluterate (2-HG). Accumulation of this oncometabolite interfere with the cell intrinsic metabolism which are strongly correlated with the tumor initiation. With the growing literature knowledge today we know that both tumor intrinsic and the direct effect of the 2-HG have strong fingerprints on the tumor microenvironment interactions. However, still remains unclear the IDH induced regulations and interactions over immune cells. In this study we aimed to understand IDH1 R132H mutation related transcriptomic changes on monocyte differentiation during tumor initiation. For this purpose, we performed RNA sequencing on to primer monocytes treated with IDH1 R132H mutant astrocyte condition media. We try to mimic tumor initiation by astrocytes including IDH R132H expressing doxycycline inducible vector system. We collect conditioned media in a time course after doxycycline treatment, then expose to primer monocyte in the presence of M-CSF.

2 GENERAL INFORMATION

2.1 Diffuse Gliomas and Grading

The brain tumor is an abnormal cell mass in any tissue inside the brain that can be benign or malignant. World Health Organization (WHO) Classification of Tumors of the Central Nervous System has been formulated and published to classify brain tumors properly. An updated version of WHO classification published in 2016 which includes genetic basis and molecular markers to diagnose CNS tumors in a comprehensive manner (Louis et al., 2016). The CNS tumors are histologically categorized into four main class with grades I to IV. These classes are categorized according to certain microscopic parameters such as the mitotic activity of the tumor, cytologic atypia, necrosis and microvascular proliferation (Gupta & Dwivedi, 2017). According to tumors malignancies and aggressiveness, WHO classication determine:

Grade I: Tumors that are non-malignant (benign) which grow slowly. Patients generally have long term survival and this type of tumors rare in adults.

Grade II: These tumors could be malignant or not. These type of tumors relatively grow slowly, sometimes spread to other tissues and recur with higher grades.

Grade III: Malignant tumors and often spread and come back with higher grades. Abnormal cells grow and reproduced continuously.

Grade IV: tumors are the most aggressive malignant tumors which rapidly grows and proliferate. They are very cancerous that can spread rapidly to close tissue (Louis et al., 2007).

Primary brain tumors arise from diverse origins in the CNS and diffuse gliomas are the most common primary brain tumors with diffuse neuropil infiltration that originate glial cells. They have been classified by their histological characters as astrocytic, oligodendroglial, or oligoastrocytic tumors with varying degrees of malignancy (WHO II-IV) (Weller et al., 2015). Histological classification (Table 1) of gliomas is important for obtaining predictive information necessary for diagnosis. It is crucial to determine diffuse glioma type for therapeutic approaches to use in which low-grade gliomas (LGGs; grade II) and high-grade gliomas (HGGs; grade III, IV) (Wesseling, Kros, & Jeuken, 2011).

Table 2.1: Histological classification of diffuse gliomas and corresponding WHO grades. IDH1 mutation frequency and distribution across the diffuse gliomas indicated as percentages (Liu, Hou, Chen, Zong, & Zong, 2016).

Diffuse Gliomas	WHO Grade	IDH1 mutation frequency(%)
Astrocytic		
Low-grade diffuse astrocytoma	II	76
Anaplastic astrocytoma	III	62.2
Primary glioblastoma	IV	5.6
Secondary glioblastoma	IV	76.4
Oligoastrocytic		
Low-grade oligoastrocytoma	II	79.8
Anaplastic oligoastrocytoma	III	69.7
Oligodendroglial		
Low-grade oligodendroglioma	II	78.8
Anaplastic oligodendroglioma	III	67.5

2.2 Genetic Basis of Diffuse Gliomas

Cancer develops through an accumulation of genetic aberrations. Diffuse gliomas also accumulate genetic alterations that differ by grade and type of gliomas. Diagnosis according to histopathological characteristics of the diffuse glioma types sometimes may be challenging due to tissue sampling problems. With the advent of genetic and epigenetic aberrations that have become important in glioma molecular diagnostics, histopathological characterization of the glioma subtypes were complemented with molecular markers (Louis et al., 2016). Genetic alterations such as mutations on IDH, TP53, ATRX, and EGFR genes, chromosomal deletion of 1p/19q, TERT promoter mutations, BRAF fusion and promoter methylation of O-6-methylguanine DNA methyltransferase (MGMT) were characterized in grade II, III, and IV gliomas (Cancer Genome Atlas Research Network et al., 2015; Omerhodžić, 2019). These mutations accumulate with tumor progression and affect the overall survival of patients with glioma. Also Eckel-Passow et al. published a genome-wide study of genetic alterations which concludes that three molecular markers are reasonably important in the diffuse gliomas' characteristics. Glioma patients carrying IDH, TERT, and chromosomal deletion of 1p/19q with

different ages have been grouped and the statistics show that overall survivals of IDH mutant patients are higher than the others(Eckel-Passow et al., 2015). In addition to this information, Arita et al. suggested IDH1 and TERT promotor mutation based grouping for WHO grade II, III and IV gliomas(Arita et al., 2016). Thereupon, in 2016, well-established molecular parameters were combined with histopathological characters of glioma with the updated version of WHO classification (Louis et al., 2016; Tateishi & Yamamoto, 2019). The integrated molecular and histological diagnostic algorithm presented for diffuse gliomas according to IDH mutation status(S. C. Lee, 2018). Genetic alterations and the classification of glial tumors summarized in Figure 2.1.

Mutations on IDH enzyme first found in colorectal cancer (Sjoblom et al., 2006), with the increasing studies on IDH mutations today, it is known that the vast majority of the glioma types bear IDH mutations (Ichimura et al., 2009; Waitkus, Diplas, & Yan, 2018). IDH mutations induce metabolic abnormalities and observed during early gliomagenesis (Watanabe, Nobusawa, Kleihues, & Ohgaki, 2009).

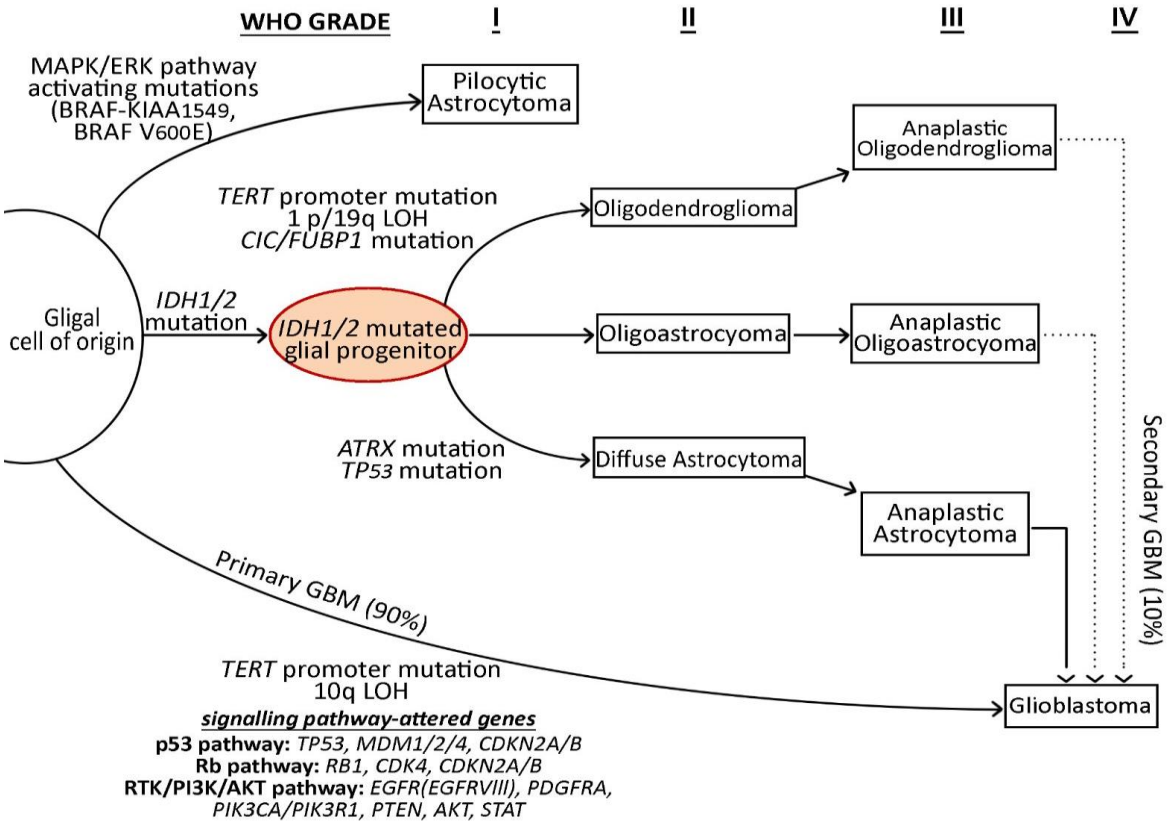

Figure 2.1 IDH mutation based diagnostic algorithm of gliomas. Common genetic alterations were indicated with the corresponding histological characters. Grade I gliomas; known as pilocytic astrocytomas characterized by the BRAF-KIAA1549 fusion transcripts leading MAPK pathway activation. Primary glioblastoma (primary GBM); altered signaling pathways are p53, Rb and RTK/ PI3K/AKT beside they have characteristic TERT promoter mutation. IDH1/2 mutations occur in the early stages of glioma and IDH mutant subtypes tend to develop secondary GBM (grade IV). Oligodendroglioma characterized by TERT promoter mutations, 1p/19q loss of heterozygosity, CIC/FUBP1 mutation. Diffuse astrocytoma tends to co-mutated with ATRX, TP53. These grade II gliomas can progress into grade III and secondary GBM.

IDH mutation is critical for secondary glioblastoma (IDH-mutant GBM) classification. Primary glioblastomas bear EGFR, PTEN, TERT promoter mutations, monosomy 10, trisomy 7 and CDKN2A deletions; secondary glioblastomas are easily differentiated by IDH mutations. Oligodendroglial tumors differentiated by the chromosomal deletion of 1p/19q with IDH mutation. TERT promotor mutation and CIC and FUBP1 also found in oligodendroglial tumors. On the other hand, ATRX and TP53 mutations observed in astrocytic tumors in addition to IDH1 mutations (Tateishi & Yamamoto, 2019). With the common genetic alterations, the majority of LGG gliomas are IDH1 mutant (Table 2.1). With these observations, it is suggested that IDH mutations are most common and early event in the gliomagenesis on the genetic basis

correlated with the impaired function of IDH enzyme (Hansen, Diplas, Becher, & Yan, 2016). The role of IDH enzyme is critical for the cellular mechanisms and epigenetic organization potentially promote tumor formation. However, the role of IDH mutations during glioma formation is not fully understood yet. All in all, it is a rapidly emerging research area to enlighten the IDH mutation induced mechanisms to understand and develop new targets to diagnose and treat.

2.3 Role of IDH Mutations

IDH is a Krebs cycle enzyme that catalyzes isocitrate oxidative decarboxylation with a key role in converting isocitrate to α-ketoglutarate (α-KG). There are three types of IDH enzyme namely IDH1, IDH2, IDH3. IDH1 found in peroxisomes and cytoplasm, the other two isoforms found in the mitochondria. IDH1/2 use NADP+ as a co-factor and they are the key enzymes to maintain cellular NADPH to catalyze many cellular processes and prevent oxidative stress in most tissues. Somatic mutations on IDH let again of function on the enzyme associated with the formation of cancer (L. Dang, Yen, & Attar, 2016). Interestingly mutation on IDH1/2 occurs in the same residue in most of the patients. Change in the amino acid located on isocitrate binding site alter the function of IDH enzymes; Arginine to Histidine at codon 132 (R132H) in IDH1(~90% of IDH1 mutations), Arginine to Lysine at codon 172 (R172K) in IDH2. Most patients also bear mutation on the one allele the other remain wild-type. Metabolomics studies showed that mutation on IDH1 results in the accumulation of 2-hydroxyglutarate (2-HG) which is called as an oncometabolite now (Lenny Dang et al., 2009). Normally IDH enzymes reduce the NAD^+ /$NADP^+$ to NADH/NADPH and release CO_2 during the conversation of isocitrate to α-KG in tricarboxylic acid (TCA) cycle. The mutated enzyme (R132H IDH1) with new function change the substrate and direction of isocitrate oxidative decarboxylation process. 2-HG is a product of glutamine which is also the source of α-KG in addition to isocitrate. Enzymatic analysis showed that mutant enzyme use α-KG as a substrate and produce D-2HG reduced form of α-KG (Figure 2.2).

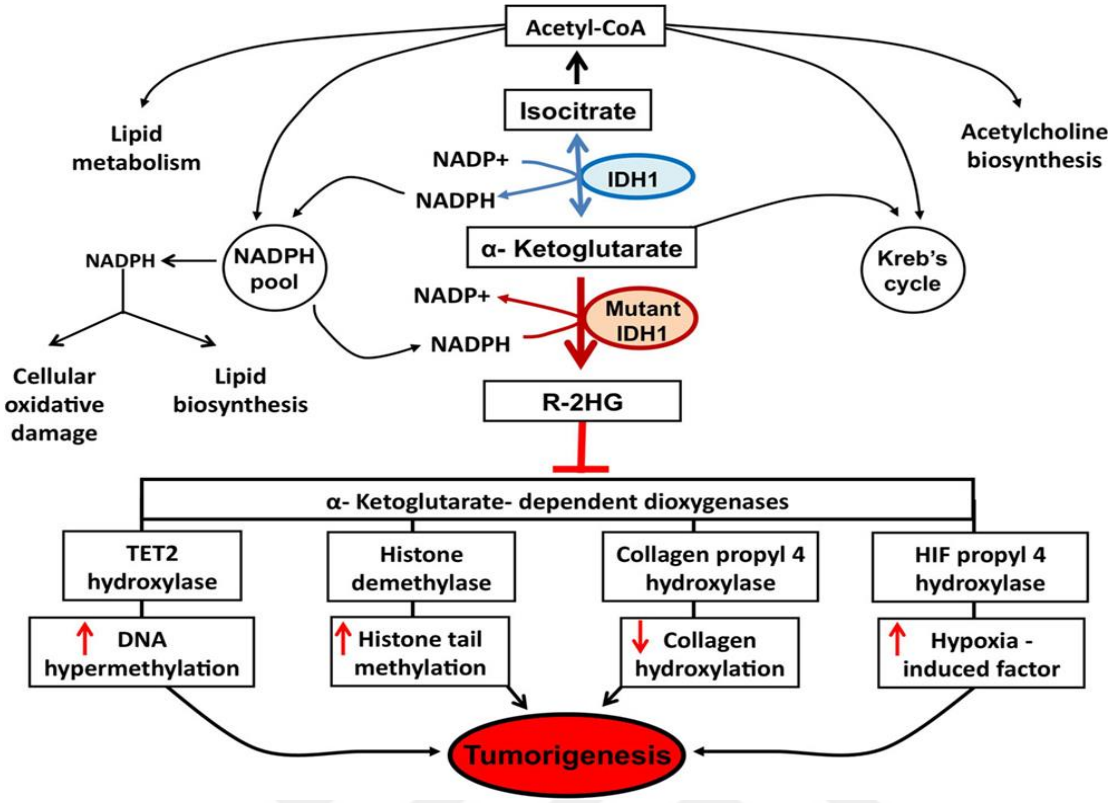

Figure 2.2 Impaired cellular mechanisms induced by IDH1 mutation. 2-HG accumulation correlated with the inhibited α-KG-dependent dioxygenases leading epigenetic alterations that potentially promote tumorigenesis (Liu et al., 2016).

This impaired function of the mutated enzyme assigns an oncogenic role to the tumor suppressor gene. Tumor driver activity of R132H IDH1 associated with several epigenetic alterations induced by inhibited α-KG-dependent dioxygenases (Figure 2.2). One of the important outcome is the increased expression of hypoxic biomarkers. Hypoxia-inducible-factor 1-alpha (HIF1-α) activation presented in most of the glioma patients which suggest that the angiogenesis and vasculogenesis of IDH1 mutant gliomas correlated with the downregulated HIF1-α targets (Lenny Dang et al., 2009; Frezza, Tennant, & Gottlieb, 2010). IDH1/2 mutation is also the molecular basis of glioma CpG island methylator phenotype (G-CIMP) observed in gliomas. Mutant IDH enzymes induce epigenetic alterations resulting impaired chromatin remodeling and gene regulation. 2-HG accumulation inhibits the DNA and histone demethylases, which normally use α-KG as a co-factor. Numerous genes hypermethylated result in these altered expression patterns in IDH1 mutant gliomas (Turcan et al., 2012). Accumulation of 2-HG triggers genome-wide epigenetic changes probably

correlated with malignant transformation as an early event. So it is important to understand potential evidence underlying tumor driver role of IDH mutation in early stages of glioma.

2.3.1 The Effect of IDH mutations in Early Stages of Glioma

There are numerous hypotheses about tumor initiation and the origin of the cancer cells. Most of these hypotheses share a common idea that cancer develops through the accumulation of the mutations leading metabolic and cellular changes. Glial tumors are heterogeneous in terms of the histological characters of different cell types in the CNS. These cells can serve as progenitors to differentiate pathologically distinct tumor subtypes. Currently, with the advent of cancer stem cell discovery, there is a strong evidence that oncogenic mutations accumulate during tumor initiation and segregate through the progenitor offsprings (de Weille, 2014).

IDH mutation is thought to be one of the driver mutation seen in early stages of glioma formation. The idea that tumor formation is the result of some modifications in sequential order; in turn, may be the IDH mutations are the initial mutations changing the course of tumor differentiation. There are well established common alterations in cellular mechanisms such signal transduction, cell growth, proliferation, cell cycle control, and apoptosis; in this part of the introduction, critical genes and pathways were discussed to a better understanding of glioma initiation (Janigro, 2006).

Different cell types in the CNS serve as cancer progenitor cell such as astrocytic, oligodendroglial, neuronal. These specific progenitors can accumulate lineage dependent genomic alterations. It is not fully understood yet, however IDH mutations correlated and superior to some of the oncogenic mutations commonly seen in glial tumors. These common genetic aberrations may contribute to tumor formation by working together. Immortal cell lines and mouse models with IDH mutation induce some changes but not enough to exhibit tumor formation by itself (Balvers et al., 2013). Studies confirmed that alteration on numerous genes such PDGFA, PIK3CA, CDKN2A, MYC, ATRX, and PTEN is needed to promote differentiation in cell and mouse models (Bardella et al., 2016b; J. H. Lee et al., 2018). The tumor driver mechanisms induced by IDH1 R132H expression and/or accumulation of 2-HG

remains unclear. Frequently dysregulated pathways are essential to understand cancer development as well as glioma formation.

Common altered signal transduction pathways role in gliomagenesis are generally activated by receptor tyrosine kinases (RTKs) and the cell cycle-arrest pathways. RTK activates growth factor-mediated signal transduction. During glioma formation signal transduction via platelet-derived growth factor/receptor (PDGF/PDGFR), epidermal growth factor/receptor (EGF/EGFR), and transforming growth factor-α receptor (TGFα/EGFR) turns the normal cell metabolism to drive tumorigenesis. Shortly, EGF and PDGF take a critical role in neural stem cell proliferation/survival and differentiation respectively (Kapoor & O'Rourke, 2003). This critical feature of the growth factor-mediated signaling cascade are the major events in the course of tumor formation. Activated RTK signaling via changes in the cytoplasmic domain with cell intrinsic signals are important to understand glioma formation and develop glioma models. For example, loss-of-function of the TP53 tumor suppressor gene is correlated with the PDGF/PDGFR overexpression in LGGs (von Deimling et al., 1992). Besides, IDH mutation may be the prior reason for the aberrant activation of PDGF/PDGFR. IDH1induced hypermethylation in CCCTC binding factor (CTCF) binding site results in overexpression of PDGRF-alpha (PDGRFA) (W. Zhang & Fine, 2006). In another study, Turcan et. al confirm that IDH1 induced extensive DNA hypermethylation in immortalized primary human astrocytes resembles a stem-like phenotype via upregulation of numerous stem cell marker genes like nestin (Turcan et al., 2012). These results show that the IDH1 mutation is affecting the differentiation via changing the chromosomal topology and epitranscriptome leading regulatory interactions on oncogenes.

Another study carried out by Namura et. al exhibit some predictor molecular signs to understand the malignant progression of LGG based on their G-CIMP profiles. They showed partial DNA demethylation profiles differences affecting cell cycle genes during progression from LGG to secondary GBM (Nomura et al., 2019). This study along with similar studies confirmed that cell cycle genes were activated as a result of G-CIMP during malignant transformation (Ceccarelli et al., 2016).

One of the regulators of cell cycle pathways namely p53 transcription factor play a crucial role in gliomagenesis. TP53 is a tumor suppressor gene and the product of this gene role in cell cycle arrest and apoptosis. The p53 signaling pathway altered ~87% of the glioblastoma

patients in the TCGA database (Y. Zhang et al., 2018). This gene is likely mutated first than IDH during tumor formation (Attolini et al., 2010). The p53 function in the abrogating apoptosis in response to oncogenic mutations and DNA damage. This mutation contributes to the gradual accumulation of the other mutations via prohibiting apoptosis.

Changes on the metabolic pathways especially energy conversation cascades are the hallmarks of cancer. The Warburg effect recognized within the cancer cells is one of the early events to drive glioma formation. IDH mutations, which play a critical role in citrate metabolism, may contribute to this metabolic shift by modifying the levels of key metabolites essential for cell growth (Vander Heiden, Cantley, & Thompson, 2009). As mentioned before the accumulation of 2-HG inhibits prolyl hydroxylases which hydroxylase the HIF-1, ones HIF-1 activated it transcriptionally activate downstream genes. Some of these downstream targets shift glucose metabolism to the glycolytic pathway that indicates IDH1 associated with the early metabolic changes during gliomagenesis (Burroughs et al., 2013).

Some of the driver mutations and altered pathways summarized regarding the occurrence of the IDH mutation. As mentioned before gliomas tend to accumulate different additional mutations depend on the cellular origins. Several reports support the hypothesis that IDH mutation is a primary alteration, probably associated with the secondary and tertiary alterations seen in the progenitor cell populations (Bardella et al., 2016). IDH mutation and CIMP induced lineage dependent seconder mutations such as TP53 and ATRX in the astrocytic tumors probably correlated with the occurrence of tertiary alterations as well (Fack et al., 2017). IDH mutant glioma progression is a result of the organized progression of changes in the cellular pathways, but the overall concept is not fully understood yet. Gliomagenesis is a complex process where cell-intrinsic paths and the tumor microenvironment interact, and such interactions still remain obscure to our knowledge. Elucidate these topics is critical to fully understand glioma initiation and progression, and therefore generate new strategies to control the disease.

2.3.2 Impact of IDH Mutations on Glioma Microenvironment

Tumor microenvironment (TME) consist of different cell types. Brain composition is distinct from other tissues and the resident cells such as neuron, microglia and astrocytes are special cells found in the glioma microenvironment. In addition to the residents, immune cells constitute approximately 30% of a tumor mass which are mainly glioma-associated microglia and macrophages (GAMs). Namely tumor-infiltrating lymphocytes(TILs), brain-resident microglia, bone marrow-derived macrophages (BMDMs), and myeloid-derived suppressive cells (MDSCs) can act as a tumor driver/suppressor and/or immune suppressors (Gieryng, Pszczolkowska, Walentynowicz, Rajan, & Kaminska, 2017). Activated immune cells have cytotoxic effects by inflammatory agent production and trigger neurodegeneration as well. Therefore, immune system interactions should be fine-tuned in the brain. Although the brain tissue remains protected from inflammation via blood-brain barrier (BBB), it is permeable to infiltration of circulating immune cells in some brain tumors (Quail & Joyce, 2017).

Tumor-associated macrophages (TAMs) (Figure 2.3A) are the mayor cell type of the tumor mass. Yolk sac originated resident microglia ($C11b^{+}$; $CD45^{low}$) found in CNS are the key components to scan and detect a threat, thereby they can be activated to produce pro or anti-inflammatory responses. On the other hand, tumor cell secretions and ECM composition alterations can attract the BMDMs ($CD11b^{+}$; $CD45^{high}$) infiltrate through the TME. Cytokines and chemokines in the ECM shape the polarization status of infiltrating BMDMs. MDSCs (Figure 2.3B) are the other immune regulator cell type that derived from the bone marrow progenitors. They can be granulocytic (G-MDSC) or monocytic (M-MDSCs). They have distinct function because of their lineage differences but MDSCs generally induce immune suppressive microenvironment in response to tumor-derived signals. They play a suppressive role in NK cells and T cell functioning and cause Treg differentiation. The other prominent immune cell type is tumor-infiltrating lymphocytes (TILs) namely CD8+ T cells and regulatory T cells (Tregs) (Figure 2.3C). Tregs and the M2 polarized TAMs in the TME result in the inhibited function of CD8+ T cells. Tumor growth and malignancy are associated with the dysregulation of anti-tumor responses in the CNS. The other immune suppressive mechanism induced by the glioma stem cells (GSCs). They generally localize nearby the perivascular site and induce immunologically quiescent phenotype via promoting M2 polarized TAMs and Treg

proliferation. In addition to these CD8+ T cell functioning inhibited and apoptosis of CD8+ T cells induced by the GSCs (Figure 2.3D) (Boussiotis & Charest, 2018).

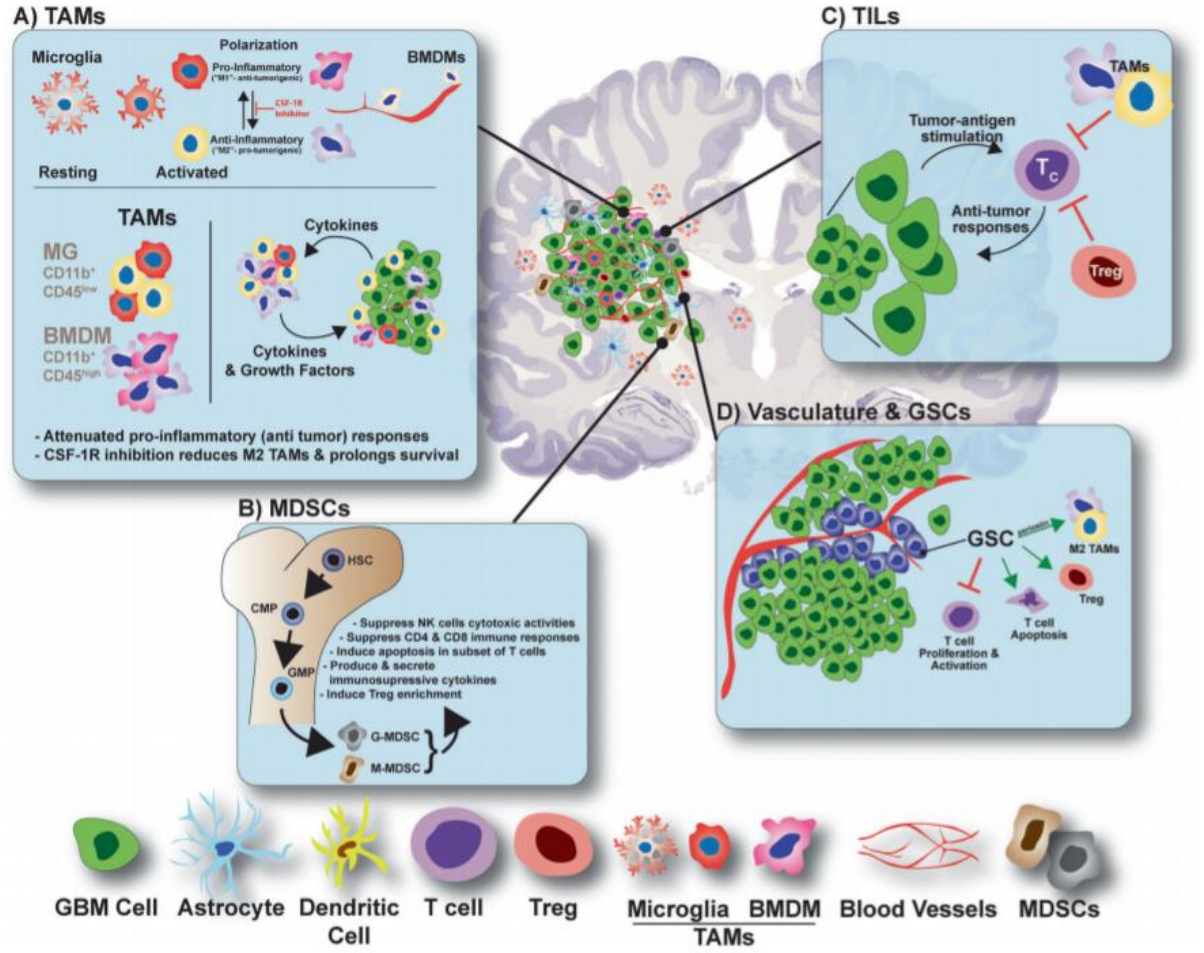

Figure 2.3 Glioma microenvironment. Cell types and the corresponding inhibitory or supportive immune related mechanisims summerized.(Boussiotis & Charest, 2018)

Tumor-mediated immunosuppression is mediated via changing the function of the immune cells in the glioma microenvironment. GAMs, lymphocytes, MDSCs, Tregs are the key immune cells deregulated to drive the immune suppressive and escape mechanisms. There are several studies querent IDH mutations effects on the glioma microenvironment. With the light of these researches now we have some clues that IDH induced reprograming of tumor microenvironment in the basis of immune responses (Amankulor et al., 2017).

Growing literature demonstrates that IDH mutant and IDH wild type tumors are different according to their TME composition and their genetic basis. With the light of these researches

now we have some clues about IDH induced reprograming of tumor microenvironment in the basis of immune responses. Tumor-specific adaptive immune responses are produced by TILs and the number of TILs is correlated with the tumor aggressiveness. Accumulation of T cells generally suppressed in the IDH mutant gliomas compare to the wild types (Saltz et al., 2018). Also, it is known that in most cancer types over expression of PD-1 (Programmed cell death protein 1) and PD-L1/2 (Programmed death- ligand 1/2) like checkpoint signals are the key regulators for T cell recruitment and functioning that is significantly correlated with glioma grade and reduced survival rates (Nduom et al., 2016). IDH mutant gliomas exhibit lower TIL infiltration and PD-L1 production (Berghoff et al., 2017). TCGA cohort studies also confirm that reduced immune-related gene expression signatures such as CD8+ T cell and interferon-γ (IFN-γ) associated genes on IDH mutant over wild type tumors. As discussed before IDH mutation induce hypermethylation and reduced PD-L1 expression in IDH mutant gliomas associated with the increased promoter methylation level on the PD-L1 gene leading downregulation of gene expression (Choi & Curry, 2017).

Impaired enzymatic function of IDH mutant gliomas results in an oncometabolite production (2-HG). As discussed before the accumulation of this oncometabolite induce epigenetic changes and alter the cellular pathways. 2-HG accumulation also affects the TME via the inhibited function of key immune-related genes (Amankulor et al., 2017). Reduced CD8+ T cell recruitment in IDH mutant gliomas is strongly correlated with the accumulation of 2-HG. IDH mutation induced suppression of signal transducer and activator of transcription 1 (STAT1) result in the reduced expression of C-X-C motif chemokine 9 (CXCL9) and C-X-C motif chemokine 10 (CXCL10). CXCL9 and CXCL10 levels indirectly reduced by the IDH mutation and/or accumulation of 2-HG leading a tumor intrinsic suppression of T cell recruitment (Figure 2.4) (Kohanbash et al., 2017; Richardson, Choi, & Curry, 2019).

Tumor intrinsic epigenetic dysregulations are strong evidence to TME deregulation in IDH mutant gliomas. However, a recent study published in Nature claim the direct effect of 2-HG on the T cell metabolism which attributes a new role to 2-HG beside being an oncometabolite (Bunse et al., 2018). The 2-HG exported from tumor cells have been shown to be imported into the T cells via the sodium-dependent dicarboxylate transport system. In addition, inhibition of ATP-dependent T cell receptor (TCR) signaling and polyamine biosynthesis pathway by 2-HG demonstrates a direct effect on the activation and proliferation of T cells. In this study, they also present that R-2HG induce alterations on calcium and

phosphatidylinositol signaling pathways. These impaired signaling cascades result in downregulation of nuclear factor kappa B (NF-κB) and nuclear factor of activated T cells (NFAT) downstream targets (Figure 2.4) (Richardson et al., 2019).

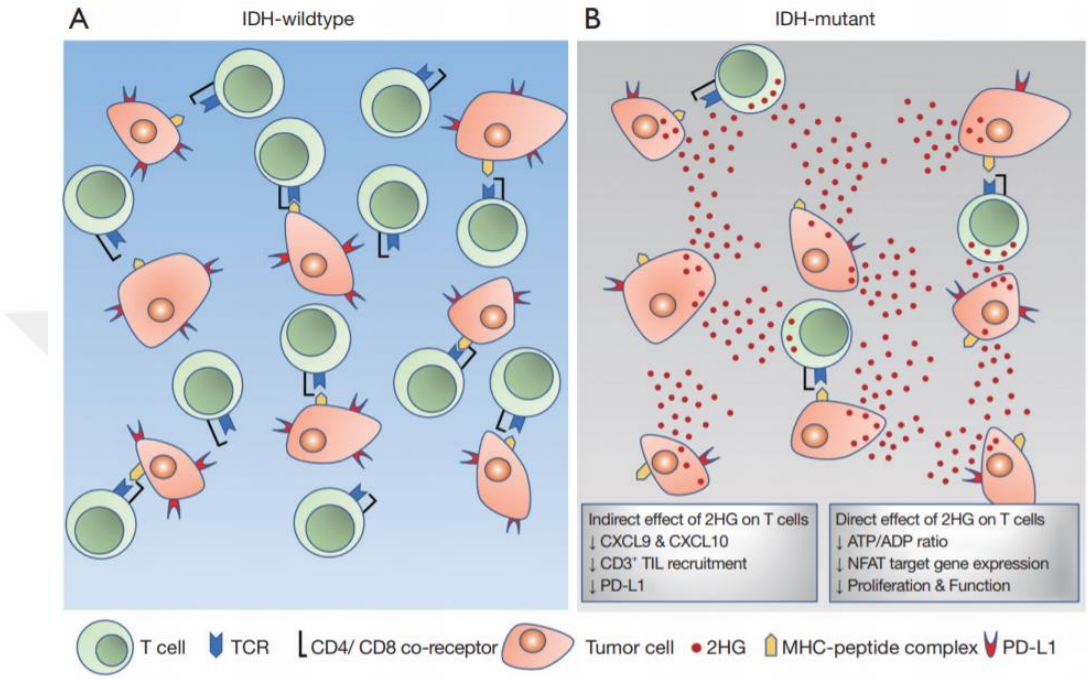

Figure 2.4 IDH-mutation induced regulation TME. IDH wildtype gliomas exhibit higher infiltration of TILs and PD-L1 expression (A). Reduced immune responses are correlated with the mutant IDH expression(B). T cell suppression can occur by glioma intrinsic mechanisms such as lower expression of CXCL9, CXCL10 and PD-L1. On the other hand, accumulation and released 2-HG can have a direct effect T cells through via paracrine fashion. The altered TCR signaling pathway on T cells, cause inhibited anti-tumor immunity.

Besides the reduced infiltration of TILs, IDH1 mutation induces a reduction of leukocyte chemotaxis thereby reducing infiltration of $CD45^+$ immune cells such as microglia/ macrophages, T cells, B cells, and dendritic cells as well. A computational study reveals IDH mutation induced hypermethylation also result in the reduction of expression levels of MHC-I type human leukocyte antigens (HLAs). The expression levels of HLA genes have been recapitulated via treatment with methyltransferase inhibitor. This study suggests that there is a reduced infiltration of immune cells in the IDH mutant gliomas correlated with the decreased MHC-I protein level result in poor antigen presentation (Luoto et al., 2018; Yeung et al., 2013).

All in all, both tumor intrinsic and the direct effect of the 2-HG have strong fingerprints on the TME interactions. However, still remains unclear the IDH induced regulations and interactions over immune cells. T cell populations are the most studied immune cells to search IDH induced mechanisms. Infiltrating myeloid cells are much more than T cells in glioma TME(Müller et al., 2017). Thus, IDH induced effects must be investigated over the myeloid cell populations such GAMs as well as other immune cell types.

2.4 Glioma-Associated Macrophages; Mechanisms of Inflammation and Polarization

2.4.1 Inflammation of Glioma-Associated Macrophages

Inflammation is defined by activated innate immune cells caused by an elevated level of cytokine secretion. This inflammatory response is mediated by evolutionary conserved pattern-recognition receptors (PRRs) which are predominantly expressed in macrophages, monocytes, dendritic cells, neutrophils, epithelial cells, and adaptive immune system cells. PRRs involves Toll-like receptors (TLRs), C-type lectins (CTLs) and NOD-like receptors (NLRs) which scans the extracellular environment and recognizes both PAMPs (Pathogen-associated molecular patterns) and DAMPs (Damage-associated molecular patterns) (Schroder & Tschopp, 2010). NLRs are multidomain proteins which are composed of C-terminal domain (rich in leucine repeats (LRR)), central nucleotide-binding domain (NACHT) and N-terminal caspase recruitment (CARD) or pyrin (PYD) domains. Among the NLR family, NLRP3 inflammasome is the most characterized one presently (Awad et al., 2017). Once PAMPs or DAMPs are recognized by NLRs; formation of inflammasomes is initiated. Inflammasomes are multiprotein complexes which are responsible for the maturation and secretion of pro-inflammatory cytokines interleukin-1β and interleukin-18 (Martinon, Burns, & Tschopp, 2002). Besides secretion of IL-1 cytokine family, inflammasomes also involve in caspase-1 activation mediated by their interaction with ASC adaptor protein (Apoptosis-associated Speck-like protein containing a Caspase recruitment domain) (Schroder & Tschopp, 2010).

Innate immune responses and inflammasome activation have a significant role in cancer development and metastasis. Different CNS cell populations can contribute to the inflammasome activation such, infiltrating macrophages, resident microglia, astrocytes,

oligodendrocytes, neurons, endothelial cells, dendritic cells (Figure 5)(Singhal, Jaehne, Corrigan, Toben, & Baune, 2014).

Production of cytokines by inflammasome activation resulting regulation of APCs functioning and differentiation of immune cells indicate that inflammasomes are associated with the complex events in the TME. Since the inflammasome activated, secreted cytokines IL-18 and IL-1β mediated mechanisms affecting cancer development and glioma progression are still controversial(Voet et al., 2019). IL-18 secretion in colon cancer and induces tumor surveillance via promoting intestinal barrier function at the mucosal surface of intestines. On the other hand, IL-1β supports immunosuppression and plays a critical role in tumor growth and metastasis in skin and breast cancer(Kantono & Guo, 2017b). IL-18 and IL-1β play a controversial role in glioma as well. IL-1β secretion induces inflammation, tumor progression and early angiogenic response. Production of IL-18 trigger IL-2 secretion which has anti-tumor activity in glioma models (XU, GUO, SENG, CUI, & QU, 2015). On the other hand, IL-18 produced by the microglia promote migration of glioma(He, Fu, Tian, & Yan, 2018).

Certain types of cancer and different cell types can exhibit different inflammasome activities. Studies on CNS inflammation and disease mostly carried out with in vitro experiments on cell lines. Accumulating studies on glioma shows that overexpression NLRP3 inflammasome correlated with the increased WHO grade. In vitro studies with glioma cell lines also shows that NLRP3 inflammasome plays a role in the proliferation, metastasis, and apoptosis (Yin et al., 2018). In one of the related study carried out with patient-derived glioma cells; while IL-1β production was observed in GBM cells, it is not observed in low-grade astrocytoma (Tarassishin, Casper, & Lee, 2014). In addition to this observations Gustin A. et al. demonstrate the NLRP3 inflammasome activation is limited with the microglial cells in the mouse model. IL-1β secretion and NLRP3 inflammasome activation could not be observed in astrocytes and some inflammasome activators such ATP can promote the production of IL-1β in microglia but not in the astrocytes(Gustin et al., 2015). Higher inflammasome activation has also been observed during chemotherapy treatment in several studies. Disrupted tumor cells with chemotherapy release ATP in a way that it can be uptaken by the P2X7 receptor of dendritic cells result in NLRP3 inflammasome formation (Karan, 2018).

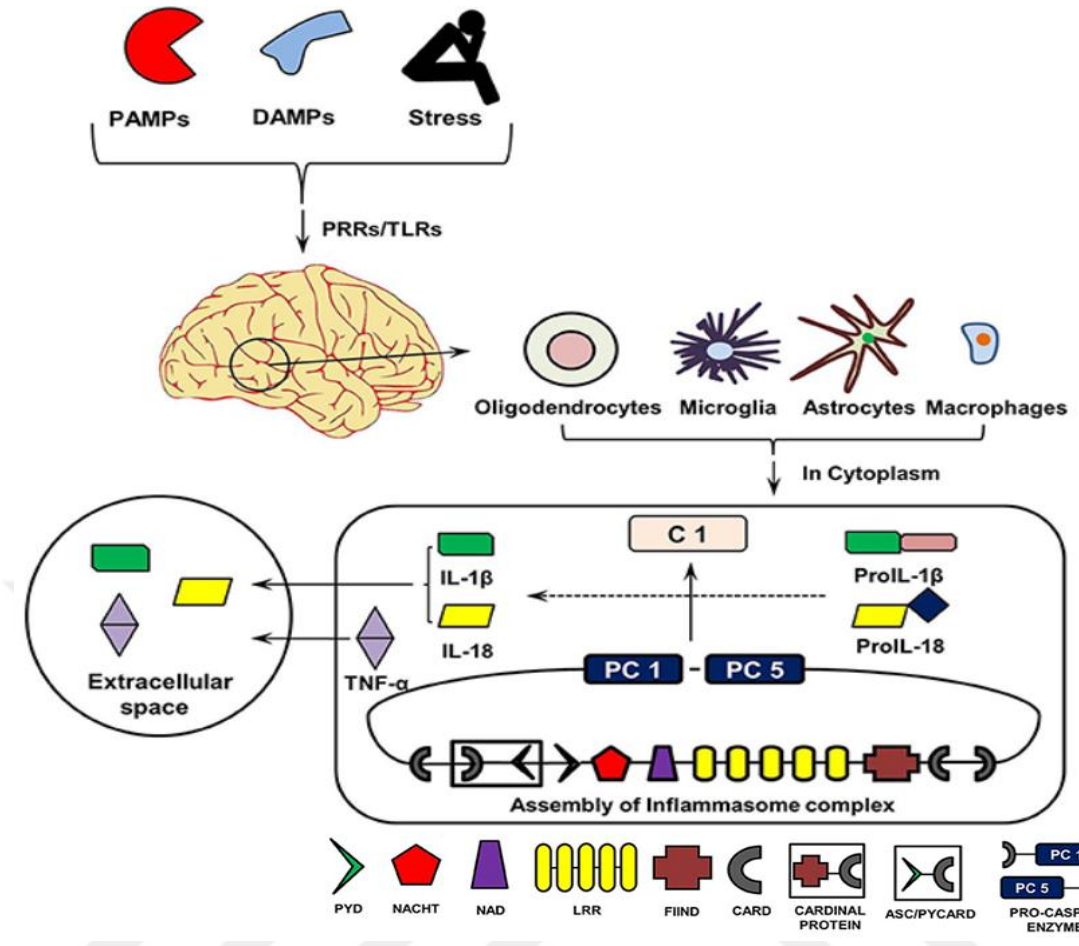

Figure 2.5 Formation of inflammasomes in brain. PAMPs, DAMPs, and stress trigger the formation of inflammasome in brain cell population such phagocytic myeloid cells. Ones the signals recognized by PRRs/TILs initiates formation of inflammasome complex. Released cytokines TNF-α, IL-18, IL-1β trigger an inflammatory reaction in the extracellular space (Singhal, Jaehne, Corrigan, Toben, & Baune, 2014). Pro-caspases: PC1 and PC5. Caspase 1: C1.

Macrophages and other cells produce IL-1β and IL-18 cytokines as an immune response. In tumor tissue release of this cytokines are correlated with the poor prognosis (Kantono & Guo, 2017). Resident or infiltrated circulating immune cells expressing PRRs can trigger these pro-inflammatory responses. It is known that GBM cells produce inflammatory cytokines such as IL-1β because of the activated NLRP3 inflammasome. In this context, it is suggested that inhibited NLRP3 activation results in an expansion of the survival rate because potentially activated NLRP3 inflammasome reduces the NK cell functioning result in the tumor invasion and proliferation (Moossavi, Parsamanesh, Bahrami, Atkin, & Sahebkar, 2018).

MDSCs can suppress the anti-tumor response via NLRP3 expression. NLRP3 activation correlated with the recruitment of the immune cells to the tumor site and metastasis as well.

Van Deventer et al. revealed that the accumulation of MDSCs decreased in Nlrp3−/− mice compared to the wild type (Condamine, Mastio, & Gabrilovich, 2015; van Deventer et al., 2010). In addition, Chow et al. shows decreased metastasis in the metastatic melanoma model when the NLRP3 activation is absent in MDSCs (Chow et al., 2012).

NK cell infiltration increased in the absence of NLRP3. Secreted chemokines such CCL5 and CXCL9 which are exhibiting the anti-metastatic activity of NK cells. Functional NLRP3 inflammasome studies on pancreatic ductal adenocarcinoma (PDA) mouse models, suggesting that tumor growth and metastasis can be controlled via targeting NLRP3 inflammasome components (Daley et al., 2017). Macrophages expressing NLRP3 inflammasome effects the cytotoxic $CD8^+$ T cells activation and CD4+ T cells differentiation through tumor promoting fission (Treg, Th2, Th17). It also alters the T helper cell polarization via triggering IL-12 production (Karan, 2018). Inoue et al. also demonstrate that NLRP3 inflammasome expressing APCs trigger the $CD4^+$ T cells to migrate CNS (Inoue, Williams, Gunn, & Shinohara, 2012).

There are a few studies investigating IDH mutation related to inflammatory mechanisms. But today we know that patients' survival rates in LGG are correlated with the IDH mutation status and histological origin of the tumor. Astrocytoma patients live longer than oligodendroglioma patients (Schomas et al., 2009). These observations may be correlated with the inflammatory responses in the TME. Gonda et al. demonstrated that inflammation-related gene expressions increased in astrocytoma compare to oligodendroglioma (Gonda et al., 2014).

Deregulation of innate and adaptive immunity via inflammasome activation is important to process to understand immune responses. We have limited information about the activation of inflammasome in glioma. Specific inflammasome targeting studies are needed to enlighten the underlying mechanisms and crosstalk in specific brain cell types. This is also important to understand both cell intrinsic pathways and paracrine signaling via specific cytokines which are responsible for the immune cell differentiation at the tumor site.

2.4.2 Macrophage Polarization: M1/M2 Like Responses

Monocytes and macrophages (MΦ) are hematopoietic-derived cells originate from bone marrow and yolk sac progenitors. They have a critical function in the mononuclear phagocyte system (MPS) to support innate immunity, help adaptive immunity and possess a high level of plasticity providing them the ability to assume specific roles required for tissue homeostasis. Monocytes are also the precursor of resident macrophages, and they can infiltrate to tissues and differentiate according to the environmental cues (Richards, Hettinger, & Feuerer, 2013). Peripheral blood monocytes are the primary source of macrophages found in lymphoid and non-lymphoid tissues.

Two major differentiation states are known as the classically-activated type 1 macrophages (M1) and the alternatively-activated type 2 macrophages (M2). Depending on the nature of the stimuli in the environment (i.e. anti- or pro-inflammation); the gene expression of macrophages is modulated to trigger them into either a pro-inflammatory M1 or an anti-inflammatory M2 phenotype (Murray, 2017). This adaptation of macrophages to their microenvironment under specific conditions is called phenotypic polarization. M1 cells are activated by interferon-γ (IFN-γ), tumor necrosis factor (TNF), and DAMPs which produce a pro-inflammatory response by secreting pro-inflammatory cytokines Interleukin-6 and TNF (Hesketh, Sahin, West, & Murray, 2017). In addition to the secretion of pro-inflammatory cytokines, activated M1 cells provide phagocytosis of microbes, elimination of tumor cells and adaptive immune response. On the other hand, exposure to anti-inflammatory cytokines such as IL-4, IL-10, IL-13 promotes M2 cell polarization. (Murray, 2017). M2 cell activation causes suppression of anti-inflammatory response, promotes digestion extracellular matrix and angiogenesis by VEGF (vascular endothelial growth factor) production. As a consequence of these features; M2 cells promotes tumor development when compared to M1 cells (Quatromoni & Eruslanov, 2012). Figure 2.6 summarizes the mediators and effectors of the M1/M2 polarization states. Role of these cytokines in the course of tumor formation and malignancies will be discussed further.

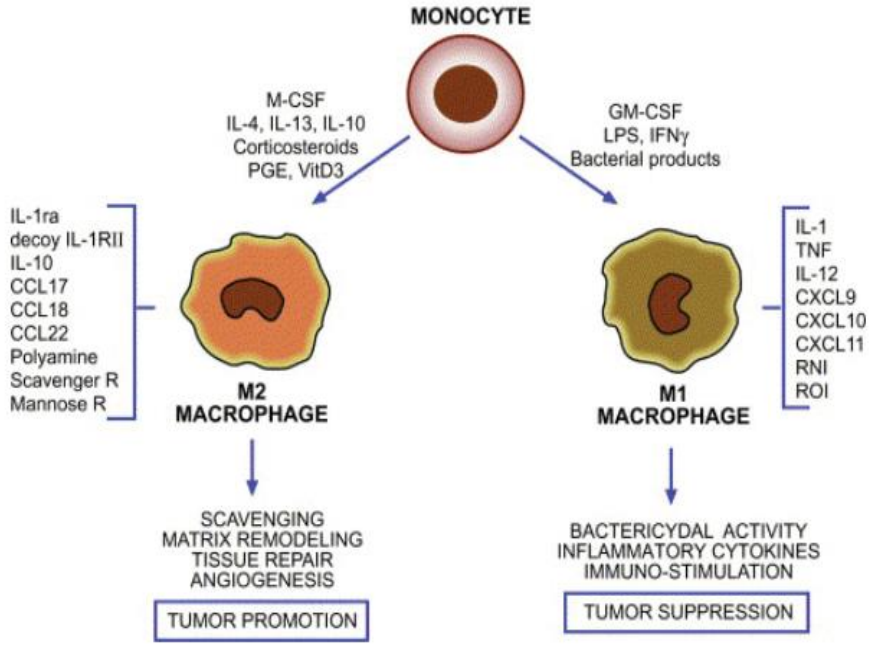

Figure 2.6 Effector and mediators of M1/M2 polarization during monocyte differentiation. Chemoattractant and released cytokine and chemokine signals summarized with the resultant biological response (Quatromoni & Eruslanov, 2012).

2.5 Glioma-Associated Macrophages and Glioma Cell Crosstalk

GAMs role in glioma immunology still remains unclear. Different subsets of macrophages are accumulated in the brain TME and they represent the vast majority of immune cells (Pyonteck et al., 2013). During tumor, progression monocytes enter the tumor tissue and differentiate to into GAMs that can promote tumor initiation, progression, and metastasis and also they are associated with the cancer-related inflammation (Hussain et al., 2006).

Significant endeavors to characterize GAMs have driven to a depiction that M2-type macrophages thought to prevail within the glioma microenvironment compare to M1-type macrophages (Kennedy et al., 2013). Since these cells do not exist at steady-state condition, GAMs are considered to a unique and different M2 myeloid population that bearing both M1 and M2 polarization signature (Allavena, Sica, Garlanda, & Mantovani, 2008; Mantovani, Schioppa, Porta, Allavena, & Sica, 2006).

TME consist of many chemoattractants to shape the environment by communicating the immune cells. These signals accumulating in the TME result in the recruitment of circulating

monocytes that give rise to M1 and M2 like responses depending on the signal. Chemoattractant such as IFN-γ lipopolysaccharides and other microbial products stimulates M1-type macrophages to produce pro-inflammatory signals like TNF-α, IL-1B, and IL-12. Surface markers like MHCII and antigen presenting molecules CD80/CD86 are upregulated as a result of M1 like differentiation. On the other hand, M2 like macrophages release immunosuppressive cytokines IL-10, IL-6, and TGF-β and upregulates the surface markers like FasL (Figure 2.7) and PD-L1 that stimulate programmed cell death of T and B cells. As mentioned before TAMs/GAMs known to resemble M2 like polarization with a signature like high IL-10 production, however at the same time they can produce IFN-inducible chemokines. Since, there is an overlap between the specific markers for M1, M2 macrophages and TAMs suggesting that TAMs have distinct transcriptome profile exhibited anti- and pro-inflammatory features (Bowman et al., 2016).

Recent studies on glioma have focused on tumor cell-intrinsic mechanisms. However, there is increasing evidence that glioma microenvironment plays an important role in the course of the disease. Increased infiltration of macrophages during disease progression dictates the immunomodulatory function of GAMs in glioma via complex communication with cytokine and chemokine signals, thus the underlying mechanisms of GAM interactions are still unclear. The potential mechanisms contributing to the recruitment and invasion of GAMs to the tumor site are illustrated in Figure 7 (Roesch et al., 2018).

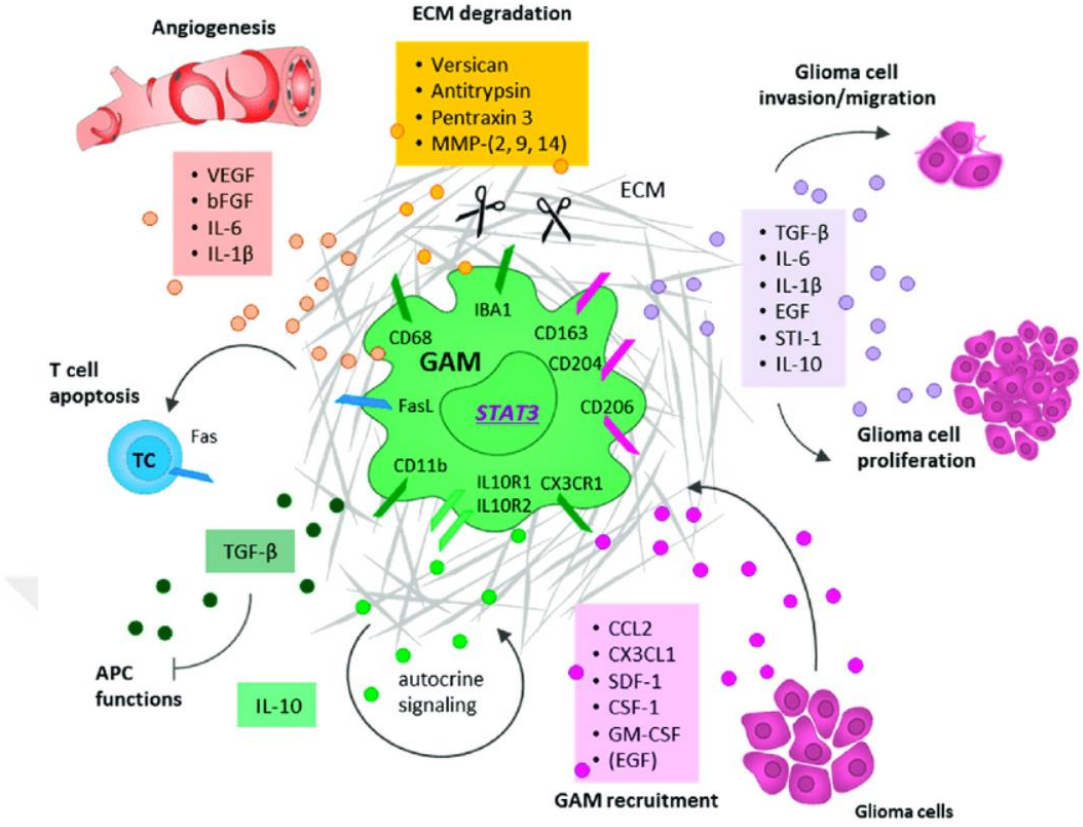

Figure 2.7 Glioma and GAMs crosstalk. The mechanisms and the signaling molecules which contribute to the glioma proliferation and deregulation of immune responses via paracrine and autocrine manner are summarized in the figure (Roesch et al., 2018).

Glioma cells secrete some signaling factors like EGF, CCL2, CXCL12 (SDF-1), CX3CL1, GDNF, CSF-1(M-CSF), GM-CSF. These type of cytokines induces M2-like responses that exert anti-inflammatory and pro-tumorigenic phenotype. In addition to these cytokines, the IL-10 cytokine secreted from GAMs in the presence of glioma can promote tumorigenesis cell proliferation and reduce inflammation (Hu et al., 2016). IL-10 receptor expressed on the GAMs contribute to the autocrine signaling and drive polarization state toward the M2 (Roesch et al., 2018). Astrocytoma and GBM cells secrete monocyte chemoattractant protein (MCP-1 or CCL2) to recruit monocyte to the TME (Platten et al., 2003; J. Zhang et al., 2012). The increased expression level of CCL2 is associated with the glioma grade (Kuratsu et al., 1993). However recent studies reported that infiltration of GAMs associated with another type of monocyte chemoattractant protein (MCP-3) (Saio et al., 2009). Another important factor released by glioma cells is the CXC motif chemokine 12 (CXCL12 or SDF-1) which plays a

critical role in the recruitment of GAMs to the intratumoral site (S.-C. Wang, Hong, Hsueh, & Chiang, 2012). Expression of CXCL12 speeds up the tumor progression in LGG patients (Salmaggi et al., 2005). Glioma also attract the GAMs recruitment and polarization state toward the immune suppressive manner via secreting myeloid colony stimulating factors (CSFs). Macrophage colony stimulating factor (M-CSF or CSF1) contribute to M2 polarization and motility of GAMs. Granulocyte macrophage colony stimulating factor (GM-CSF) is another member of the CSF family released from glioma cells. Effect of these CSFs on the macrophage lineages are different (Lacey et al., 2012). GM-CSF induce production of cytokines such as TNF, IL-6, IL-12p70 and IL-23 following LPS stimulation leading them toward M1 polarization state. However, M-CSF treated macrophages release IL-10 and CCL2. Some reviews claim that M-CSF-exposed macrophage populations tend to retain their steady-state but tent to M2 type responses (Hamilton, 2008).

Another important protein secreted from human glioma cells along with GAMs is the signal transducer and activator of transcription protein 3 (STAT3). In most cancer and GBM (PTEN mutant) cells, STAT3 gene is constitutively active (de la Iglesia, Puram, & Bonni, 2009), and the overexpression of STAT3 protein propagate reduction of some immune-related factors such CD80, CD86, and MHC II. Therefore STAT3 is one of the key immunosuppression mechanism in glioma progression and the persistent activation of STAT3 activation affects the macrophage polarization and inhibits M1 type responses in the TME (Sica & Bronte, 2007). The cytokines IL-10, EGF, FGF, and IL-6 are known to activate SAT3. Secreted IL-6 various cell types in the TME can activate STAT3 via paracrine as well as autocrine signaling. As a result of STAT3 activation Il-6 expression increased and this loop of IL-6 expression upregulates various kind of growth factor and cytokine production such CCL2, IL1-β, VEGF, EGFR, CCL3, and GM-CSF (Yuan, Zhang, & Niu, 2016). STAT3 is a potential therapeutic target and “molecular hub” which associated with the several pathways in GBM progression (Brantley & Benveniste, 2008; W. Li & Graeber, 2012).

Ones GAMs are recruited to the tumor site and polarized, upregulated surface markers are useful to characterize M2 macrophages. Macrophage scavenger receptors; CD204 and CD163, and mannose receptor-1; CD206 is the well-established markers for TAMs as well as GAMs (Soldano et al., 2016). Some microglia and macrophage markers (CD68, IBA1, CX3CR, CD11b) are also used to characterize GAMs. Lately, several studies on GAMs demonstrate that

poor prognosis and glioma aggressiveness correlated with the accumulation of $CD68^+$, $CD11b^+$, $CD163^+$ GAMs (Lu-Emerson et al., 2013). In various cancer types, $CD68^+$ TAMs are associated with the reduction of survival rates (Ojalvo et al., 2018). $CD68^+$ GAM accumulation also correlated with the glioma patients' survivals (L. Wang et al., 2018). $CD68^+$ GAMs tend to exhibit M1 type responses and interestingly activated $CD68^+$ M1 cells associated with IDH mutations in LGG (Jansen, Spliet, Leng, & Robe, 2018). These M1 type immune responses may be the potential mechanism result in longer survival rates of IDH mutant gliomas.

The invasion of the GAMs alters the ECM composition resulting in degradation. Several factors like matrix metalloproteinases (MMPs-2,9,14) promote ECM degradation, angiogenesis, glioma cell proliferation, and migration and T cell apoptosis (Figure 7). TAMs transcriptomic signatures present that ECM protein expression decreased while ECM degrading enzyme increase. Recently, Madsen et al. characterize a $CCR2^+$ (chemokine receptor of CCL2) monocyte-derived TAM population which degrade collagen (Madsen et al., 2017). Crosstalk between glioma cells and GAMs result in various pro-tumorigenic phenotype and it is crucial to clarify tumor progression.

GAMs exhibit pro-tumorigenic responses by secreting molecules such as TGF-β, IL-6, IL-1β, EGF, STI-1, and IL-10 promoting cell proliferation and glioma cell migration. It is important to highlight that the expression levels of these cytokines are depending on the interaction with the glioma cells. For example, microglia cells release a lower amount of transforming growth factor-beta (TGF-β) in monoculture compare to co-culture with glioma cells. This increased TGF-β in the presence of the glioma cells reduces the expression of MHC II molecules and surface markers (CD80, CD86) (Wesolowska et al., 2008), suggesting that reduced expression of the stimulatory factors results in the impaired phagocytosis. In another study, with rodent glioma model, was claimed the changeable expression levels in the presence of the glioma cells, showing that expression of surface markers and MHC II increased after isolation of GAMs from TME (Badie, Bartley, & Schartner, 2002).

GAMs also secrete pro-angiogenic factors such as IL-6, IL-1β, VEGF to promote vascularization. High expression of VEGF is associated with the myeloid cell accumulation and the blockage of the both VEGF and VEGF receptor recapitulates the phenotype and reduce myeloid cell infiltration in GBM mouse models (Piao et al., 2012). Similarly, another study shows that, IL-6 receptor blockage reduce the expression and angiogenesis in murine models

(X. Chen et al., 2014). However genetic lineages of GAMs are important to exhibit pro-angiogenic effects. Brandenburg et al. demonstrate that resident microglia promotes vascularization rather than MDSCs (Brandenburg et al., 2016).

Consequently, GAMs exhibit distinct responses in TME depending on their genetic lineages as resident microglia and blood-borne macrophages. Infiltrating GAMs characterized in the LGG is mostly resident microglia while blood-borne macrophages in the higher grades. Since the crosstalk between glioma and immune cells is curtail to understand glioma progression, the underlying mechanisms suggest new potential therapeutic targets for glioma patients. There is wide literature on GAMs supporting tumor progression but it is still controversial M1/M2 polarization states during tumor formation. Today, we have knowledge about the IDH mutations effects on the glioma formation but the whole mechanisms still lack of understanding. This thesis study aimed to put emphasis on the effect of IDH1 mutation on blood-borne macrophages during tumor development. This study is a step forward in determining new molecular targets by contributing to the literature in explaining the interaction of IDH mutant glioma and the immune system.

3 MATERIALS AND METHODS

3.1 Cell Culture

3.1.1 Astrocytic Cell Culture

In this thesis study, previously Immortalized Human Astrocyte (IHA) cells (Sonoda et al., 2001) which infected with the pLVX-Tet-On retrovirus to exhibit IDH1 mutant phenotype were used (Gift from Prof. Timothy A. Chan and Sevin Turcan). IHAs exhibit hTERT expression, ras pathway activation, p53 inactivation, and pRb/p16 pathway inactivation as genetic background to model the grade III Astrocytoma. With the tetracycline-inducible expression system, the coding sequence of IDH1 R132H placed in the downstream of the Tet-responsive promoter. Three different cell line; including vector encoding the inducible empty vector, wild type and mutant IDH1 (IDH1 R132H) respectively were cultured.

These three types of astrocytic cell lines were cultured in Astrocyte Media (Astrocyte Media / AM, ScienCell, 1801) (AM, 500 ml basal medium; 10 ml FBS (ScienCell, 0010), 5 ml Astrocyte Growth Support (AGS, ScienCell, 1852) and 5 ml of penicillin / streptomycin (P / S, ScienCell, 0503). They were stimulated with doxycycline (Sigma-Aldrich, D9891). All the cell lines were cultured in the presence (1mg /ml) and the absence of doxycycline. Stocks were opened when the cells at passage number 0 and cultured along the passage number 9. Cell samples were taken from 3., 6. and 9. passages. RNA and protein isolation were performed to be able to detect mutant IDH1 R132H proteins, samples used for the downstream western analysis.

3.1.2 Collection of Conditioned Media from IDH1-mutant IHAs

From the stimulation of doxycycline, conditioned media (CM) were collected from the astrocyte cell lines along 9 passages and they filtered through a 0.22 μm filter than stored at -20 ° C. The CM collected from first three passages of IDH1 R132H IHAs were pooled and labeled as 1st Time Point CM (**TP1**); the 4.-6. passages labeled as 2nd Time Point CM (**TP2**)

and the last three passages called as 3rd Time Point CM (**TP3**). IHAs with empty vector used as control condition and collected CM from whole 9 passage pooled and labelled as Empty Control CM (**EC**). Control group was generated with the macrophage medium with M-CSF and labelled as Control (**C**).

3.1.3 Primer Monocyte Isolation and Culturing

The blood samples were taken from the blood bank (DEU) with buffy coat pooling bag. Monocyte isolation was performed from the peripheral blood by two-stage gradient centrifugation method. Monocytes isolated via this method were treated with CM collected from immortalized IDH1 R132H mutant and empty vector carrying astrocytes.

First density gradient; isolation of mononuclear cells from Buffy Coat

Buffy coat was distributed to 50 ml falcon tubes,20 ml per tube. Blood samples were diluted with a 1: 1 ratio of 1X PBS (Gibco, 10010023) solution. The samples, diluted in 20 ml, were carefully and slowly laid over the 15 ml Ficoll (GE Healthcare, 17-1440-03) solution (1.077 g/ml) to separate phases clearly. Centrifugation step was performed at room temperature(RT),400g, without acceleration/brake for 30 minutes. The middle nebula layer with peripheral blood mononuclear cells (PBMCs) were collected with the help of pipette then washed two times in RPMI1640 (Gibco, 21875034) medium and/or 1X PBS. The RPMI1640 medium used in the experiments contains 5% heat-inactivated FBS, 1mM sodium pyruvate, 1% L-glutamine, 1% penicillin-streptomycin and phenol red.

Isolation of monocytes from mononuclear cells

The mononuclear cells isolated in the previous step were suspended in 20ml RPMI1640 medium without phenol red (Gibco, 1183506). For the second density gradient, the iso-osmotic Percoll (GE Healthcare, 17-5445-02) solution was prepared. 23.13 ml Percoll solution (density: 1.131 g/ml) was mixed with 1.87 ml 10X PBS in a 50 ml falcon tube. Then 23ml was taken from this solution and mixed 27ml RPMI1640 with phenol red. The mixture with three ingredients divided into new falcon tubes each with 25 ml mixture. 46% iso-osmotic Percoll solution obtained to perform a second density gradient. 20 ml of mononuclear cell suspension

in RPMI1640 medium without phenol red was slowly laid on the iso-osmotic Percoll solution. At this stage, since the suspension of the cells is transparent and the percoll solution is pink in color due to phenol red, it was possible to differentiate whether the phases are mixed or not. The tubes were then centrifuged at RT, 550g, without braking for 30 minutes. The nebula layer between the pink and transparent phases was collected with the help of a pipette. The collected monocytes were washed two times in RPMI1640 medium. After the final wash, the cells suspended in RPMI1640 medium and counted with hemocytometer in a 1:10 dilution in Trypan blue stain (0.4% w/v) (Sigma-Aldrich, T8154).

3.1.4 Differentiation of Monocytes to Macrophage

In this thesis study, three different donor blood samples used to isolate monocyte. Two donors used to downstream analysis for RNA sequencing (RNA-seq). All three donors were used for RT-qPCR and western analyses. The isolated monocytes were incubated with RPMI1640 medium and different CM containing human M-CSF (Macrophage Colony Stimulating Factor) (Peprotech, cat no. 300-25). The monocytes isolated from the same donor blood sample were separated in equal numbers for 5 different conditions ($4x10^6$ cells per well). Conditions described in Table 3.1 respectively.

Table 3.1: Medium composition used to differentiate monocytes to GAM. Different CM collected from the IHAs at different time points through the 9 passages used to set differentiation condition. Monocytes cultured with RPMI 1640 with M-CSF as a control condition. Same amount of M-CSF and CM collected from the Empty vector carriying IHAs used as an Empty control

Ingredients	TP1	TP2	TP3	C	EC
CM from IDH1mutat IHAs	30%	30%	30%	-	-
CM from IHA including empty vector	-	-	-	-	30%
RPMI 1640	70%	70%	70%	100%	70%
M-CSF	10ng/ml	10ng/ml	10ng/ml	10ng/ml	10ng/ml

Medium stocks for the condition TP1, TP2, and TP3 were collected and pooled from the passages of the IDH1R132H mutant vector carrying astrocytes. Empty condition medium stocks were collected and pooled from the empty vector carrying astrocytes along the nine passages. RPMI1640 with M-CSF used as control medium stock.

Differentiation protocol lasted seven days. Monocytes from donors have seeded into Corning® Costar® Ultra-Low Attachment six-well plates (Life Sciences, 3471) in five different conditions for differentiation. Differentiation started with the $4x10^6$ cells with 5ml medium per well. A day after seeding 2 ml medium stock was added onto the wells and repeated with one-day intervals along the seven days. After seven days' cells were collected from the low attachment plates and centrifuged at 400g for 5 min. Old medium removed and all the macrophages seeded into tissue culture plates in 5ml rest medium for one-day rest. The RPMI1640 medium used as a resting medium without M-CSF contains 5% heat-inactivated FBS, 1mM sodium pyruvate, 1% L-glutamine, 1% penicillin-streptomycin and phenol red. Macrophages that attached to the bottom of the tissue culture plates were harvested at the end of the one-day rest. Plates were placed into the ice and medium with unattached cells removed to harvest macrophages. Lysis buffer was poured directly on to the macrophages for RNA and protein isolation.

3.2 RT-qPCR analysis

In order to investigate expression levels of the selected genes (Table 2.1) RT-qPCR was performed to the macrophage samples. 25µl reaction mixture prepared containing 50ng RNA, 0.2µl forward, 0.2µl reverse primers (Table 2.1) and 12,5µl 2X GM SYBR qPCR Mix (GeneMarkbio, cat no: QPSY02-1). Triplicate of each condition RT-qPCR experiment performed via Applied Biosystems® 7500 Real-Time PCR thermal cycler. The reaction condition set up as; 1 cycle at 95 ˚C for 2 min, 40 cycle at 95 ˚C 15 seconds, 60 ˚C 30 seconds. Results normalized according to the GAPDH levels and statistical analysis was performed via GraphPad Prism.

Table 3.2: Gene names and primer sequences used for RT-qPCR analysis.

Gene Name	Forward Sequence	Reverse Sequence
IRF5	5′- CCAGCCAGGACGGAGATAAC-3′	5′- TATGTGGCTTCCGCACCTAC-3′
TNF-α	5′- GAGGCCAAGCCCTGGTATG-3′	5′- CGACTCTAGTTAGCCGGGC-3′
MRC1	5′- CTACAAGGGATCGGGTTTATG-3′	5′- ACCTCTGGAGCACAGATT-3′
CCL17	5′- CGGGACTACCTGGGACCTC-3′	5′- GCTTCTTCTCGGTGTCACTCC-3′
NEK7	5′-TTTACACTCCTGACAGCG -3′	5′-GCAACAGGAACTTTAGAACT -3′
NLRP3	5′- GCAGCAAACTGGAAAGGAAG-3′	5′- CTTCTCTGATGAGGCCCAAG-3′
Asc	5′-AGTTTCACACCAGCCTGGAA -3′	5′- TTTTCAAGCTGGCTTTTCGT-3′
Caspase1	5′-CTCAGGCTCAGAAGGGAATG -3′	5′-CGCTGTACCCCAGATTTTGT -3′
IL-18	5′-GCTTGAATCTAAATTATCAGTC-3′	5′-GAAGATTCAAATTGCATCTTAT -3′
GAPDH	5′-TGCACCACCAACTGCTTAGC -3′	5′-GGCATGGACTGTGGTCATGAG -3′

3.2.1 RNA isolation

Total RNA isolation was performed from the samples taken from immortal human astrocytes and differentiated macrophages, which were used for RNA-seq analysis and RT-qPCR. All RNAs were isolated according to the user protocol using the NucleoSpin® RNA (MN, cat no. 740955.50) kit. Cells were destroyed by adding 350µl of RA1 buffer solution and 3.5 β-ME. The cell lysis, loaded onto the purple filter, was centrifuged at 11.000 g for 1 min and then mixed with 350µl of 70% EtOH. The mixture is then loaded on a light blue filter and centrifuged at 11,000 g for 30 seconds. 35oµl of MDB buffer solution loaded onto RNAs attached to the light blue filter were re-centrifuged at 11.000g for 1 min. The 95 µl rDNase reaction mixture was prepared and loaded onto the filter for 15 min incubation at RT to remove DNA. In order to stop the reaction, 200µl of RAW2 buffer solution was added and centrifuged at 11.000g for 30 seconds. After washing the filter twice with RA3 buffer solution, the RNAs were eluted with 35µl RNase-free water.

3.2.2 cDNA Synthesis

RNA samples were converted to cDNA by using ProtoScript® First Strand cDNA Synthesis Kit (NEB, E6300). Random primer mix was used to convert RNA to cDNA according to manufacturer's instruction. 600ng RNA sample were taken (up to 6µl) and mixed with primers (2 µl), M-MuLV Reaction Mix (10 µl), M-MuLV Enzyme Mix (2 µl). The reaction filled with water to total volume 20 µl and incubated 25°C for 5 minutes and then at 42°C for one hour. Enzyme was inactivated at 80°C for 5 minutes. The cDNA products were stored at -20°C for downstream RT-qPCR analysis.

3.3 Western Blot analysis

Western blot analysis was performed to investigate NLRP3 inflammatory activity on macrophages which has been differentiated in IHA CM.

3.3.1 Protein Isolation

Proteins used in this study were isolated via NucleoSpin® Triprep (MN, cat no: 740966.50) protein isolation kit for use in Western blotting experiments. In accordance with the user protocol, the cultured cells were first destroyed by 350µl of RP1 and 3.5µl β-ME, then centrifuged for 1 min at 11.000g and filtered through a purple filter. The lysis cleansed from cell debris with the first filter then loaded onto a light blue filter by mixing with 350µl 70% EtOH. Filter column centrifuged at 11.000g for 30 seconds. RNA and DNA remain attached to the column filter after centrifugation step and the lysis that has moved away from the column was mixed with 1:1 ratio of PP solution and incubated for 10 minutes at RT. The proteins precipitated by centrifugation at 11.000g for 5 minutes. Pellets were washed with 50% EtOH. Then the pellets precipitated again by centrifugation at 11.000g for 1 min. Pellets allowed to dry at RT for 5-10 minutes. According to the pellet size, all of them dissolved in 20-100µl PSB-TCEP buffer. Proteins boiled at 95-98 °C for 3 minutes. After boiling the samples cooled down

to RT and centrifuged again for 1 minute. The supernatant was transferred to another Eppendorf tube. Isolated proteins stored at -20 °C for further analysis.

3.3.2 Bicinchoninic Acid Protein Assay

Bicinchoninic Acid (BCA) Protein Assay Kit (TAKARA, cat no: T9300A) was used to calculate isolated protein amounts. Working solution was prepared by mixing BCA reagents A and B in 100:1 ratio according to the manufacturer's instructions. Then, protein standards prepared to set a standard curve with different concentrations (2000, 1500, 1000, 750, 500, 250, 125 and 0- ug/ml). Serially diluted standards and prepared protein samples (1:5 diluted) were separated as duplicate (25 ul for each) to the microtiter plate. 200 ul working solution was added onto the samples and incubated at 37°C for 30 minutes. Absorbance's measured at 562 nm via microplate reader (BioRad) and water used as a blank solution. Standard curve plotted and sample concentrations calculated according to the curve.

3.3.3 Western Blotting

Table 3.3: SDS-PAGE gel compositions used in the western blot analysis.

Resolving Gel 10%	Stacking Gel 5%
1.3 ml 1.5 M Tris (pH 8.8)	0.38 ml 0.5M Tris (pH 6.8)
1.7 ml Acrylamide (30%)	0.5 ml Acrylamide (30%)
1.9 ml Water	2.1 ml Water
50µl SDS (10%)	30µl SDS (10%)
50µl APS (10%)	30µl APS (10%)
2 µl TEMED	3 µl TEMED
Total=5,002ml	Total=3,043ml

To perform SDS-PAGE gel electrophoresis, one small and one large glass were clamped and placed on pouring stand. Resolving (4ml) and stocking (2ml) gels were prepared as indicated in Table 2.2 and poured into the gap between the glasses. Once the resolving gel has been polymerized, stocking gel poured into the top of the gel and comb was placed properly to form wells. SDS-PAGE gel in the holder was transferred to the running tank. Running tank filled with Running buffer (25 mM Tris, 192 mM glycine, 0.1% SDS, PH=8.3). Protein amounts calculated with BCA assay, then the proteins were prepared and boiled at 95 ° C. They were separated on prepared SDS-PAGE gel for about 2 hours(18mA) after the protein samples mixed with 3X loading dye (cell signaling, cat no:7722S) adding the calculated amounts of protein(20µg) and water. SDS-PAGE gel placed on the transfer system filled with transfer buffer (48mM Tris-Base, 39mM Glycine, %20 methanol) and transferred to the membrane (2hrs, 250mA). Then the membrane blocked with 5% milk powder in TTBS solution (50 mM Tris-Cl, 150 mM NaCl, pH 7.6) for 1 hour at RT. The membrane was washed 3 times with TBS to remove excess milk powder than incubated with the desired primer antibody overnight at +4ºC. Membrane was washed before HRP-linked seconder antibody treatment and incubated with the suitable seconder antibody for 1-2 hours at RT. The membrane will then be washed again three times, and the proteins were imaged using Luminata ™ Forte Western HRP Substrate (Millipore, cat no: WBLUF0500) on imaging system.

Table 3.4: Antibody names, dilutions and the brands of supplyers

Antibody	Dilution	Brand	Catalog Number
Anti-mouse IgG	1:2000	Cell Signaling	7076S
Anti-rabbit IgG	1:2000	Cell Signaling	7074S
Anti-NLRP3/NALP3	1:1000	Adipogene Life Sciences	AG-20B-0014
Anti-NEK7	1:10000	Abcam	Ab133514
Anti-Asc	1:1000	Adipogene Life Sciences	AG-25B-0006
Anti-Caspase-1	1:500	Abcam	Ab1872
Anti-beta Actin	1:2000	Abcam	Ab8227
Anti-Human IDH1 R132H	1:2000	LifeSpan BioScences	LS-C336969-100

3.4 Bioinformatic Analysis

RNA-seq was performed via Illumina HiSeq/NovaSeq 6000 S2 PE150 XP genom sequencer platform using paired-end (30 Mio each) sequencing method.

3.4.1 RNA-seq data quality control and removal of adaptor sequences

Firstly, FastQC software used to clean the raw reads from the low-quality reads and the Trimmomatic software v0.39 (Bolger, Lohse, & Usadel, 2014) used to remove excess adaptor sequences from the raw data.

3.4.2 Alignment of the reads to the reference genome and transcriptome assembly

High-quality reads were mapped to the reference genome *H. sapiens*, GRCh38.p12 (Genecode release 30) (Frankish et al., 2019) by using HISAT2 v2.1.0 software (Kim, Langmead, & Salzberg, 2015) which is a spliced aware-alignment tool. Aligned reads were than assembled to potential transcripts using StringTie v1.3.6 (Pertea, Kim, Pertea, Leek, & Salzberg, 2016).

3.4.3 Quantification of differentially expressed genes

Assembled transcripts filtered and normalized via R v3.5.1 statistical computing environment. After normalization Raw TPM counts (58870) reduced to filtered TPM count (13935). PCA plot analysis correlation heat map plot was performed to each data set to reveal the variance between each condition and the biologic replicates. The edgeR package (v.3.24.3) (Robinson, McCarthy, & Smyth, 2010)housed in the R v3.5.2 statistical computing environment was used for differential expression analysis with the filtered TPMs. Differential expression

analysis was performed for 2 replicate individually according to the control group TPMs (Control_1 vs EmptyControl_1, TP1_1, TP2_1, TP3_1 and Control_2, EmptyControl_2, TP1_2, TP2_2, TP3_2). Then gene expression levels normalized according to z-score and Log2 values.

3.4.4 Gene ontology analysis with differentially expressed genes in TP1, TP2,TP3 and common differentially expressed genes in three time point

After differential expression analysis enriched GO terms obtained by using Enrichr a web-based tool (https://amp.pharm.mssm.edu/Enrichr/) (E. Y. Chen et al., 2013). Data filtered according to their fold changes (FC >1) and false discovery rates (FDR> 0.01). After filtering the genes, the group of genes that are differentially expressed in the EC extracted from the TP1, TP2 and TP3 (TP1 vs EC, TP2 vs EC, TP3 vs EC) to eliminate the CM induced changes. Then GO analysis performed for these gene sets (Figure 3.8). Then the common differentially expressed genes in TP1, TP2 and TP3 (not expressed in the EC) selected to understand IDH1 R132H related changes during differentiation of the monocytes. Total 21 gene extracted with the threshold FDR<0.01 and FC>1(for each TP1, TP2 and TP3) (Figure3.7, Table 3.2) and these genes should be examined in depth later. Then we change threshold values as FDR<0.05 and FC>1 (at least in one time point). The genes with the new threshold were used for GO analysis as common differentially expressed genes in TP1, TP2 and TP3. Results evaluated according to their calculated p-values and z-scores (Figure 3.10).

4 RESULTS

4.1 Validation of Mutant IDH1 Expression

In order to detect mutant-IDH1(R132H) expression at protein level western blot analysis was performed with mutant specific antibody. Three different IHA cell lines including vector encoding the inducible empty vector, wild type and mutant IDH1 were cultured and the protein samples collected to perform western analysis at three different passages representing the time intervals which CM collected.

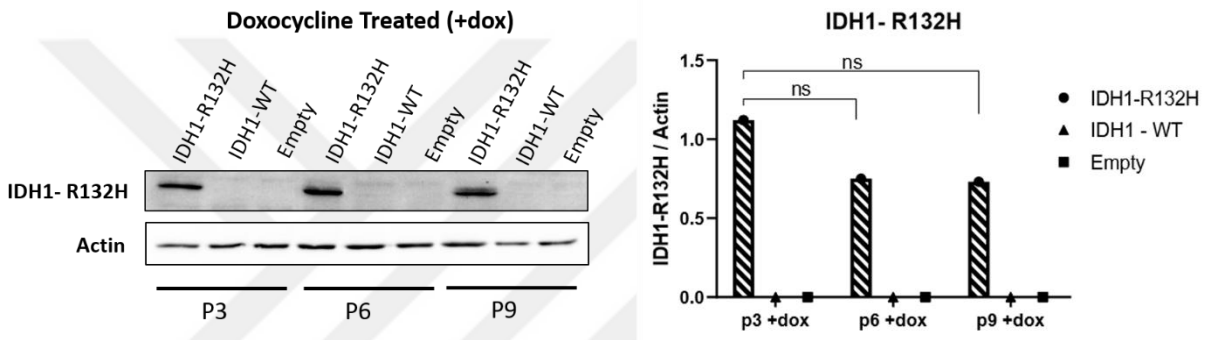

Figure 4.1 Expression of IDH1-R132H in IHA cell lines. Samples taken at passage 3, 6 and 9 (P3, P6, P9 respectively) from **t**hree different cell lines including vector encoding the inducible empty vector (Empty), wild type (IDH1-WT) and mutant IDH1 (IDH1-R132H)**.** 2-way-ANOVA analysis was performed to estimate p-values.

Expression of IDH1-R132H slightly decreased at passages 46 and 49 compare to passage 43. IDH1-R132H expression was not observed in the IDH-WT and Empty cell lines as expected (Figure 4.1).

4.2 NLRP3 inflammasome complex components' protein expressions during differentiation of the human monocytes treated with IDH mutant IHA CM

Western blot analysis was performed using an anti-NLRP3, an anti-ASC, an anti-caspase-1 antibody to introduce inflammasome protein expression in the different IHA CM treated macrophages from three independent donors.

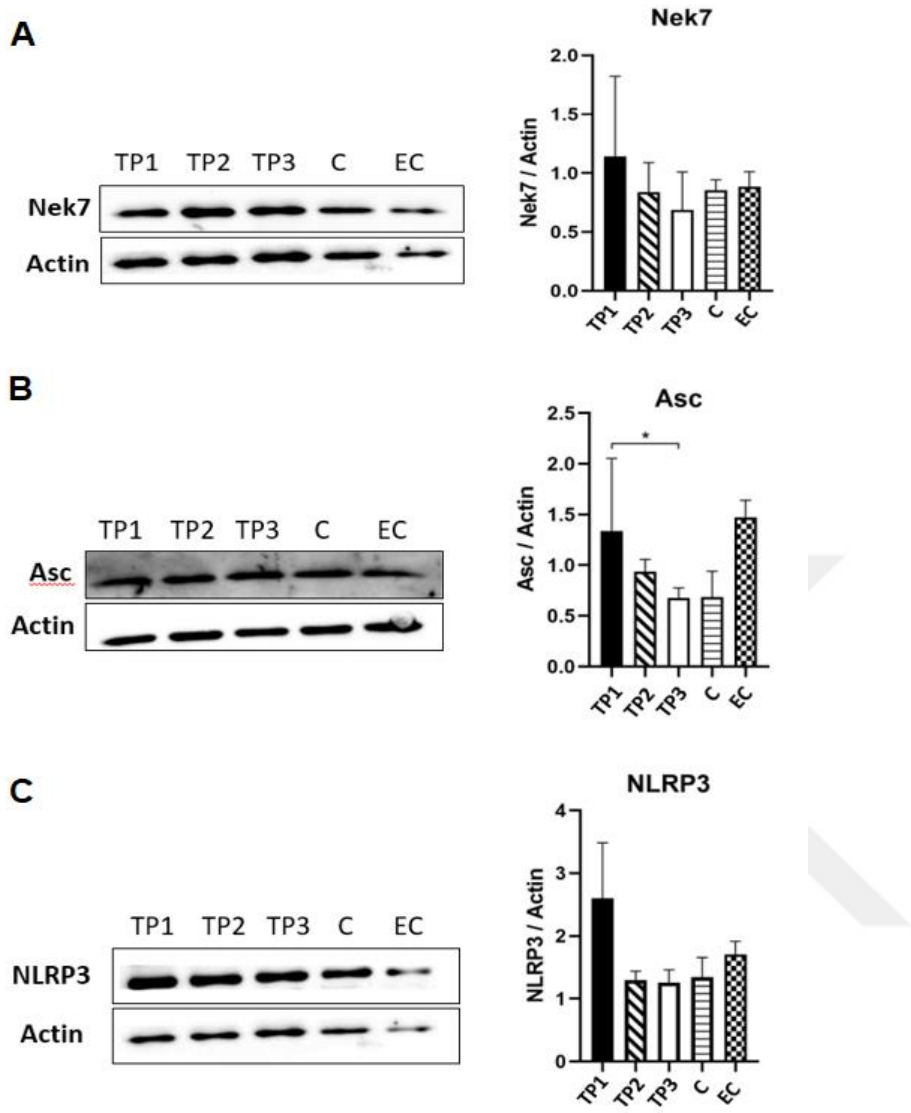

Figure 4.2 Expression levels of Nek7, Asc, NLRP3 proteins during differentiation of human primer monocytes cultured in IHA CM. The monocytes cultured with different IHA CM (TP1, TP2, TP3, C and EC respectively). The SDS-PAGE gel images represented and the relative expressions were plotted for Nek7 (A), Asc (B) and NLRP3 (C) respectively (n=3, *$p<0,05$). Unpaired t test analysis was performed to estimate p-values.

Before the activation of NLRP3 iflammasomes caspase-1 is detectable as pro-caspase1 (p45) in cell lysates. The activation of the inflammoseme results in the proteolytically cleavage of the pro-caspase1 to p20 and p10 forms. These cleaved forms of the Caspase1 later participate to the bulk form of the inflammasomes and secreted through the culture medium. During the western blot experiments with the protein samples collected from the differentiated monocytes Caspase 1 could not be observed in both pro-caspase1 and cleaved forms.

The expression levels of the NLRP3, Asc, Nek7 proteins showed no significant change during differentiation of monocytes which treated with different CM. However, expression levels of all three proteins slightly and gradually decreases from TP1 to TP2 and TP3 respectively. In the control groups expression of the inflammasome components was slightly increased in EC compare to the other control counterpart C. Also expression patterns of the three proteins in TP1 and EC showed similar changes.

4.3 NLRP3 inflammasome complex components' gene expressions during differentiation of the primer human monocytes treated with IDH mutant IHA CM

RT-qPCR analysis was performed to investigate gene expressions of the NLRP3 inflammasome complex.

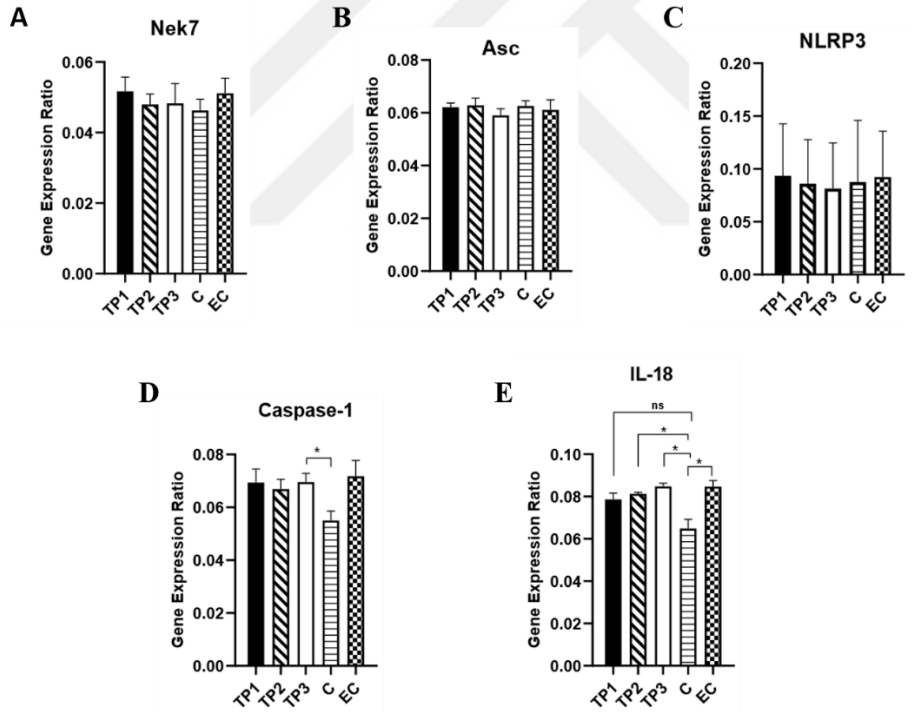

Figure 4.3 Gene expression levels of Nek7, Asc, NLRP3, Caspase-1 and IL-18 during differentiation of human primer monocytes cultured in IHA CM. The monocytes cultured with different IHA CM (TP1, TP2, TP3, C and EC respectively). The relative expressions were plotted for Nek7 (A), Asc (B), NLRP3 (C), Caspase-1(D) and IL-18 (E) respectively (n=3, $*p<0,05$). GraphPad used to calculate expression ratios by ΔCT method and unpaired t test analysis was performed to estimate p-values.

Expression levels shows no significant change during monocyte differentiation cultured in different IHA CM. Caspase-1 expression level increased in TP3 compare to the EC. During NLRP3 inflammsome activation IL-18 expression increased and secreted to the ECM. During monocyte differentiation in TP2, TP3 and EC shows significant increase compare to the C (Figure 4.3 E).

4.4 RNA sequnencing results

4.4.1 Evaluation of alignment scores and transcript variance between cases

HISAT2 results were evaluated to reveal the alignment scores via flagstat / samtools toolkit. For the conditions TP1, TP2, TP3, EC and C with the two biologic replicates aligned to the reference genome. Average read counts and aligned reads calculated (Table 4.1) and approximately 31895423,8 read obtained from the RNA-seq mapped and 30682452,2 of them aligned to the genome. Mean mapped read percentage is calculated as 96,20%.

Table 4.1: Read counts obtained from RNA-seq and the corresponding alignment scores. Read counts and aligned reads were given for two biological replicate in each condition. Results generated via HISAT2 and evaluated with flagstat tool of samtools toolkit.

Condition	Biologic Replicate	Total Read Count	Aligned Reads	Overall Aligned Reads Percentage (%)
TP1	1	30890671	29539639	95,62
	2	33728206	32357099	95,93
TP2	1	30953291	29756424	96,13
	2	31395118	30374811	96,75
TP3	1	30091749	28913452	96,08
	2	31314267	30374071	96,99
EC	1	28693030	27586859	96,14
	2	30020216	28936647	96,39
C	1	37596801	36108853	96,04
	2	34270889	32876667	95,93
Average		31895423,8	30682452,2	96,20

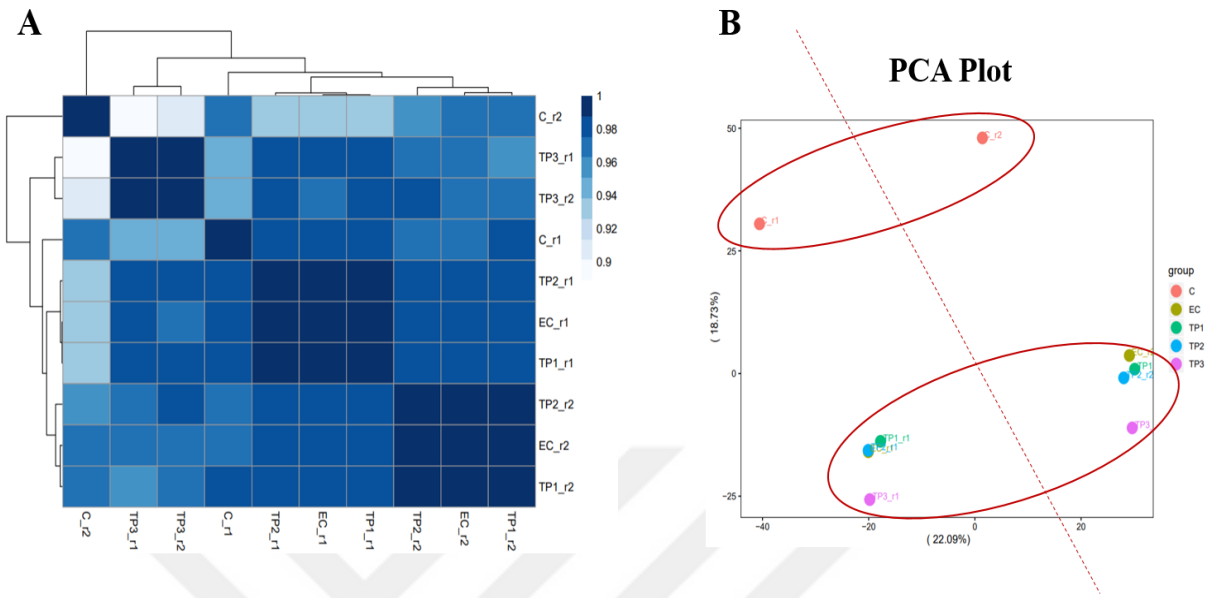

Figure 4.4 Heat map representation of correlation of clustered transcripts (A) and principal component analysis of transcript variance between two biological replicate (B) stimulated with different conditions. (A) Brighter color represents the decreased correlation, in contrast darker color represents strong correlation between conditions (TP1, TP2, TP3, EC and C). (B) PCA plot analysis of monocytes differentiated in different conditions represented with different colors and the replicates represented as _r1 and _r2 respectively.

Principle component analysis demonstrates that the two biologic replicate is significantly different from each other. It is significantly clear that the control groups (C) (Figure 4.4, C_r1 and C_r2) which are not stimulated with the IHA CM shows distinct transcriptomic profile compare to the other. While TP1, TP2 and EC segregate together, the regression of TP3 is shown clearly and this slight change consistent in the two biological replicate. Consistent with the PCA plot results. Correlation map shows the condition C is significantly different from the other counterparts. While EC, TP1 and TP2 correlated with each other, TP3 significantly different with the other time point counterparts.

4.4.2 General transcriptomic changes between cases

In the EC group; while total 10758 genes were not significantly change according to the expression levels compare to the control group, 1609 genes were up-regulated and 1568 genes were down-regulated. In the TP1 10546 genes were not significantly change, on the other hand, while 1619 genes were up-regulated, 1761 genes were down-regulated. In the TP2 group; 10566 genes were not significantly change but 1646 genes up-regulated regulated and 1716 genes down regulated. Compare to the other time point counterparts it is observed that the number of up and down regulated genes significantly increase. While 9904 genes were not significantly change, 1970 genes were up-regulated and 2020 genes down regulated.

The set of genes were filtered (FDR<0.01 and FC>1) and evaluated to understand time specific gene expressions. While 11 genes were expressed in only macrophages treated with TP1 CM, 7 and 164 genes were expressed only in TP2 and TP3 respectively. Time specific genes indicated with yellow dots on the Figure 4.5.

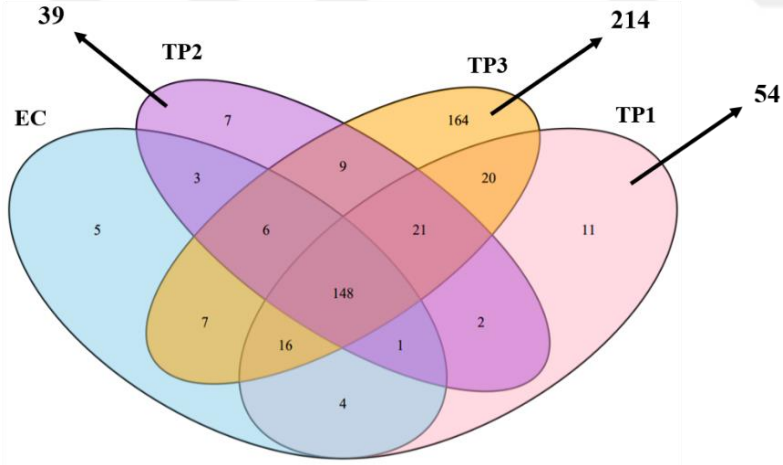

Figure 4.5 Venn diagram representing the differentially expressed genes in differentiated macrophages different conditions. Differentially expressed genes in TP1, TP2, TP3 and EC obtained via comparison with Control group (FDR<0.01, FC>1). Arrows indicate that the differentially expressed gene counts in TP1 (54), TP2 (39) and TP3 (214) compare to the genes in EC group. Common differentially expressed genes (21) in TP1, TP2 and TP3 indicated with red circle.

Differential expression results indicate that compare to the control group total 223, 197, 391, and 190 genes are differentially expressed in TP1, TP2, TP3 and EC respectively. Most of these genes are common in the EC group. These common genes extracted from the TP1, TP2 and TP3 to eliminate the AM (Astrocyte Medium), which is used as CM, doxycycline and the vector effect during differentiation of monocytes to macrophages. Then the filtered 54, 39 and 214 (for TP1, TP2, TP3 respectively) genes were used for GO analysis to exhibit enriched pathways during differentiation process (Figure 4.5). Mevalonate pathway is the most significant term enriched during TP1 and TP2, on the other hand complement activation is the most significant enriched pathway in TP3. Complement activation is commonly enriched in the three time points but it is observed that the significance of the term increased towards the TP3. Enriched pathways indicate that the overall molecular changes during monocyte differentiation directing M1 like response in each time point.

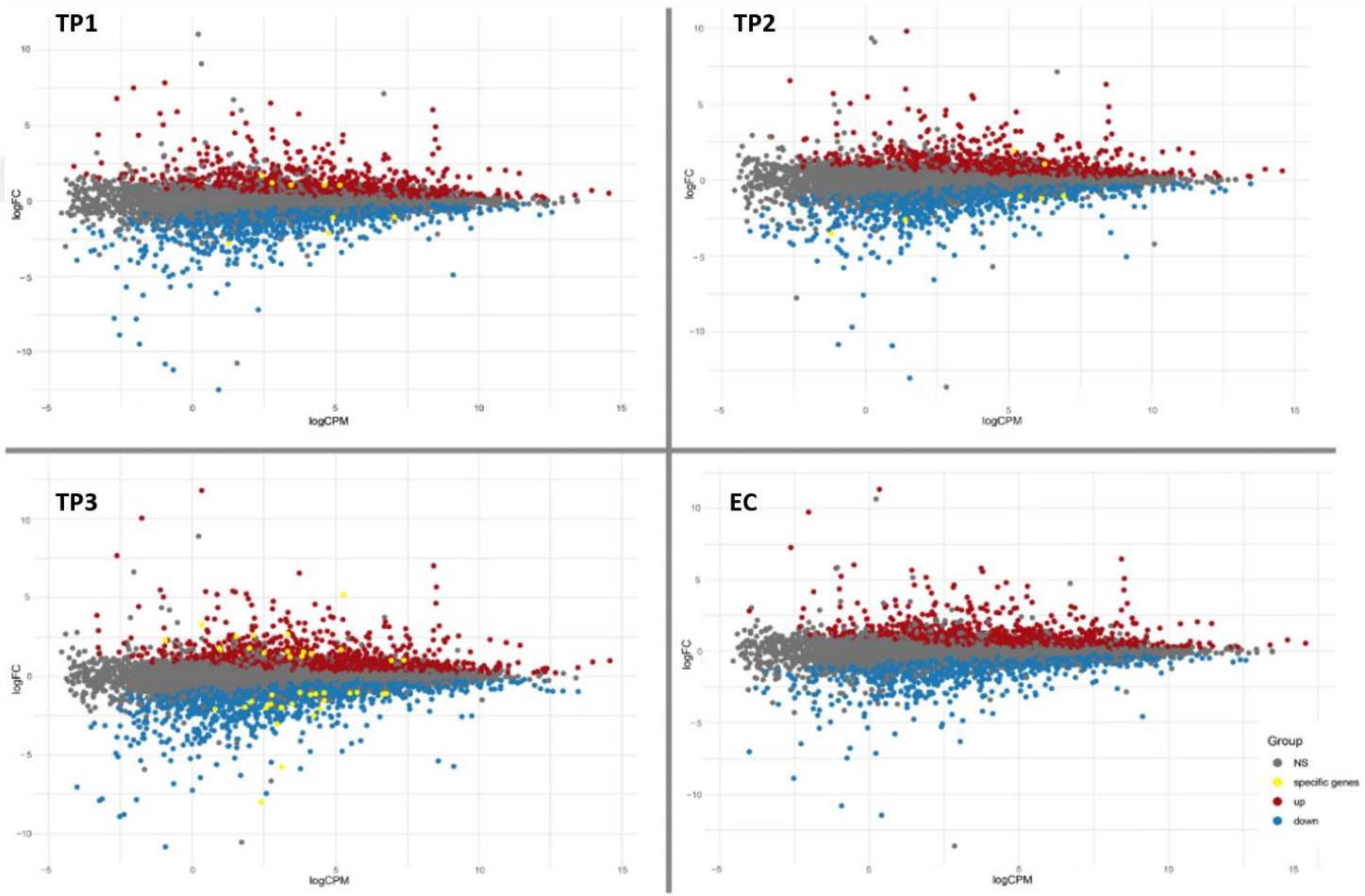

Figure 4.6 MA plot representation of up and down regulated genes in the TP1, TP2, TP3 and EC groups respectively. Filtered genes (FDR<0.01) represented as up/down regulated (red/blue), not significantly changed (NS) and yellow dots represents the time specific genes in each group.

4.4.3 Gene Ontology analysis for total differentially expressed genes and common differentially expressed genes in TP1, TP2 and TP3

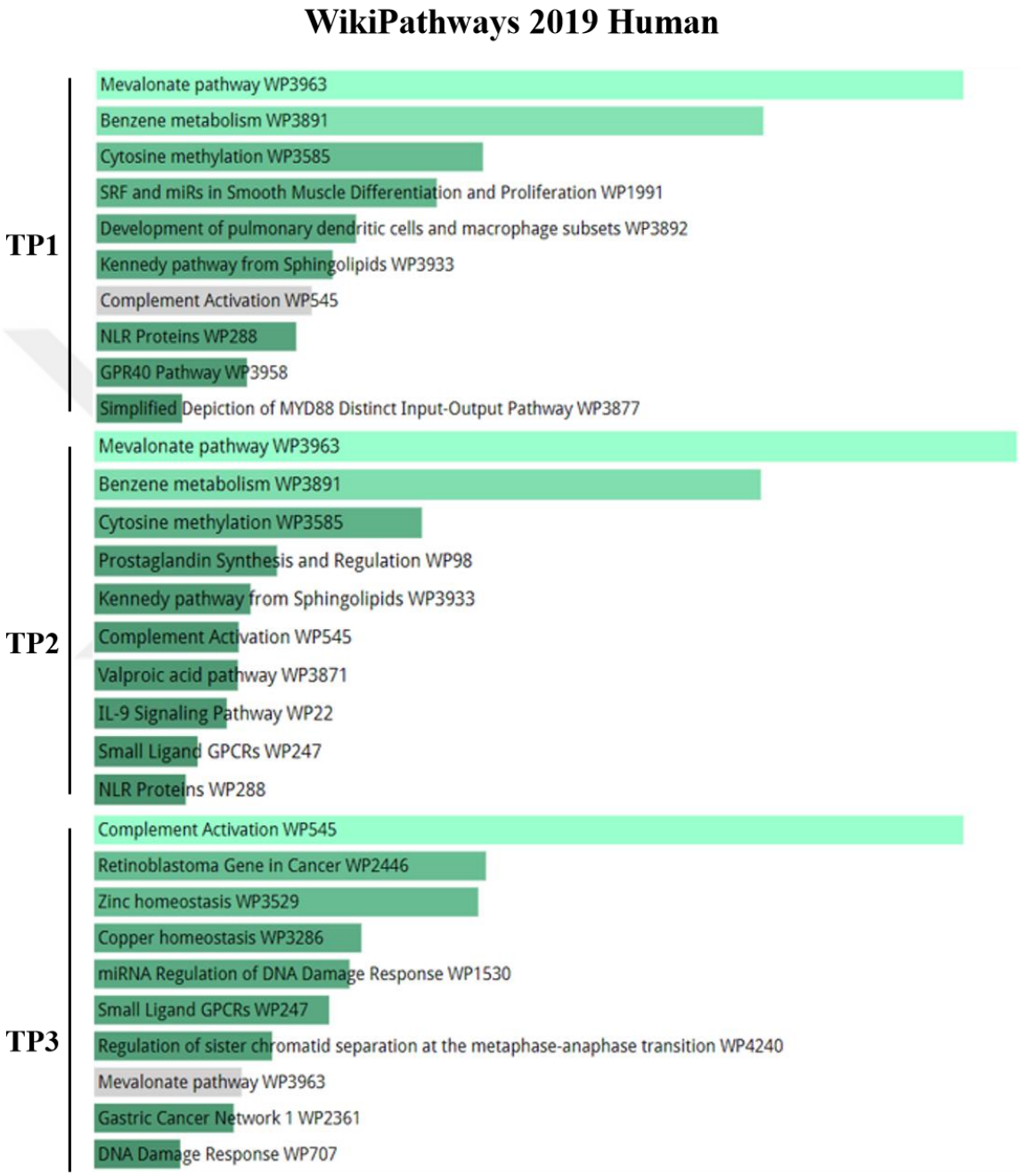

Figure 4.7 Enriched WikiPathways during differentiation of human primer monocytes cultured in IHA CM. Enriched GO terms obtained from WikiPathways (Slenter et al., 2018) a multifaceted pathway database by using Enrichr a web-based tool (https://amp.pharm.mssm.edu/Enrichr/) for GO analysis. Results ordered according to their combined z-scores and P-values. Brighter color and longer bars indicates the most significantly enriched pathways. Three different condition indicated as TP1, TP2 and TP3 respectively.

Common differentially expressed genes extracted to understand IDH1 R132H related changes in the TP1, TP2 and TP3. Most significantly differentially expressed 124 gene listed in Table 4.2 with the corresponding FC's for each time point. While expression levels of the common differentially expressed genes were similar, three genes GAL, HS3ST2, MRGPRF-AS1 were exhibit severe change in TP3.

In order to understand IDH R132H effect in the basis of transcriptomic changes total 124 gene selected to further analysis. GO analysis of these common genes indicate that p53 signaling pathway most significantly regulated GO term according to the KEGG pathway analysis. Complement and coagulation cascades seem to be enriched and negatively regulated according to GO Biological Process terms. Also Th1 and Th2 cell differentiation pathways enriched fallowing Carbohydrate digestion and absorption and Neomycin, kanamycin and gentamicin biosynthesis. ABC transports, Sphingolipid metabolism and Mineral absorption are also enriched pathways during differentiation of monocytes treated with IDH R132H mutant astrocytic CM. Steroid hormone biosynthesis is not significant according to p-value threshold but slightly enriched during treatment (Fgure 4.8).

Table 4.2: Common Differentially expressed genes in three time points compare to the EC. Seventeen genes represented with their corresponding fold changes ($FC=2^{\wedge logFC}>1$ at least in 1 TP) and filtered according to their FDR (<0.05). Red boxes indicate severe changes in TP3 compare to TP1 and TP3.

Gene. Name	TP1 - FC	P-Value	FDR	TP2 - FC	P-Value	FDR	TP3 - FC	P-Value	FDR
GAL	-2,1	0,000125664	0,007483459	-2,3	4,87144E-05	0,005065934	-4,3	1,85072E-06	0,000751598
FSCN1	-2,3	2,27675E-05	0,003292986	-2,2	3,04401E-05	0,004001724	-2,4	1,73555E-05	0,001895475
EPHB2	2,4	1,1487E-05	0,002389119	2,4	1,2143E-05	0,002685919	2,7	4,86496E-06	0,001133499
TEC	2,1	0,00016535	0,008471163	2,1	0,000159139	0,009057221	2,1	0,000159967	0,005992318
COX5B	-2,0	3,32943E-05	0,004034396	-2,1	2,68227E-05	0,003775492	-2,1	1,92584E-05	0,001987899
TDG	2,0	3,09728E-05	0,003959688	2,3	1,38529E-05	0,002699512	2,0	3,77044E-05	0,002742392
HK3	-2,2	4,1E-05	0,004263693	-2,2	4,22733E-05	0,004750627	-2,3	2,81746E-05	0,002382738
ACAT2	-2,3	1,57242E-05	0,002786328	-2,5	8,00707E-06	0,00210008	-2,6	6,00197E-06	0,001161632
C19orf38	-2,0	5,93898E-05	0,005278344	-2,0	6,30539E-05	0,005857706	-2,4	1,7076E-05	0,001888528
CFP	2,3	0,000102599	0,006840739	2,7	3,34323E-05	0,004150272	2,6	4,37414E-05	0,002973346
TLR7	2,4	0,000122382	0,007414738	2,3	0,000172043	0,009513579	2,9	3,94601E-05	0,002843051
ABCA3	2,0	0,000616119	0,017526214	2,0	0,00054222	0,017571721	2,1	0,000389593	0,009441705
ABCC5	2,1	0,000791239	0,019680477	1,9	0,002255527	0,037057012	2,1	0,000935662	0,015062349
AC008074.2	-1,9	0,00148672	0,027558975	-2,0	0,001235807	0,027291555	-2,4	0,000310331	0,008480221
AC106782.2	-1,8	0,003014753	0,041996651	-1,9	0,001593549	0,030886403	-2,1	0,000984777	0,015506071
AC110995.1	4,9	0,001496884	0,027627925	4,2	0,002648093	0,040685287	4,8	0,001568755	0,019850137
ACOT7	-1,6	0,000424534	0,01440344	-1,7	0,000173893	0,00954016	-2,0	3,69674E-05	0,002740108
ADAP1	2,0	0,002536778	0,038005	2,0	0,003069185	0,044091848	2,7	0,00036322	0,009122452
AL590666.2	-5,4	0,002221495	0,034880666	-4,9	0,002940669	0,043200531	-11,6	0,000392258	0,009473343
AMIGO1	-2,2	0,000837446	0,020366168	-1,8	0,00301436	0,043603264	-2,4	0,000471419	0,010514323
AP2A2	1,7	3,53488E-05	0,004096051	1,8	2,48995E-05	0,003614319	2,1	5,53125E-06	0,001133499
ARG2	2,5	0,001586317	0,028656383	2,1	0,003803618	0,049042437	3,4	0,000275685	0,00785619
ARHGEF35	-4,8	0,001033572	0,022645954	-5,7	0,000620698	0,018968034	-3,0	0,006289489	0,046126655
ASAP2	-2,0	0,000692422	0,018693711	-2,8	6,906E-05	0,006129628	-2,5	0,000157998	0,005963639
ATL1	-2,1	0,001416047	0,026737964	-1,9	0,003428204	0,046543472	-2,4	0,000534255	0,011296232
ATP8A1	2,1	0,000276045	0,011022038	2,0	0,000394114	0,014567572	3,1	2,46223E-05	0,002257301

BCL7A	-3,2	0,000413686	0,014283467	-2,4	0,00171041	0,031864394	-2,2	0,002935178	0,028743289
BMP1	-1,8	0,000159785	0,008452815	-1,9	9,60106E-05	0,007271238	-2,5	1,15886E-05	0,001563586
C2	1,9	4,74065E-05	0,004637666	1,9	4,17039E-05	0,004724752	2,9	2,04719E-06	0,000792432
CCNB1	-2,0	0,00107734	0,023096505	-2,4	0,000285985	0,012453738	-2,8	0,000133161	0,005522597
CCNB2	-2,0	0,002747536	0,039817377	-2,3	0,000929557	0,023968027	-3,3	0,000134498	0,00554507
CD55	1,7	0,001011931	0,022418535	2,0	0,000297658	0,012645937	2,1	0,000204841	0,006764126
CEP70	-2,0	0,003635587	0,046833152	-2,1	0,00231616	0,037617359	-2,1	0,002684917	0,027190637
CERS4	1,8	0,003063887	0,042440624	2,1	0,000753899	0,021172723	2,3	0,000357726	0,009066585
COL8A2	-2,1	8,73883E-05	0,006309614	-1,9	0,000227242	0,011013355	-1,9	0,000186927	0,006470829
CR1	-2,5	0,001597515	0,028698962	-2,5	0,001906686	0,033976562	-2,0	0,006793298	0,048604804
CRABP2	-2,6	0,000352167	0,012914346	-2,3	0,000796877	0,02181626	-2,8	0,000234409	0,007210788
CRHBP	2,9	0,003503034	0,045749555	3,0	0,002951339	0,043200531	3,9	0,001008013	0,01569679
CRTAP	1,6	7,17627E-05	0,00581403	1,7	5,88051E-05	0,005574481	2,1	4,75736E-06	0,001133499
CYP2U1	2,7	0,000974397	0,022148528	2,2	0,002910625	0,042920169	2,9	0,000676795	0,012541409
DBH-AS1	-4,7	0,001510317	0,027728936	-4,6	0,001623461	0,031290352	-4,5	0,001719608	0,021038396
DCSTAMP	-2,0	5,31655E-05	0,004947899	-1,9	9,41926E-05	0,007172538	-2,1	5,04113E-05	0,003252231
DHRS11	-1,7	0,00236978	0,036163196	-1,7	0,001892748	0,033814664	-2,3	0,000132251	0,005522597
DLGAP5	-2,5	0,001531381	0,028041775	-3,0	0,000677747	0,020009337	-5,0	7,26498E-05	0,003970096
DOK2	2,3	0,00065472	0,018030687	2,1	0,001277596	0,027686443	2,2	0,000817828	0,013930243
EMP3	1,8	0,000349719	0,012914346	2,1	7,66513E-05	0,006396026	1,8	0,00034211	0,008977959
ERVK3-1	2,1	0,001671007	0,029663038	2,0	0,002990864	0,043504901	1,9	0,00497386	0,040367349
FAM161B	2,0	0,000769999	0,019429405	1,8	0,001658566	0,031530864	1,9	0,001288799	0,017959421
FDX1	-1,8	0,000256185	0,010752842	-1,8	0,000283894	0,012401451	-2,0	7,71167E-05	0,004099052
FGD2	2,0	0,000123292	0,007430058	2,1	7,20109E-05	0,006211611	2,5	2,12495E-05	0,002108048
FGGY	-1,7	0,000516086	0,015946033	-1,7	0,000747285	0,021172723	-2,1	0,000105694	0,004851144
GGA2	1,6	3,65068E-05	0,004096051	1,6	3,00389E-05	0,003988892	2,0	3,28984E-06	0,000980523
HECTD2	2,1	0,000210399	0,009612811	1,7	0,001534619	0,030133522	1,9	0,000570579	0,011526857
HHAT	-1,9	0,001059719	0,02300922	-2,3	0,000246541	0,011519646	-2,1	0,000565244	0,011515603
HMG20B	-1,7	0,000651533	0,017990704	-2,0	0,000118163	0,007767006	-1,6	0,001298744	0,018007952
HMGB2	-3,4	5,67234E-06	0,00147107	-1,8	0,000399856	0,014677434	-2,7	2,06052E-05	0,002108048
HS3ST2	3,8	0,003617783	0,046722713	5,3	0,001210765	0,027158032	8,1	0,000382086	0,009402429

HSD11B1	-2,8	0,001163707	0,024088079	-2,5	0,002171046	0,036318751	-2,9	0,001004807	0,01569679
IL12RB1	1,9	0,002041367	0,033454566	2,0	0,001566612	0,030575262	2,8	0,000145193	0,005780742
IL2RG	-1,7	0,000498698	0,015651693	-2,0	0,000105916	0,007551585	-2,4	3,25099E-05	0,002530869
IPP	-2,0	0,001702501	0,029938728	-2,1	0,001344231	0,028029179	-2,3	0,000669938	0,012526796
ITGAE	-1,7	0,003633325	0,046833152	-1,7	0,00270329	0,041183535	-2,1	0,000404001	0,009681214
ITSN1	2,1	0,000395768	0,0139621	1,7	0,002029478	0,034794587	1,9	0,000691761	0,012700507
LANCL3	-4,5	0,000341919	0,012842688	-3,4	0,000926683	0,023957933	-5,7	0,000154	0,005943304
LDLRAD3	2,0	0,001357988	0,026226786	2,0	0,001289451	0,027686443	2,4	0,000326933	0,008768988
LILRB1	1,9	0,001164289	0,024088079	2,0	0,000699103	0,020423484	1,8	0,001920227	0,022523876
LMTK2	-1,9	0,000163779	0,008452815	-1,8	0,0002795	0,012325421	-2,2	3,63302E-05	0,002707279
MBOAT1	-1,9	0,002500596	0,037630453	-1,9	0,002844718	0,042533415	-2,1	0,001195578	0,017282553
METTL9	-1,8	0,002041097	0,033454566	-2,0	0,000836217	0,022365998	-1,7	0,003209366	0,030052942
MFSD2A	-2,2	0,000138643	0,007852008	-2,0	0,000308136	0,012817555	-1,8	0,000515545	0,011131618
MFSD6	-0,6	0,000271789	0,011022038	-1,7	0,000100865	0,007397671	-2,1	1,91173E-05	0,001987899
MND1	-5,9	0,000882108	0,020986119	-4,0	0,002816049	0,042240738	-3,8	0,003401589	0,031287886
MOB3B	-2,0	0,000258998	0,010760125	-2,0	0,000252343	0,011643699	-2,4	6,97434E-05	0,003913968
MPZL3	-2,0	0,000225558	0,00988412	-1,8	0,000755488	0,021172723	-2,1	0,000166342	0,006116872
MRGPRF-AS1	-7,5	0,003847787	0,048387386	-9,1	0,002710643	0,041236693	-19,8	0,000755238	0,013346563
MS4A6A	2,9	0,001816712	0,031254179	0,4	0,00331996	0,045677965	3,0	0,001458148	0,019222225
MT1F	-4,5	0,000431516	0,014453037	-3,8	0,00082916	0,022348824	-5,0	0,000305112	0,008411626
MT1X	-2,9	0,00281404	0,040343263	-3,5	0,001186124	0,026740003	-4,3	0,000500532	0,010932459
MYO7A	2,1	1,68404E-05	0,002793704	2,0	2,17633E-05	0,003296425	2,1	1,39448E-05	0,001719651
NEK2	-2,7	0,003157807	0,043056793	-3,5	0,001031226	0,02521077	-5,4	0,000200275	0,006757449
NLN	1,9	0,000224792	0,009881635	2,3	3,97715E-05	0,004618471	2,1	9,58635E-05	0,004654555
NOTCH1	1,7	0,000686169	0,018682889	1,7	0,000565578	0,018035082	2,2	6,77098E-05	0,003883504
NUSAP1	-1,9	0,002224906	0,034880666	-2,0	0,001511934	0,029842501	-2,9	0,000107571	0,004851144
OSBP2	-2,2	0,002744075	0,039817377	-2,6	0,000958588	0,024199132	-3,4	0,000260073	0,007613701
OTOAP1	1,9	0,001898597	0,032212478	2,4	0,000301655	0,012677678	2,5	0,000200902	0,006762251
PDE3B	-1,8	0,000108551	0,006916997	-1,8	0,000139301	0,008476666	-2,1	3,27514E-05	0,002535502
PIK3R5	1,8	0,000635818	0,017863164	1,9	0,000341353	0,013358958	2,4	6,367E-05	0,003727902
PLCD1	-2,0	0,000162762	0,008452815	-2,0	0,000201189	0,010345276	-2,1	0,000141814	0,005731822

PLEKHF1	-1,8	0,000720865	0,018882068	-2,2	0,000156765	0,008989783	-2,2	0,000133055	0,005522597
PLXNA1	1,7	0,000140334	0,007852008	1,6	0,000256744	0,011691919	2,0	2,7889E-05	0,002382738
PMAIP1	-2,3	0,00034763	0,012914346	-2,0	0,001134808	0,026422838	-2,4	0,000247247	0,007443462
RAB3IL1	1,9	8,03004E-05	0,006042913	2,0	7,26582E-05	0,006211611	2,6	8,28882E-06	0,001377854
RETREG1	-1,9	0,001801569	0,031057569	-1,9	0,001335763	0,028029179	-2,5	0,000220575	0,007001614
RGS10	2,3	0,000270257	0,011022038	1,9	0,001314175	0,027831353	2,2	0,000344216	0,008986279
RGS20	-2,1	9,59243E-05	0,006599763	-1,9	0,000187744	0,009985567	-2,5	2,61271E-05	0,002275506
RHOBTB2	-2,0	2,62265E-05	0,003514096	-2,0	3,09136E-05	0,004013877	-2,2	1,28138E-05	0,001618726
RTL5	2,1	0,00034711	0,012914346	2,4	0,000132142	0,008257382	2,3	0,000170588	0,00620666
RWDD2A	-1,8	0,001449993	0,027158131	-1,7	0,002341198	0,037716214	-2,3	0,000240169	0,007328349
SAMD4A	2,1	0,001675747	0,02970934	2,1	0,002125521	0,035901984	2,3	0,001062258	0,016116683
SAMSN1	1,9	8,28271E-05	0,006042913	1,6	0,000480196	0,016461624	2,2	2,58125E-05	0,002262246
SEC14L2	-1,8	0,002596427	0,038655141	-1,7	0,003023654	0,043617622	-3,4	3,0265E-05	0,002437823
SEMA4A	1,8	0,000772109	0,019429405	1,8	0,000564305	0,018035082	2,4	7,48173E-05	0,00400992
SLC16A7	1,6	0,001112545	0,023483822	1,5	0,003630121	0,048036397	2,1	8,51673E-05	0,004375916
SLC2A5	-2,2	0,002710581	0,039745663	-2,1	0,003581136	0,047572092	-2,6	0,001024037	0,015767905
SLC6A7	-6,1	0,000954617	0,021987755	-8,0	0,00048118	0,016461624	-6,7	0,000716428	0,012948664
SPTLC3	4,4	0,002212659	0,034879422	4,4	0,002274792	0,037075125	4,4	0,00214163	0,024060969
SSBP3	-2,0	3,83079E-05	0,004096051	-1,8	0,000126254	0,008010976	-2,2	2,11498E-05	0,002108048
ST6GALNAC4	-2,0	3,329E-05	0,004034396	-1,8	6,74042E-05	0,006029986	-2,0	2,54615E-05	0,002257301
STAC	-4,3	0,001720883	0,03001314	-4,1	0,001853597	0,03353772	-3,2	0,004928886	0,040095751
STEAP3	1,8	0,00025998	0,010760125	1,8	0,000202478	0,010373297	2,1	6,64785E-05	0,003854993
STK39	-2,2	0,000525314	0,01606769	-2,1	0,000675512	0,020008157	-1,8	0,002013905	0,023154924
TCF4	2,0	0,000191624	0,009176225	1,8	0,000467071	0,016110482	1,7	0,001075006	0,016212344
TEX2	-1,9	6,36787E-05	0,00547079	-2,0	4,02717E-05	0,004637907	-2,3	1,442E-05	0,001747329
TGM2	-2,3	2,57901E-06	0,001239259	-2,0	6,53745E-06	0,001902703	-1,9	1,1879E-05	0,001563586
TMEM86A	1,9	0,00017523	0,008815275	1,8	0,000344874	0,013395859	2,8	1,17577E-05	0,001563586
TMOD2	2,5	0,000124234	0,007430058	2,2	0,000289954	0,012470697	2,9	5,52555E-05	0,003437435
TNFSF12	1,9	0,00095778	0,022024189	2,0	0,000427435	0,015170936	2,6	8,54732E-05	0,004375916
TNFSF14	-2,1	0,000703011	0,018695528	-2,0	0,000960468	0,024202747	-2,2	0,000576683	0,011596071
TOGARAM2	-2,7	0,002008924	0,033353751	-2,7	0,002338046	0,037716214	-2,3	0,00512564	0,040820008

TPD52L1	-2,5	0,000468852	0,015088791	-2,6	0,000340174	0,013358958	-1,9	0,003193114	0,030013662
TRAF1	-1,9	0,00022298	0,009881635	-1,8	0,000425552	0,015170936	-2,1	0,000119136	0,005195293
TSC22D1	-1,7	0,003548508	0,046170362	-1,7	0,002549099	0,039627051	-2,2	0,000345984	0,008986279
WWTR1	-2,0	0,000218425	0,009850329	-1,7	0,000835163	0,022365998	-2,0	0,000154394	0,005943304
ZCCHC24	1,8	0,000369346	0,013324139	1,8	0,000320607	0,013057481	2,0	0,000124711	0,005336157

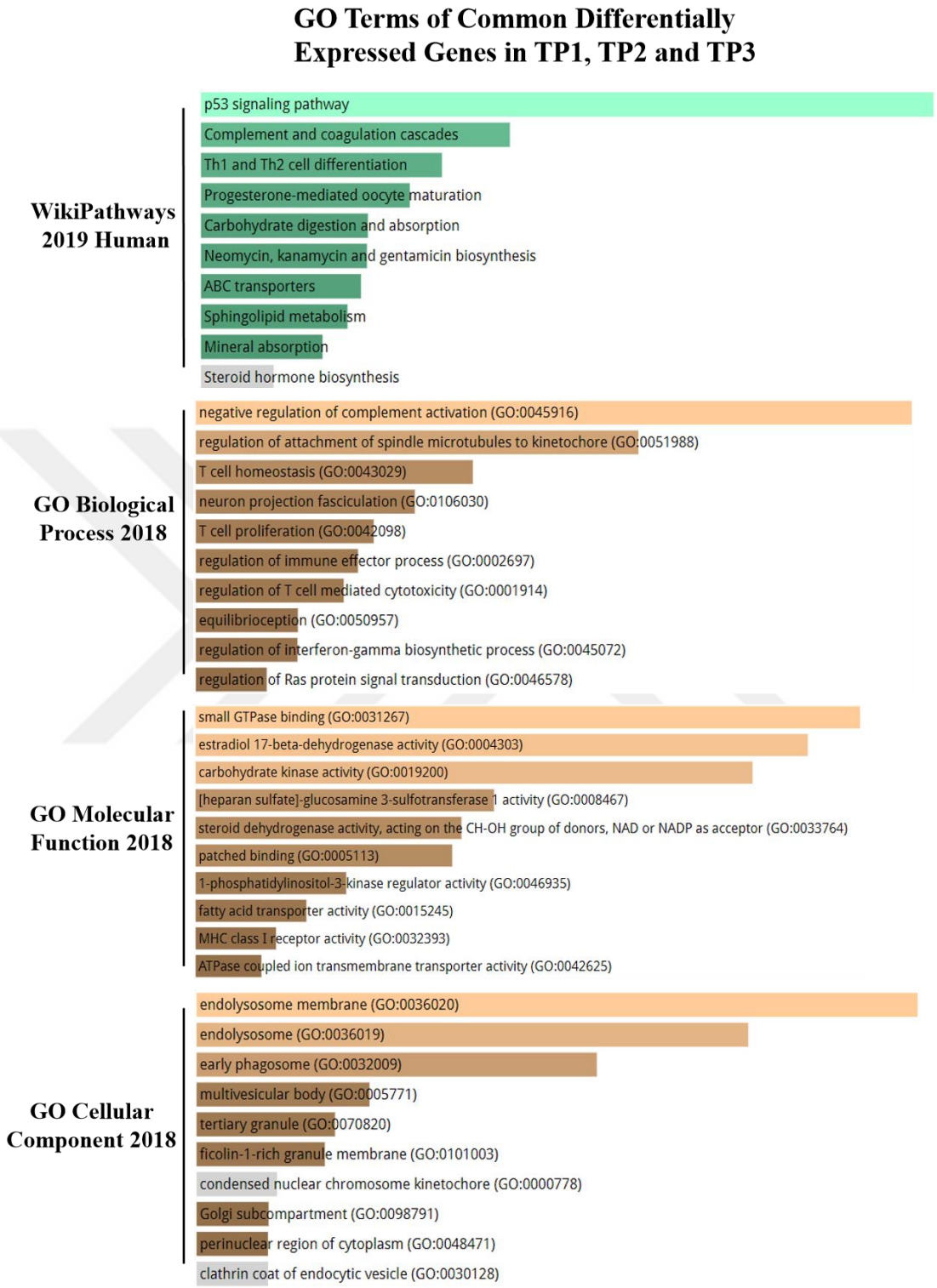

Figure 4.8 Enriched GO Terms of commonly differentially expressed genes in TP1,TP2 and TP3 during differentiation of human primer monocytes cultured in IHA CM. GO analysis for enriched pathways and corresponding molecular functions', biological processes' and cellular components' visualized by using Enrichr a web-based tool (https://amp.pharm.mssm.edu/Enrichr/). Results ordered according to their P-values. Brighter color and longer bars indicates the most significantly enriched pathways. Three different condition indicated as TP1, TP2 and TP3 respectively.

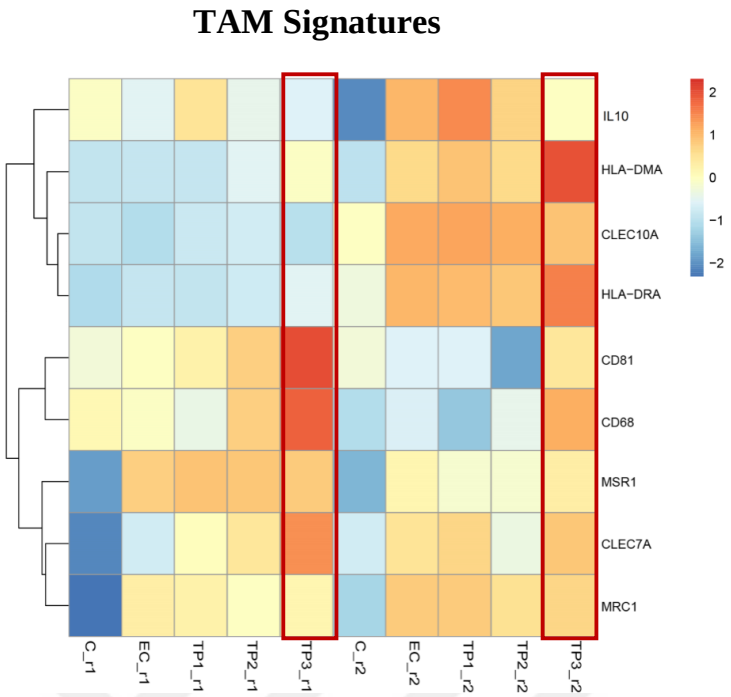

Figure 4.9 TAM signature genes represented as heat map according to TPMs of two biological replicate in TP1,TP2,TP3, EC and C. Correlation represented according to log2 and z-score values for two replicate individually.

A gene set constituted with TMA markers to plot a heat map (Figure 4.9). These data indicate that the expression levels of the TAM marker genes increase toward TP3. Two biologic replicate shows different patterns but according to their control counterparts upregulation of the TAM signatures exhibits similar pattern.

Protein association network analysis performed to common differentially expressed genes to understand protein interaction in the given genes of interest (Figure 4.10). Un-connected nodes extracted and the remaining genes shows the protein interaction correlated with each other. IDH1 gene edited to the given set of genes manually. The results show that IDH1 gene is may be correlated with the NOTCH1 gene leading cell cycle regulation (interaction predicted via text mining). Also CFP, CR1, C2 and CD55 genes are in the association and same cluster with the IDH1 gene.

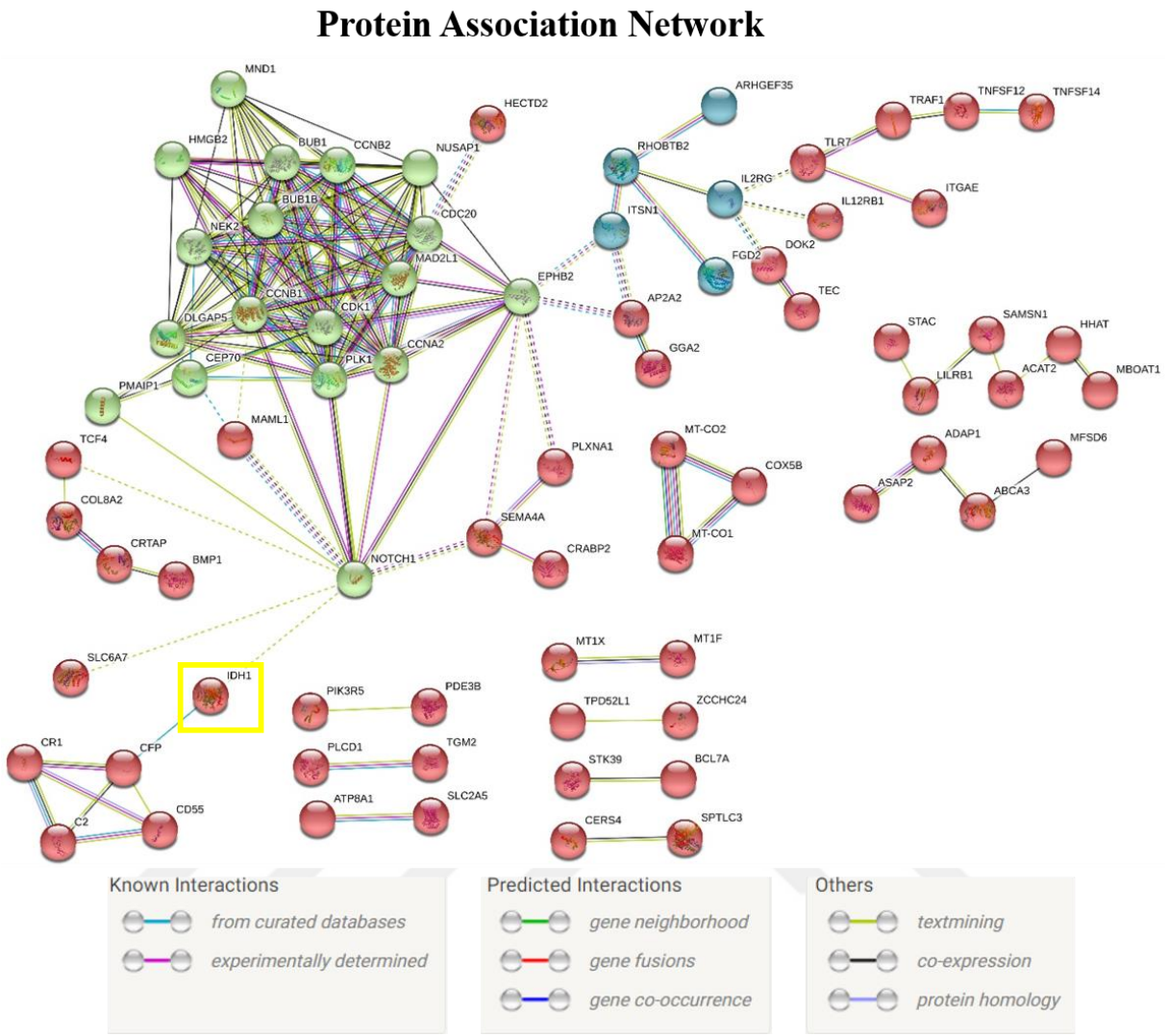

Figure 4.10 Protein association network of common differentially expressed genes in TP1,TP2 and TP3. MCL clustering applied to the given gene set and 4 different node identified. Red node includes cell cycle genes associated with the NOTCH1 gene (green node) and IDH1gene (blue node) was edited to the gene set manually. Yellow node indıcates the cytochrome c related genes.

RT-qPCR analysis was performed to M2 and M1 related marker genes (Figure 4.11 B, C). MRC1 is a type I membrane receptor which takes the glycoproteins and towards the polarization to M2 type response (Jablonski et al., 2015). We could not observe significant changes in MRC1 gene expression but it slightly increases in the CM treated monocytes during differentiation. CCL17 is another M2 related marker for macrophages associated with promoting tumorigenesis (IL-4 polarized) (Hsu et al., 2018). We observed significant increase in the CCL17 expression in TP3 compare to the control group. CCL17 expression slightly decreased in the TP2 compare to the other counterparts (non-significant). While M1 type

inflammatory response marker TNF-α gene expression significantly decrease from TP1 to TP3 compare to the control group, IRF5 expression ratios are not significantly change in CM treated macrophages and control group. TNF-α expression associated with the differentiation, cell proliferation, apoptosis and lipid metabolism (Batra et al., 2018). These increased TNF-α expression may be correlated with the enriched mevalonate pathway in the CM treated macrophages. IRF5 encodes a transcription factor leading production of IFNA and INFB and inflammatory cytokines like TNF-α and generally overexpressed in newborn macrophages (Schneider et al., 2018). We observed increased IRF expression level in each CM treated macrophages and control group. Similar expression pattern of IRF5 may be associated with the M-CSF stimulation.

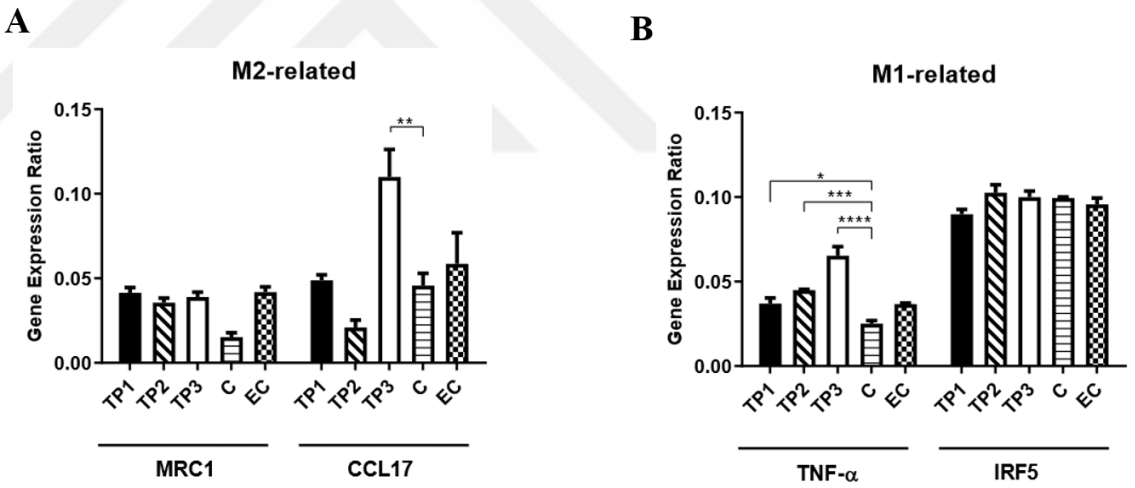

Figure 4.11 Gene expression levels of M2 related (MRC1, CCL17)(B) and M1 related (TNF-α, IRF5) during differentiation of human primer monocytes cultured in IHA CM. The monocytes cultured with different IHA CM (TP1, TP2, TP3, C and EC respectively). The relative expressions were plotted MRC1, CC17, TNF-α and IRF genes (n=3; *p<0,05, **p<0,01, ***p<0,001, ****p<0,0001). GraphPad used to calculate expression ratios by ΔCT method and 2-Way-ANOVA analysis was performed to estimate p-values.

5 DISCUSSION

TME responses plays critical role in the course of the glioma progression as well as the other cancers. In the context of IDH1 R132H mutations it is critical to understand that mutation may attribute immune regulatory role during the glioma formation associated with the prolonged survival of the IDH1 mutant glioma patients. We investigate the transcriptomic changes on monocyte differentiation during glioma initiation mimicked by the time course. The identified enriched pathways and related mechanisms must be evaluated properly to understand and reveal the potential genes and pathways will be targeted for further analysis.

Cancer cells changes their metabolic pathways to adapt metabolic stress and govern more energy to proliferate rapidly. AKT and AMPK pathways are the two major pathways that are critical for responding metabolic stress. AMPK pathway promotes energy production and balance redox reactions. Glucose uptake, fatty acid (FA) oxidation upregulated and FA synthesis limited via AMPK pathway. Also, FOXO and mTOR are the downstream effectors of the AMPK pathway. FOXO is upregulated leading maintenance of redox balance and mTOR down regulated result in inhibited protein synthesis. AMPK pathway activation towards the cell that via inhibited mTOR pathway leading autophagy activation. During metabolic stress response, AKT act as an antagonist of the AMPK pathway. mTOR signaling stimulated by the AKT pathway and stimulate glucose metabolism. Contrarily, FOXO inhibited result in reactive oxygen species (ROS) production (Zhao et al., 2017).

Down regulation of the AMPK pathway and activation of the AKT pathway lead FA synthesis, cholesterol synthesis and ROS production. Cholesterol is mainly contributing to plasma membrane and lipid rafts and important to maintenance of vitamin D and steroid hormones (Wei et al., 2016). Cholesterol production and homeostasis is important to maintain cell function. In the brain because of the BBB cholesterol homeostasis is different from the other tissues. Different cell types contribute to cholesterol synthesis, but the major cell type producing hydroxylated sterol (especially 24(S)-hydroxycholesterol) is the astrocytes in brain (Sun et al., 2016). Cholesterol is synthesized in brain mainly via mevalonate pathway (Goldstein & Brown, 1990). Upregulated mevalonate pathway is observed in the GBM patients (Geng et al., 2016; Kambach et al., 2017; Lewis et al., 2015). Beside the cancer cell intrinsic

role, cholesterol is also important for the immune cell functioning. Modulating cholesterol metabolism in $CD8^+$ T cells improves the antitumor activity and also cholesterol analog negatively regulate TCR signaling (F. Wang, Beck-García, Zorzin, Schamel, & Davis, 2016; Yang et al., 2016). Immune cells activated via mevalonate pathway in PI3K-AKT-mTOR dependent manner. Macrophages activated via mavelonate pathway is associated with the AKT pathway activation and indicates that the increased mevalonate pathway is associated with the M1 type responses (Gruenbacher & Thurnher, 2017).

It is a complex mechanism that transcellular mevalonate pathway can be activated via the lipid intermediates synthesized by another cell (Guijas et al., 2012). According to our observations astrocytic CM may induce transcellular mevalonate pathway activation. Normally, frequency of transcellular mevalonate pathway activation is low (%5) but it can be increased in combination to starvation (%30) and concentrated isoprenols in ECM can contribute to transcellular mevalonate metabolism up to %50 percentage (Onono et al., 2013). Also p53 mutations effect the transccelular The CM usage may reduce the nutrient supply needed for the normal growth and metabolism of the monocytes during differentiation. However, it is also a clue that may be astrocytic oxidized low density lipoproteins (oxLDL) contribute to the transcellular mavelonate pathway activation. Recent studies indicate that lipid scavenger receptor CD36 mediate the uptake of extracellular isoprenoids and oxLDL can increase CD36 expression (Anderson et al., 2015; Rao et al., 2019). In consistent with these observations we also observed increased CD36 expression in the astrocytic CM treated macrophages.

Another enriched pathway is the associated with the benzene metabolism and prostaglandin synthesis. Benzene is not metabolized in macrophages but its secondary metabolites in bone marrow like hydroquinone and phenol is converted to metabolites both bound to cellular macromolecules and free ones by peroxidase activity of the macrophage. These metabolites supress RNA-synthesis in dose dependent manner, different doses recorded for different metabolites. (Post, Sayder, & Kalf, 1986). Benzene was also reported to involve in alteration in resident macrophages in vivo (Laskin et al. 1989) and when bone-marrow macrophages treated with hydroquinone in vitro, they were secreting less interleukine-1 which is a cytokine involving in regulation of hematopoietic growth factors (Thomas, Reasor, &

Wierda, 1989). May be the secondary metabolites of the benzene like phenol, catechol and hydroquinone in astrocytic CM interfere with the macrophage metabolism.

Prostaglandin is a lipid compound derived from arachidonic acid. In the generation of the inflammatory reaction, prostaglandins play an important part. Krebs cycle of M1-polarized macrophages. M1 type macrophages treated with LPS/IFN-γ tend to accumulate citrate via transcriptional repression of IDH enzyme. Citrate is required for the FA synthesis and FA biosynthesis promotes the production of prostaglandins and nitric oxide which are the key drivers of inflammatory responses. Enriched prostaglandin metabolism in TP1 and TP2 may be the result of FA production via mevalonate pathway. An also there is need for further analysis to understand may be the 2-HG produced by the IDH1 R123H astrocytes interfere with the crebs-cycle in the macrophages result in the enriched prostaglandin metabolism (Mills & O'Neill, 2016). These results also suggesting that according to the total transcriptomic changes (Figure 4.7) astrocyte CM treated macrophages act like M1 type inflammatory macrophage.

Consistent with the PCA plot analysis macrophage subsets in TP3 different from the TP1, and TP2 in terms of the enriched pathways. Complement system activation observed in all tree time point case but the term is significantly enriched in TP3 compare to the other counterparts. The complement system a pathway takes a role in synaptic pruning and host defense. Innate and partially adaptive immune system responses are regulated via the complement system and it serves as a bridge between the two types of immune responses. The complement system can be activated by classically, alternatively, or with the lectin pathways. Each pathway result in the production of a protease called a C3 convertase. In order to induce host defense, membrane attack complex (MAC) pores are formed with the activated complement. Activated C3 convertase produces inflammatory mediator C3a and C3b acting as an opsonin in such mechanisms that C3b receptors expressed on phagocytes to detect the target and undergo phagocytosis (Kaminska, Czapski, Guzik, Król, & Gielniewski, 2019).The activation of the complement system towards the macrophage polarization through the M1 type. In our total transcript analysis with the differentially expressed genes for TP1, TP2 and TP3 indicating that the complement system activated which is associated with the inflammatory response (Figure 4.7). However, when we filter the genes which are thought to be associated with the IDH1 R123H mutation / 2-HG accumulation, these genes exhibit negative regulation of the complement system signals. Activated complement sytem may be associated with the

CM usage and may be the amount of 2-HG is not enough to suppress complement activation during initiation of the glioma.

It is known that IDH mutant gliomas associated with the inhibited complement system in TME. Decreased number of infiltrating immune cells in IDH mutant gliomas may be associated with the complement. There are only a few studies investigating the effect of the complement system on glioma initiation and progression. A recent study with astrocytoma grade IV patient samples reveals increased C1 inhibitor (C1-IA) expression levels associated with inactivation of C1 and this phenotype recapitulated using antibodies against C1-IA. Results suggesting that therapies targeting to inactivated complement system can trigger the host defense and expand the survival of glioma patients (Förnvik et al., 2017). The other studies about complement activation on glioma suggesting that IDH mutation/2-HG accumulation inhibits the complement activation and leading reduced host immune response with lowering $CD4^+$ and $CD8^+$ T cells infiltration (L. Zhang et al., 2018). It is also presented direct effects of complement on T cell functioning via interacting with G-protein coupled receptors (C3aR, C5aR) on antigen-presenting cells (APC) and T cells (Kwan, van der Touw, & Heeger, 2012). In consistent with the literature we identified negative regulation of complement activation as enriched pathway associated with the IDH1 R123H mutation (Figure 4.8).

In case of TP3 Retinoblastoma (Rb) associated pathways and zinc homeostasis is the other two pathways significantly enriched after treatment of astrocytic CM. Maintenance of zinc homeostasis is vital for normal cellular function as irregularities in Zn homeostasis results in several abnormalities like growth retardation, immunodeficiency, neuronal and sensory dysfunctions (Fukada, Yamasaki, Nishida, Murakami, & Hirano, 2011). Zn homeostasis involves widely in the regulation of immune system and Zn deficiency causes complex immune deficiency. In the immune system, zinc plays a significant part and impacts both inborn and adaptive immune cells. Many studies have discovered that zinc deficiency can lead to lower immune response and enhanced infection susceptibility. In addition, the amount and function of multiple immune cell types, including macrophages, neutrophils, dendritic cells, mastic cells, T cells, and B cells, have been indicated to be affected by endogenous Zn. Distinct expression patterns of importer and exporter proteins for Zn in macrophages, involves in several functions of macrophages in response to infectious stimuli. Zn homeostasis is not only involving in macrophage function, but also determines the cellular fate of macrophages. Low Zn level was shown to promote Zn-depleted-monocyte to macrophage differentiation and high Zn level

decrease viability of monocytes. Zn concentration level has different mode of action for different cell types in macrophage differentiation. Besides role in macrophage differentiation, excessive and deficient zinc level can also induce apoptosis in macrophages (Gao, Dai, Zhao, Min, & Wang, 2018). Enriched zinc homeostasis is associated with the M1 like responses during macrophage differentiation (Dierichs, Kloubert, & Rink, 2018). In TP3 case enriched pathways strongly associated with the M1 type response consistent with the other time point counterparts.

In our RT-qPCR experiments, selected macrophage marker genes show no significant change to predict polarization states of the differentiated cells in TP1, TP2 and TP3. However, in TP3 both M1 and M2 marker gene expression levels elevated (CCL17, TNF-α; Figure 4.11 B, C). Also, TAM marker gene expression levels seems to be elevated in TP3 compare to the TP1 and TP2 (Figure 4.9). Generally, TAMs tend to be act like M2 type macrophages but the M1/M2 classification is not proper for the TAMs, they are distinct subset of macrophages with transcriptionally distinct phenotypes in M1/M2 mysterious. GAMs also exhibit different transcriptomic changes compare to the other macrophage subsets (Hambardzumyan, Gutmann, & Kettenmann, 2016). According to our enriched pathway analysis all three time point cases seems to be associated M1 type response, but in TP3 elevated in TAM signatures and M1, M2 marker gene expressions can be associated with the morphological changes observed during experiments.

It is still mysterious that IDH mutation induced changes in glioma TME. There are a few studies investigating IDH mutation related to NLR dependent inflammatory mechanisms regulating TME. Astrocytoma patients exhibit elevated inflammation-related gene expression compare to the oligodendroglioma patients (Gonda et al., 2014). Also, GBM cells produce inflammatory cytokines such as IL-1β because of the activated NLRP3 inflammasome and inhibited NLRP3 activation results in an expansion of the survival rate because potentially activated NLRP3 inflammasome reduces the NK cell functioning result in the tumor invasion and proliferation (Moossavi et al., 2018). In this context, it is important to understand cell intrinsic pathways and paracrine signaling via specific cytokines which are responsible for the immune cell differentiation at the tumor site. We investigate the NLRP3 inflammasome activation in CM treated macrophages by western blot and RT-qPCR analysis. Macrophages producing IL-1β and IL-18 cytokines as an immune response to NLRP3 activation. Release of this cytokines are correlated with the poor prognosis in glioma patients (Kantono & Guo, 2017).

Also, NLRP3 activation inhibits the NK cell infiltration and NLRP3 activated APCs trigger the $CD4^+$ T cells to the tumor side (Inoue et al., 2012). In this concept our NLRP3 western blot and RT-qPCR results shows no significant change in the CM treated macrophages (Figure 4.2, Figure 4.3). However, in western blot analysis of NLRP3 inflammasome components (Asc, Nek7, NLRP3) there is a slight decrease in the TP3 compare to the other counterparts and in TP1 elevated expression levels observed. We could not observe the caspase1 cleavage and pro-caspase1 during western blot analysis. RT-qPCR result also shows no significant change in terms of the gene expression levels. However, IL-18 production significantly increase in astrocytic CM treated macrophages compare to control. These result need further investigation to reveal cleavage of caspase1 and cytokine (IL-1β and IL-18) secretion to demonstrate overall NLRP3 activation mechanism. NLR proteins seems to be enriched in the TP2 (Figure 4.7). Also we identified NEK2 (downregulated in three time point case) as a potential gene related with the IDH1 R132H glioma crosstalk with macrophages. Therefore, there is need for further analysis and specific inflammasome targeting studies to enlighten the underlying mechanisms and crosstalk in specific cell types.

Beside the overall changes exhibited by the differentiated monocytes with astrocytic CM, we identified a subset of genes potentially related with the IDH R132H mutation role in crosstalk during monocyte differentiation exposed to IDH1 mutant astrocytic CM. P53 signaling pathway is the most significantly enriched pathway during macrophage differentiation following complement and coagulation cascade, Th1 and Th2 cell differentiation and progesterone-mediated oocyte maturation (Figure 4.8). P53 is a transcription factor for regulation of the expression of genes involving in apoptosis, cell cycle arrest, metabolism and DNA repair (Vazquez, Bond, Levine, & Bond, 2008). P53 regulates wide range of cellular pathways as it upregulates genes involving in cell cycle arrest, vesicle transport and activation in immune signalling, but it downregulates cell proliferation and ECM. Because of these function it is main regulator of cancer pathology. While inflammation is an important factor of cancer predisposition; the exact role of p53 in inflammation is not very well understood. It was shown that $p53^{-/-}$ mice showed increased pro-inflammatory cytokine secretion in response to LPS. Also in humans it was reported that p53 upregulates Toll-like receptor family and therefore promotes TLR-dependent pro-inflammatory cytokine formation (Shatz, Menendez, & Resnick, 2012). It was also shown that p53 supresses M2 macrophage polarization. Nutlin-3a reported to activate p53 and destabilizes p53-MDM2 complex in IL-4 treated macrophages and

causes downregulation of M2 marker genes. On the other hand, phosphorylation of Akt provides MDM2 activation and p53 inactivation; therefor promotes M2 polarization of macrophages (L. Li et al., 2015). On the other hand, in TME p53 signalling can be activated via a paracrine signals facilitating IL-6 expression. P53 may associated with the senescence together with the NF-κB which are cytokine/chemokine gene regulators in TAMs. Thus, signaling can be promoting tumor formation via secreted cytokines and chemokines like IL-6 and CXCL1 (Lowe et al., 2014). In this study enriched p53 signaling pathway identified as a potential result of IDH mutation induced changes during monocyte differentiation. Glioma cell intrinsic IDH mutations may be contribute to the macrophage functioning through tumor promoting phenotype. The cell viability and cell cycle asrrest targeting studies needed to understand p53 singnaling activation on monocytes in association with IDH R132H mutation derived signals in tumor initiating cells.

The enriched Th1 and Th2 cell differentiation pathway, and the corresponding GO biological process terms T cell homeostasis, T cell proliferation and T cell mediated cytotoxicity. Macrophages crosstalk with T cells in order to bring about T cell activation and functioning. In TME, Th cells are key regulators of immune response through antigen-specific effector cells activation and recruitment such as macrophages and mast cells. Th1 and Th2 are the predominant subtypes. Th activation governs via APC or directly by MHC II expressing tumor cells. Th1 cells characterized by production of IFNγ and the Th2 cells producing IL4, IL5 and IL13 (Amsen, Spilianakis, & Flavell, 2009). In a recent study, Schumacher T at al., identify IDH R132H mutation specific $CD4^+$ T cell response around the tumor side. They screen IDH R132H mutant and wild type patients and detect IDH1(R132H)-specific IFN-c-producing T cells (Th1) in 4 of 24 IDH R132H mutant glioma patient (Schumacher et al., 2014). Enriched Th1 and Th2 differentiation pathway and the cytotoxic T cell signatures associated with the antigen presenting activity of the differentiated monocytes in IDH1 R132H mutant astrocytic CM.

Another enriched pathway potentially associated with the IDH1 R132H mutation is ABC transporters. The ABC transporter proteins are localized on membranes of most cells regulating active transport of endo- and xenobiotics. ABC proteins role in TME in cross talking with cancer cells. The transportation of molecules into the TME, such as signaling lipids with established roles in tumor biology and effects the immune ABC transporter substrates (Fletcher, Williams, Henderson, Norris, & Haber, 2016). In a recent study Chen et al. demonstrate that

ABCG2 a member of ABC transporter family expressed only in glioma stem cell, but not in the normal astrocytes (L. Chen et al., 2017). ABCC5 major ABC family in astrocytic tumors (Bronger et al., 2005). In consistent with the literature we observe increase expression level in ABCC5. However, we have little about ABCC5 function in macrophages. The other elevated ABC transport family is ABCA3 which also overexpressed in glioma stem cells. These observations are important to evaluate crosstalk between macrophages and glioma initiation. It is important to understand full mechanisms and there is still need for functional studies to discover new targets fueling tumor initiation. In the light of this study we identified potential mode of action of IDH mutant glioma crosstalk with the infiltrating monocytes and induced changes during macrophage differentiation.

6 CONCLUSION AND FUTURE DIRECTIONS

In this thesis study the effects of IDH1 R123H mutation on monocyte differentiation investigated during early stages of glioma initiation. Potential mechanisms evaluated with potential gene set of interest though to be associated IDH1 mutation induced regulations and interactions over monocyte derived macrophages. We identified potential associated pathways during monocyte differentiation treated with IDH mutant astrocytic CM. We try to mimic glioma initiation with time course dependent experimental design to catch time specific changes and common transcriptomic changes in response to IDH1 mutation. We only observe slight change in TP3 compare to the TP1, TP2 and EC. Also RT-qPCR analysis for macrophage specific markers did not show any predictory results in terms of the polarization states of the CM treated macrophages. Overall transcriptomic changes are strongly associated with the M1 like response but the further analysis needed to understand phenotype of the CM treated macrophages. It is also observed that EC group have similar transcriptomic changes with the TP1, TP2 and slightly TP3. These may be strongly associated with the CM usage. Co-culture methods with different cell type can be more useful to understand direct interaction of two cell types. Also, stimulation with specific cytokines addition to 2-HG is another way to reveal 2-HG dependent regulation of macrophage differentiation. However, in this thesis study we try to understand two distinct differentiation step; monocyte differentiation and glioma initiation. Also primer monocytes obtained from different donors shows different transcriptomic profiles in the same condition. The number of the replicates can be elevated to reduce the varience.

All in all, predicted mechanisms should be elegantly evaluated and further analysis needed to understand full processes. It is a preliminary study to enlighten the paths correlated with the IDH1 R132H induced regulatory mechanism in the myeloid cell precursor.

7 REFERENCES

Allavena, P., Sica, A., Garlanda, C., & Mantovani, A. (2008). The Yin-Yang of tumor-associated macrophages in neoplastic progression and immune surveillance. *Immunological Reviews*, *222*(1), 155–161. https://doi.org/10.1111/j.1600-065X.2008.00607.x

Amankulor, N. M., Kim, Y., Arora, S., Kargl, J., Szulzewsky, F., Hanke, M., … Holland, E. C. (2017). Mutant IDH1 regulates the tumor-associated immune system in gliomas. *Genes & Development*, *31*(8), 774–786. https://doi.org/10.1101/gad.294991.116

Amsen, D., Spilianakis, C. G., & Flavell, R. A. (2009). How are T(H)1 and T(H)2 effector cells made? *Current Opinion in Immunology*, *21*(2), 153–160. https://doi.org/10.1016/j.coi.2009.03.010

Anderson, C. M., Kazantzis, M., Wang, J., Venkatraman, S., Goncalves, R. L. S., Quinlan, C. L., … Stahl, A. (2015). Dependence of Brown Adipose Tissue Function on CD36-Mediated Coenzyme Q Uptake. *Cell Reports*, *10*(4), 505–515. https://doi.org/10.1016/J.CELREP.2014.12.048

Arita, H., Yamasaki, K., Matsushita, Y., Nakamura, T., Shimokawa, A., Takami, H., … Ichimura, K. (2016). A combination of TERT promoter mutation and MGMT methylation status predicts clinically relevant subgroups of newly diagnosed glioblastomas. *Acta Neuropathologica Communications*, *4*(1), 79. https://doi.org/10.1186/s40478-016-0351-2

Attolini, C. S.-O., Cheng, Y.-K., Beroukhim, R., Getz, G., Abdel-Wahab, O., Levine, R. L., … Michor, F. (2010). A mathematical framework to determine the temporal sequence of somatic genetic events in cancer. *Proceedings of the National Academy of Sciences*, *107*(41), 17604–17609. https://doi.org/10.1073/pnas.1009117107

Awad, F., Assrawi, E., Jumeau, C., Georgin-Lavialle, S., Cobret, L., Duquesnoy, P., … Karabina, S. A. (2017). Impact of human monocyte and macrophage polarization on NLR expression and NLRP3 inflammasome activation. *PLoS ONE*, *12*(4). https://doi.org/10.1371/journal.pone.0175336

Badie, B., Bartley, B., & Schartner, J. (2002). Differential expression of MHC class II and B7 costimulatory molecules by microglia in rodent gliomas. *Journal of Neuroimmunology*, *133*(1–2), 39–45. https://doi.org/10.1016/S0165-5728(02)00350-8

Balvers, R. K., Kleijn, A., Kloezeman, J. J., French, P. J., Kremer, A., van den Bent, M. J., … Lamfers, M. L. M. (2013). Serum-free culture success of glial tumors is related to specific molecular profiles and expression of extracellular matrix–associated gene modules. *Neuro-Oncology*, *15*(12), 1684–1695. https://doi.org/10.1093/neuonc/not116

Bardella, C., Al-Dalahmah, O., Krell, D., Brazauskas, P., Al-Qahtani, K., Tomkova, M., … Tomlinson, I. (2016a). Expression of Idh1R132H in the Murine Subventricular Zone Stem Cell Niche Recapitulates Features of Early Gliomagenesis. *Cancer Cell*, *30*(4), 578–594. https://doi.org/10.1016/j.ccell.2016.08.017

Bardella, C., Al-Dalahmah, O., Krell, D., Brazauskas, P., Al-Qahtani, K., Tomkova, M., … Tomlinson, I. (2016b). Expression of Idh1R132H in the Murine Subventricular Zone Stem Cell Niche Recapitulates Features of Early Gliomagenesis. *Cancer Cell*, *30*(4), 578–594.

https://doi.org/10.1016/j.ccell.2016.08.017

Batra, R., Suh, M. K., Carson, J. S., Dale, M. A., Meisinger, T. M., Fitzgerald, M., … Baxter, B. T. (2018). IL-1β (Interleukin-1β) and TNF-α (Tumor Necrosis Factor-α) Impact Abdominal Aortic Aneurysm Formation by Differential Effects on Macrophage Polarization. *Arteriosclerosis, Thrombosis, and Vascular Biology*, *38*(2), 457–463. https://doi.org/10.1161/ATVBAHA.117.310333

Berghoff, A. S., Kiesel, B., Widhalm, G., Wilhelm, D., Rajky, O., Kurscheid, S., … Preusser, M. (2017). Correlation of immune phenotype with IDH mutation in diffuse glioma. *Neuro-Oncology*, *19*(11), 1460–1468. https://doi.org/10.1093/neuonc/nox054

Bolger, A. M., Lohse, M., & Usadel, B. (2014). Trimmomatic: a flexible trimmer for Illumina sequence data. *Bioinformatics*, *30*(15), 2114–2120. https://doi.org/10.1093/bioinformatics/btu170

Boussiotis, V. A., & Charest, A. (2018). Immunotherapies for malignant glioma. *Oncogene*, *37*(9), 1121–1141. https://doi.org/10.1038/s41388-017-0024-z

Bowman, R. L., Klemm, F., Akkari, L., Pyonteck, S. M., Sevenich, L., Quail, D. F., … Joyce, J. A. (2016). Macrophage Ontogeny Underlies Differences in Tumor-Specific Education in Brain Malignancies. *Cell Reports*, *17*(9), 2445–2459. https://doi.org/10.1016/J.CELREP.2016.10.052

Brandenburg, S., Müller, A., Turkowski, K., Radev, Y. T., Rot, S., Schmidt, C., … Vajkoczy, P. (2016). Resident microglia rather than peripheral macrophages promote vascularization in brain tumors and are source of alternative pro-angiogenic factors. *Acta Neuropathologica*, *131*(3), 365–378. https://doi.org/10.1007/s00401-015-1529-6

Brantley, E. C., & Benveniste, E. N. (2008). Signal Transducer and Activator of Transcription-3: A Molecular Hub for Signaling Pathways in Gliomas. *Molecular Cancer Research*, *6*(5), 675–684. https://doi.org/10.1158/1541-7786.MCR-07-2180

Bronger, H., König, J., Kopplow, K., Steiner, H.-H., Ahmadi, R., Herold-Mende, C., … Nies, A. T. (2005). ABCC Drug Efflux Pumps and Organic Anion Uptake Transporters in Human Gliomas and the Blood-Tumor Barrier. *Cancer Research*, *65*(24), 11419–11428. https://doi.org/10.1158/0008-5472.CAN-05-1271

Bunse, L., Pusch, S., Bunse, T., Sahm, F., Sanghvi, K., Friedrich, M., … Platten, M. (2018). Suppression of antitumor T cell immunity by the oncometabolite (R)-2-hydroxyglutarate. *Nature Medicine*, *24*(8), 1192–1203. https://doi.org/10.1038/s41591-018-0095-6

Burroughs, S. K., Kaluz, S., Wang, D., Wang, K., Van Meir, E. G., & Wang, B. (2013). Hypoxia inducible factor pathway inhibitors as anticancer therapeutics. *Future Medicinal Chemistry*, *5*(5), 553–572. https://doi.org/10.4155/fmc.13.17

Cancer Genome Atlas Research Network, Brat, D. J., Verhaak, R. G. W., Aldape, K. D., Yung, W. K. A., Salama, S. R., … Zhang, J. (2015). Comprehensive, Integrative Genomic Analysis of Diffuse Lower-Grade Gliomas. *New England Journal of Medicine*, *372*(26), 2481–2498. https://doi.org/10.1056/NEJMoa1402121

Ceccarelli, M., Barthel, F. P., Malta, T. M., Sabedot, T. S., Salama, S. R., Murray, B. A., … Verhaak, R. G. W. (2016). Molecular Profiling Reveals Biologically Discrete Subsets and

Pathways of Progression in Diffuse Glioma. *Cell*, *164*(3), 550–563. https://doi.org/10.1016/j.cell.2015.12.028

Chen, E. Y., Tan, C. M., Kou, Y., Duan, Q., Wang, Z., Meirelles, G., … Ma'ayan, A. (2013). Enrichr: interactive and collaborative HTML5 gene list enrichment analysis tool. *BMC Bioinformatics*, *14*(1), 128. https://doi.org/10.1186/1471-2105-14-128

Chen, L., Shi, L., Wang, W., Zhou, Y., Chen, L., Shi, L., … Zhou, Y. (2017). ABCG2 downregulation in glioma stem cells enhances the therapeutic efficacy of demethoxycurcumin. *Oncotarget*, *8*(26), 43237–43247. https://doi.org/10.18632/oncotarget.18018

Chen, X., Zhang, L., Zhang, I. Y., Liang, J., Wang, H., Ouyang, M., … Badie, B. (2014). RAGE Expression in Tumor-Associated Macrophages Promotes Angiogenesis in Glioma. *Cancer Research*, *74*(24), 7285–7297. https://doi.org/10.1158/0008-5472.CAN-14-1240

Choi, B. D., & Curry, W. T. (2017). IDH mutational status and the immune system in gliomas: a tale of two tumors? *Translational Cancer Research*, *6*(Suppl 7), S1253–S1256. https://doi.org/10.21037/tcr.2017.09.37

Chow, M. T., Sceneay, J., Paget, C., Wong, C. S. F., Duret, H., Tschopp, J., … Smyth, M. J. (2012). NLRP3 Suppresses NK Cell-Mediated Responses to Carcinogen-Induced Tumors and Metastases. *Cancer Research*, *72*(22), 5721–5732. https://doi.org/10.1158/0008-5472.CAN-12-0509

Condamine, T., Mastio, J., & Gabrilovich, D. I. (2015). Transcriptional regulation of myeloid-derived suppressor cells. *Journal of Leukocyte Biology*, *98*(6), 913–922. https://doi.org/10.1189/jlb.4RI0515-204R

Daley, D., Mani, V. R., Mohan, N., Akkad, N., Pandian, G. S. D. B., Savadkar, S., … Miller, G. (2017). NLRP3 signaling drives macrophage-induced adaptive immune suppression in pancreatic carcinoma. *The Journal of Experimental Medicine*, *214*(6), 1711–1724. https://doi.org/10.1084/jem.20161707

Dang, L., White, D. W., Gross, S., Bennett, B. D., Bittinger, M. A., Driggers, E. M., … Su, S. M. (2009). Cancer-associated IDH1 mutations produce 2-hydroxyglutarate. *Nature*, *462*(7274), 739–744. https://doi.org/10.1038/nature08617

Dang, L., Yen, K., & Attar, E. C. (2016). IDH mutations in cancer and progress toward development of targeted therapeutics. *Annals of Oncology*, *27*(4), 599–608. https://doi.org/10.1093/annonc/mdw013

de la Iglesia, N., Puram, S. V, & Bonni, A. (2009). STAT3 regulation of glioblastoma pathogenesis. *Current Molecular Medicine*, *9*(5), 580–590. Retrieved from http://www.ncbi.nlm.nih.gov/pubmed/19601808

de Weille, J. (2014). On the Genesis of Neuroblastoma and Glioma. *International Journal of Brain Science*, *2014*, 1–14. https://doi.org/10.1155/2014/217503

Dierichs, L., Kloubert, V., & Rink, L. (2018). Cellular zinc homeostasis modulates polarization of THP-1-derived macrophages. *European Journal of Nutrition*, *57*(6), 2161–2169. https://doi.org/10.1007/s00394-017-1491-2

Eckel-Passow, J. E., Lachance, D. H., Molinaro, A. M., Walsh, K. M., Decker, P. A., Sicotte,

H., … Jenkins, R. B. (2015). Glioma Groups Based on 1p/19q, IDH , and TERT Promoter Mutations in Tumors. *New England Journal of Medicine*, *372*(26), 2499–2508. https://doi.org/10.1056/NEJMoa1407279

Fack, F., Tardito, S., Hochart, G., Oudin, A., Zheng, L., Fritah, S., … Niclou, S. P. (2017). Altered metabolic landscape in IDH-mutant gliomas affects phospholipid, energy, and oxidative stress pathways. *EMBO Molecular Medicine*, *9*(12), 1681–1695. https://doi.org/10.15252/emmm.201707729

Fletcher, J. I., Williams, R. T., Henderson, M. J., Norris, M. D., & Haber, M. (2016). ABC transporters as mediators of drug resistance and contributors to cancer cell biology. *Drug Resistance Updates*, *26*, 1–9. https://doi.org/10.1016/J.DRUP.2016.03.001

Förnvik, K., Maddahi, A., Persson, O., Osther, K., Salford, L. G., & Nittby Redebrandt, H. (2017). C1-inactivator is upregulated in glioblastoma. *PloS One*, *12*(9), e0183086. https://doi.org/10.1371/journal.pone.0183086

Frankish, A., Diekhans, M., Ferreira, A.-M., Johnson, R., Jungreis, I., Loveland, J., … Flicek, P. (2019). GENCODE reference annotation for the human and mouse genomes. *Nucleic Acids Research*, *47*(D1), D766–D773. https://doi.org/10.1093/nar/gky955

Frezza, C., Tennant, D. A., & Gottlieb, E. (2010). IDH1 Mutations in Gliomas: When an Enzyme Loses Its Grip. *Cancer Cell*, *17*(1), 7–9. https://doi.org/10.1016/j.ccr.2009.12.031

Fukada, T., Yamasaki, S., Nishida, K., Murakami, M., & Hirano, T. (2011). Zinc homeostasis and signaling in health and diseases. *Journal of Biological Inorganic Chemistry*. https://doi.org/10.1007/s00775-011-0797-4

Gao, H., Dai, W., Zhao, L., Min, J., & Wang, F. (2018). The Role of Zinc and Zinc Homeostasis in Macrophage Function. *Journal of Immunology Research*, *2018*, 1–11. https://doi.org/10.1155/2018/6872621

Geng, F., Cheng, X., Wu, X., Yoo, J. Y., Cheng, C., Guo, J. Y., … Guo, D. (2016). Inhibition of SOAT1 Suppresses Glioblastoma Growth via Blocking SREBP-1-Mediated Lipogenesis. *Clinical Cancer Research*, *22*(21), 5337–5348. https://doi.org/10.1158/1078-0432.CCR-15-2973

Gieryng, A., Pszczolkowska, D., Walentynowicz, K. A., Rajan, W. D., & Kaminska, B. (2017). Immune microenvironment of gliomas. *Laboratory Investigation*, *97*(5), 498–518. https://doi.org/10.1038/labinvest.2017.19

Goldstein, J. L., & Brown, M. S. (1990). Regulation of the mevalonate pathway. *Nature*, *343*(6257), 425–430. https://doi.org/10.1038/343425a0

Gonda, D. D., Cheung, V. J., Muller, K. A., Goyal, A., Carter, B. S., & Chen, C. C. (2014). The Cancer Genome Atlas expression profiles of low-grade gliomas. *Neurosurgical Focus*, *36*(4), E23. Retrieved from http://www.ncbi.nlm.nih.gov/pubmed/24812719

Goodenberger, M. L., & Jenkins, R. B. (2012). Genetics of adult glioma. *Cancer Genetics*, *205*(12), 613–621. https://doi.org/10.1016/j.cancergen.2012.10.009

Gruenbacher, G., & Thurnher, M. (2017). Mevalonate metabolism governs cancer immune surveillance. *Oncoimmunology*, *6*(10), e1342917. https://doi.org/10.1080/2162402X.2017.1342917

Guijas, C., Pérez-Chacón, G., Astudillo, A. M., Rubio, J. M., Gil-de-Gómez, L., Balboa, M. A., & Balsinde, J. (2012). Simultaneous activation of p38 and JNK by arachidonic acid stimulates the cytosolic phospholipase A2-dependent synthesis of lipid droplets in human monocytes. *Journal of Lipid Research*, *53*(11), 2343–2354. https://doi.org/10.1194/jlr.M028423

Gupta, A., & Dwivedi, T. (2017). A Simplified Overview of World Health Organization Classification Update of Central Nervous System Tumors 2016. *Journal of Neurosciences in Rural Practice*, *8*(4), 629–641. https://doi.org/10.4103/jnrp.jnrp_168_17

Gustin, A., Kirchmeyer, M., Koncina, E., Felten, P., Losciuto, S., Heurtaux, T., … Dostert, C. (2015). NLRP3 Inflammasome Is Expressed and Functional in Mouse Brain Microglia but Not in Astrocytes. *PLOS ONE*, *10*(6), e0130624. https://doi.org/10.1371/journal.pone.0130624

Hambardzumyan, D., Gutmann, D. H., & Kettenmann, H. (2016). The role of microglia and macrophages in glioma maintenance and progression. *Nature Neuroscience*, *19*(1), 20–27. https://doi.org/10.1038/nn.4185

Hamilton, J. A. (2008). Colony-stimulating factors in inflammation and autoimmunity. *Nature Reviews Immunology*, *8*(7), 533–544. https://doi.org/10.1038/nri2356

Hansen, L. J., Diplas, B. H., Becher, O., & Yan, H. (2016). Genetics of glioma. In J. H. Sampson (Ed.), *The Duke Glioma Handbook* (pp. 1–23). Cambridge: Cambridge University Press. https://doi.org/10.1017/CBO9781107588721.002

He, Q., Fu, Y., Tian, D., & Yan, W. (2018). The contrasting roles of inflammasomes in cancer. *American Journal of Cancer Research*, *8*(4), 566–583. Retrieved from http://www.ncbi.nlm.nih.gov/pubmed/29736304

Hesketh, M., Sahin, K. B., West, Z. E., & Murray, R. Z. (2017). Macrophage phenotypes regulate scar formation and chronic wound healing. *International Journal of Molecular Sciences*. https://doi.org/10.3390/ijms18071545

Hsu, A. T., Lupancu, T. J., Lee, M.-C., Fleetwood, A. J., Cook, A. D., Hamilton, J. A., & Achuthan, A. (2018). Epigenetic and transcriptional regulation of IL4-induced CCL17 production in human monocytes and murine macrophages. *Journal of Biological Chemistry*, *293*(29), 11415–11423. https://doi.org/10.1074/JBC.RA118.002416

Hu, M., Du, J., Cui, L., Huang, T., Guo, X., Zhao, Y., … Song, J. (2016). IL-10 and PRKDC polymorphisms are associated with glioma patient survival. *Oncotarget*, *7*(49), 80680–80687. https://doi.org/10.18632/oncotarget.13028

Hussain, S. F., Yang, D., Suki, D., Aldape, K., Grimm, E., & Heimberger, A. B. (2006). The role of human glioma-infiltrating microglia/macrophages in mediating antitumor immune responses. *Neuro-Oncology*, *8*(3), 261–279. https://doi.org/10.1215/15228517-2006-008

Ichimura, K., Pearson, D. M., Kocialkowski, S., Bäcklund, L. M., Chan, R., Jones, D. T. W., & Collins, V. P. (2009). IDH1 mutations are present in the majority of common adult gliomas but rare in primary glioblastomas. *Neuro-Oncology*, *11*(4), 341–347. https://doi.org/10.1215/15228517-2009-025

Inoue, M., Williams, K. L., Gunn, M. D., & Shinohara, M. L. (2012). NLRP3 inflammasome

induces chemotactic immune cell migration to the CNS in experimental autoimmune encephalomyelitis. *Proceedings of the National Academy of Sciences of the United States of America*, *109*(26), 10480–10485. https://doi.org/10.1073/pnas.1201836109

Jablonski, K. A., Amici, S. A., Webb, L. M., Ruiz-Rosado, J. de D., Popovich, P. G., Partida-Sanchez, S., & Guerau-de-Arellano, M. (2015). Novel Markers to Delineate Murine M1 and M2 Macrophages. *PLOS ONE*, *10*(12), e0145342. https://doi.org/10.1371/journal.pone.0145342

Janigro, D. (Ed.). (2006). *The Cell Cycle in the Central Nervous System*. Totowa, NJ: Humana Press. https://doi.org/10.1007/978-1-59745-021-8

Jansen, Spliet, W. G. M., Leng, W. de, & Robe, P. A. (2018). Histologic characterization of the immune infiltrate in isocitrate dehydrogenase wild-type and mutant World Health Organization Grade II and III gliomas. *Glioma*, *1*(6), 196. https://doi.org/10.4103/GLIOMA.GLIOMA_42_18

Kambach, D. M., Halim, A. S., Cauer, A. G., Sun, Q., Tristan, C. A., Celiku, O., … Stommel, J. M. (2017). Disabled cell density sensing leads to dysregulated cholesterol synthesis in glioblastoma. *Oncotarget*, *8*(9), 14860–14875. https://doi.org/10.18632/oncotarget.14740

Kaminska, B., Czapski, B., Guzik, R., Król, S. K., & Gielniewski, B. (2019). Consequences of IDH1/2 Mutations in Gliomas and an Assessment of Inhibitors Targeting Mutated IDH Proteins. *Molecules (Basel, Switzerland)*, *24*(5). https://doi.org/10.3390/molecules24050968

Kantono, M., & Guo, B. (2017a). Inflammasomes and Cancer: The Dynamic Role of the Inflammasome in Tumor Development. *Frontiers in Immunology*, *8*, 1132. https://doi.org/10.3389/fimmu.2017.01132

Kantono, M., & Guo, B. (2017b). Inflammasomes and Cancer: The Dynamic Role of the Inflammasome in Tumor Development. *Frontiers in Immunology*, *8*, 1132. https://doi.org/10.3389/fimmu.2017.01132

Kapoor, G. S., & O'Rourke, D. M. (2003). Receptor Tyrosine Kinase Signaling In Gliomagenesis: Pathobiology And Therapeutic Approaches. *Cancer Biology & Therapy*, *2*(4), 330–342. https://doi.org/10.4161/cbt.2.4.507

Karan, D. (2018). Inflammasomes: Emerging Central Players in Cancer Immunology and Immunotherapy. *Frontiers in Immunology*, *9*, 3028. https://doi.org/10.3389/fimmu.2018.03028

Kennedy, B. C., Showers, C. R., Anderson, D. E., Anderson, L., Canoll, P., Bruce, J. N., & Anderson, R. C. E. (2013). Tumor-associated macrophages in glioma: friend or foe? *Journal of Oncology*, *2013*, 486912. https://doi.org/10.1155/2013/486912

Kim, D., Langmead, B., & Salzberg, S. L. (2015). HISAT: a fast spliced aligner with low memory requirements. *Nature Methods*, *12*(4), 357–360. https://doi.org/10.1038/nmeth.3317

Kohanbash, G., Carrera, D. A., Shrivastav, S., Ahn, B. J., Jahan, N., Mazor, T., … Okada, H. (2017). Isocitrate dehydrogenase mutations suppress STAT1 and CD8+ T cell accumulation in gliomas. *The Journal of Clinical Investigation*, *127*(4), 1425–1437.

https://doi.org/10.1172/JCI90644

Kuratsu, J., Yoshizato, K., Yoshimura, T., Leonard, E. J., Takeshima, H., & Ushio, Y. (1993). Quantitative study of monocyte chemoattractant protein-1 (MCP-1) in cerebrospinal fluid and cyst fluid from patients with malignant glioma. *Journal of the National Cancer Institute*, *85*(22), 1836–1839. Retrieved from http://www.ncbi.nlm.nih.gov/pubmed/8230263

Kwan, W., van der Touw, W., & Heeger, P. S. (2012). Complement regulation of T cell immunity. *Immunologic Research*, *54*(1–3), 247–253. https://doi.org/10.1007/s12026-012-8327-1

Lacey, D. C., Achuthan, A., Fleetwood, A. J., Dinh, H., Roiniotis, J., Scholz, G. M., … Hamilton, J. A. (2012). Defining GM-CSF- and macrophage-CSF-dependent macrophage responses by in vitro models. *Journal of Immunology (Baltimore, Md. : 1950)*, *188*(11), 5752–5765. https://doi.org/10.4049/jimmunol.1103426

Laskin, D. L., MacEachern, L., & Snyder, R. (1989). Activation of bone marrow phagocytes following benzene treatment of mice. *Environmental Health Perspectives*, *82*, 75–79. https://doi.org/10.1289/ehp.898275

Lee, J. H., Lee, J. E., Kahng, J. Y., Kim, S. H., Park, J. S., Yoon, S. J., … Lee, J. H. (2018). Human glioblastoma arises from subventricular zone cells with low-level driver mutations. *Nature*, *560*(7717), 243–247. https://doi.org/10.1038/s41586-018-0389-3

Lee, S. C. (2018). Diffuse Gliomas for Nonneuropathologists: The New Integrated Molecular Diagnostics. *Archives of Pathology & Laboratory Medicine*, *142*(7), 804–814. https://doi.org/10.5858/arpa.2017-0449-RA

Lewis, C. A., Brault, C., Peck, B., Bensaad, K., Griffiths, B., Mitter, R., … Schulze, A. (2015). SREBP maintains lipid biosynthesis and viability of cancer cells under lipid- and oxygen-deprived conditions and defines a gene signature associated with poor survival in glioblastoma multiforme. *Oncogene*, *34*(40), 5128–5140. https://doi.org/10.1038/onc.2014.439

Li, L., Ng, D. S. W., Mah, W. C., Almeida, F. F., Rahmat, S. A., Rao, V. K., … Lane, D. P. (2015). A unique role for p53 in the regulation of M2 macrophage polarization. *Cell Death and Differentiation*, *22*(7), 1081–1093. https://doi.org/10.1038/cdd.2014.212

Li, W., & Graeber, M. B. (2012). The molecular profile of microglia under the influence of glioma. *Neuro-Oncology*, *14*(8), 958–978. https://doi.org/10.1093/neuonc/nos116

Liu, A., Hou, C., Chen, H., Zong, X., & Zong, P. (2016). Genetics and Epigenetics of Glioblastoma: Applications and Overall Incidence of IDH1 Mutation. *Frontiers in Oncology*, *6*, 16. https://doi.org/10.3389/fonc.2016.00016

Louis, D. N., Ohgaki, H., Wiestler, O. D., Cavenee, W. K., Burger, P. C., Jouvet, A., … Kleihues, P. (2007). The 2007 WHO Classification of Tumours of the Central Nervous System. *Acta Neuropathologica*, *114*(2), 97–109. https://doi.org/10.1007/s00401-007-0243-4

Louis, D. N., Perry, A., Reifenberger, G., von Deimling, A., Figarella-Branger, D., Cavenee, W. K., … Ellison, D. W. (2016). The 2016 World Health Organization Classification of

Tumors of the Central Nervous System: a summary. *Acta Neuropathologica*, *131*(6), 803–820. https://doi.org/10.1007/s00401-016-1545-1

Lowe, J. M., Menendez, D., Bushel, P. R., Shatz, M., Kirk, E. L., Troester, M. A., … Resnick, M. A. (2014). p53 and NF-κB Coregulate Proinflammatory Gene Responses in Human Macrophages. *Cancer Research*, *74*(8), 2182–2192. https://doi.org/10.1158/0008-5472.CAN-13-1070

Lu-Emerson, C., Snuderl, M., Kirkpatrick, N. D., Goveia, J., Davidson, C., Huang, Y., … Jain, R. K. (2013). Increase in tumor-associated macrophages after antiangiogenic therapy is associated with poor survival among patients with recurrent glioblastoma. *Neuro-Oncology*, *15*(8), 1079–1087. https://doi.org/10.1093/neuonc/not082

Luoto, S., Hermelo, I., Vuorinen, E. M., Hannus, P., Kesseli, J., Nykter, M., & Granberg, K. J. (2018). Computational Characterization of Suppressive Immune Microenvironments in Glioblastoma. *Cancer Research*, *78*(19), 5574–5585. https://doi.org/10.1158/0008-5472.CAN-17-3714

Madsen, D. H., Jürgensen, H. J., Siersbæk, M. S., Kuczek, D. E., Grey Cloud, L., Liu, S., … Bugge, T. H. (2017). Tumor-Associated Macrophages Derived from Circulating Inflammatory Monocytes Degrade Collagen through Cellular Uptake. *Cell Reports*, *21*(13), 3662–3671. https://doi.org/10.1016/j.celrep.2017.12.011

Mantovani, A., Schioppa, T., Porta, C., Allavena, P., & Sica, A. (2006). Role of tumor-associated macrophages in tumor progression and invasion. *Cancer and Metastasis Reviews*, *25*(3), 315–322. https://doi.org/10.1007/s10555-006-9001-7

Martinon, F., Burns, K., & Tschopp, J. (2002). The Inflammasome: A molecular platform triggering activation of inflammatory caspases and processing of proIL-β. *Molecular Cell*, *10*(2), 417–426. https://doi.org/10.1016/S1097-2765(02)00599-3

Mills, E. L., & O'Neill, L. A. (2016). Reprogramming mitochondrial metabolism in macrophages as an anti-inflammatory signal. *European Journal of Immunology*, *46*(1), 13–21. https://doi.org/10.1002/eji.201445427

Moossavi, M., Parsamanesh, N., Bahrami, A., Atkin, S. L., & Sahebkar, A. (2018). Role of the NLRP3 inflammasome in cancer. *Molecular Cancer*, *17*(1), 158. https://doi.org/10.1186/s12943-018-0900-3

Müller, S., Kohanbash, G., Liu, S. J., Alvarado, B., Carrera, D., Bhaduri, A., … Diaz, A. (2017). Single-cell profiling of human gliomas reveals macrophage ontogeny as a basis for regional differences in macrophage activation in the tumor microenvironment. *Genome Biology*, *18*. https://doi.org/10.1186/S13059-017-1362-4

Murray, P. J. (2017). Macrophage Polarization. *Annual Review of Physiology*, *79*(1), 541–566. https://doi.org/10.1146/annurev-physiol-022516-034339

Nduom, E. K., Wei, J., Yaghi, N. K., Huang, N., Kong, L.-Y., Gabrusiewicz, K., … Heimberger, A. B. (2016). PD-L1 expression and prognostic impact in glioblastoma. *Neuro-Oncology*, *18*(2), 195–205. https://doi.org/10.1093/neuonc/nov172

Nomura, M., Saito, K., Aihara, K., Nagae, G., Yamamoto, S., Tatsuno, K., … Mukasa, A. (2019). DNA demethylation is associated with malignant progression of lower-grade

gliomas. *Scientific Reports*, *9*(1), 1903. https://doi.org/10.1038/s41598-019-38510-0

Ojalvo, L. S., Thompson, E. D., Wang, T.-L., Meeker, A. K., Shih, I.-M., Fader, A. N., … Emens, L. A. (2018). Tumor-associated macrophages and the tumor immune microenvironment of primary and recurrent epithelial ovarian cancer. *Human Pathology*, *74*, 135–147. https://doi.org/10.1016/j.humpath.2017.12.010

Omerhodžić, I. (2019). Introductory Chapter: Glioma - Merciless Medical Diagnosis. In *Glioma - Contemporary Diagnostic and Therapeutic Approaches*. IntechOpen. https://doi.org/10.5772/intechopen.82863

Onono, F., Subramanian, T., Sunkara, M., Subramanian, K. L., Spielmann, H. P., & Morris, A. J. (2013). Efficient use of exogenous isoprenols for protein isoprenylation by MDA-MB-231 cells is regulated independently of the mevalonate pathway. *The Journal of Biological Chemistry*, *288*(38), 27444–27455. https://doi.org/10.1074/jbc.M113.482307

Ostrom, Q. T., Gittleman, H., Truitt, G., Boscia, A., Kruchko, C., & Barnholtz-Sloan, J. S. (2018). CBTRUS Statistical Report: Primary Brain and Other Central Nervous System Tumors Diagnosed in the United States in 2011–2015. *Neuro-Oncology*, *20*(suppl_4), iv1-iv86. https://doi.org/10.1093/neuonc/noy131

Pertea, M., Kim, D., Pertea, G. M., Leek, J. T., & Salzberg, S. L. (2016). Transcript-level expression analysis of RNA-seq experiments with HISAT, StringTie and Ballgown. *Nature Protocols*, *11*(9), 1650–1667. https://doi.org/10.1038/nprot.2016.095

Piao, Y., Liang, J., Holmes, L., Zurita, A. J., Henry, V., Heymach, J. V., & de Groot, J. F. (2012). Glioblastoma resistance to anti-VEGF therapy is associated with myeloid cell infiltration, stem cell accumulation, and a mesenchymal phenotype. *Neuro-Oncology*, *14*(11), 1379–1392. https://doi.org/10.1093/neuonc/nos158

Platten, M., Kretz, A., Naumann, U., Aulwurm, S., Egashira, K., Isenmann, S., & Weller, M. (2003). Monocyte chemoattractant protein-1 increases microglial infiltration and aggressiveness of gliomas. *Annals of Neurology*, *54*(3), 388–392. https://doi.org/10.1002/ana.10679

Post, G., Sayder, R., & Kalf, G. F. (1986). Metabolism of benzene and phenol in macrophages in vitro and the inhibition of RNA synthesis by benzene metabolites. *Cell Biology and Toxicology*, *2*(2), 231–246. https://doi.org/10.1007/BF00122692

Pyonteck, S. M., Akkari, L., Schuhmacher, A. J., Bowman, R. L., Sevenich, L., Quail, D. F., … Joyce, J. A. (2013). CSF-1R inhibition alters macrophage polarization and blocks glioma progression. *Nature Medicine*, *19*(10), 1264–1272. https://doi.org/10.1038/nm.3337

Quail, D. F., & Joyce, J. A. (2017). The Microenvironmental Landscape of Brain Tumors. *Cancer Cell*, *31*(3), 326–341. https://doi.org/10.1016/j.ccell.2017.02.009

Quatromoni, J. G., & Eruslanov, E. (2012). Tumor-associated macrophages: function, phenotype, and link to prognosis in human lung cancer. *American Journal of Translational Research*, *4*(4), 376–389.

Rao, X., Zhao, S., Braunstein, Z., Mao, H., Razavi, M., Duan, L., … Zhong, J. (2019). Oxidized LDL upregulates macrophage DPP4 expression via TLR4/TRIF/CD36 pathways.

EBioMedicine, *41*, 50–61. https://doi.org/10.1016/J.EBIOM.2019.01.065

Richards, D. M., Hettinger, J., & Feuerer, M. (2013). Monocytes and Macrophages in Cancer: Development and Functions. *Cancer Microenvironment*, *6*(2), 179–191. https://doi.org/10.1007/s12307-012-0123-x

Richardson, L. G., Choi, B. D., & Curry, W. T. (2019). (R)-2-hydroxyglutarate drives immune quiescence in the tumor microenvironment of IDH-mutant gliomas. *Translational Cancer Research*, *8*(Suppl 2), S167–S170. https://doi.org/10.21037/tcr.2019.01.08

Robinson, M. D., McCarthy, D. J., & Smyth, G. K. (2010). edgeR: a Bioconductor package for differential expression analysis of digital gene expression data. *Bioinformatics (Oxford, England)*, *26*(1), 139–140. https://doi.org/10.1093/bioinformatics/btp616

Roesch, S., Rapp, C., Dettling, S., Herold-Mende, C., Roesch, S., Rapp, C., … Herold-Mende, C. (2018). When Immune Cells Turn Bad—Tumor-Associated Microglia/Macrophages in Glioma. *International Journal of Molecular Sciences*, *19*(2), 436. https://doi.org/10.3390/ijms19020436

Saio, M., Saio, M., Kito, Y., Ohe, N., Yano, H., Yoshimura, S., … Takami, T. (2009). Tumor-associated macrophage/microglia infiltration in human gliomas is correlated with MCP-3, but not MCP-1. *International Journal of Oncology*, *34*(6), 1621–1627. https://doi.org/10.3892/ijo_00000292

Salmaggi, A., Gelati, M., Pollo, B., Marras, C., Silvani, A., Balestrini, M. R., … Boiardi, A. (2005). CXCL12 Expression is Predictive of a Shorter Time to Tumor Progression in Low-Grade Glioma: A Single-Institution Study in 50 Patients. *Journal of Neuro-Oncology*, *74*(3), 287–293. https://doi.org/10.1007/s11060-004-7327-y

Saltz, J., Gupta, R., Hou, L., Kurc, T., Singh, P., Nguyen, V., … Mariamidze, A. (2018). Spatial Organization and Molecular Correlation of Tumor-Infiltrating Lymphocytes Using Deep Learning on Pathology Images. *Cell Reports*, *23*(1), 181–193.e7. https://doi.org/10.1016/j.celrep.2018.03.086

Schneider, A., Weier, M., Herderschee, J., Perreau, M., Calandra, T., Roger, T., & Giannoni, E. (2018). IRF5 Is a Key Regulator of Macrophage Response to Lipopolysaccharide in Newborns. *Frontiers in Immunology*, *9*, 1597. https://doi.org/10.3389/fimmu.2018.01597

Schomas, D. A., Laack, N. N. I., Rao, R. D., Meyer, F. B., Shaw, E. G., O'Neill, B. P., … Brown, P. D. (2009). Intracranial low-grade gliomas in adults: 30-year experience with long-term follow-up at Mayo Clinic. *Neuro-Oncology*, *11*(4), 437–445. https://doi.org/10.1215/15228517-2008-102

Schroder, K., & Tschopp, J. (2010). The Inflammasomes. *Cell*. https://doi.org/10.1016/j.cell.2010.01.040

Schumacher, T., Bunse, L., Pusch, S., Sahm, F., Wiestler, B., Quandt, J., … Platten, M. (2014). A vaccine targeting mutant IDH1 induces antitumour immunity. *Nature*, *512*(7514), 324–327. https://doi.org/10.1038/nature13387

Shatz, M., Menendez, D., & Resnick, M. A. (2012). The human TLR innate immune gene family is differentially influenced by DNA stress and p53 status in cancer cells. *Cancer Research*, *72*(16), 3949–3957. https://doi.org/10.1158/0008-5472.CAN-11-4134

Sica, A., & Bronte, V. (2007). Altered macrophage differentiation and immune dysfunction in tumor development. *Journal of Clinical Investigation*, *117*(5), 1155–1166. https://doi.org/10.1172/JCI31422

Singhal, G., Jaehne, E. J., Corrigan, F., Toben, C., & Baune, B. T. (2014a). Inflammasomes in neuroinflammation and changes in brain function: a focused review. *Frontiers in Neuroscience*, *8*, 315. https://doi.org/10.3389/fnins.2014.00315

Singhal, G., Jaehne, E. J., Corrigan, F., Toben, C., & Baune, B. T. (2014b). Inflammasomes in neuroinflammation and changes in brain function: a focused review. *Frontiers in Neuroscience*, *8*, 315. https://doi.org/10.3389/fnins.2014.00315

Sjoblom, T., Jones, S., Wood, L. D., Parsons, D. W., Lin, J., Barber, T. D., … Velculescu, V. E. (2006). The Consensus Coding Sequences of Human Breast and Colorectal Cancers. *Science*, *314*(5797), 268–274. https://doi.org/10.1126/science.1133427

Slenter, D. N., Kutmon, M., Hanspers, K., Riutta, A., Windsor, J., Nunes, N., … Willighagen, E. L. (2018). WikiPathways: a multifaceted pathway database bridging metabolomics to other omics research. *Nucleic Acids Research*, *46*(D1), D661–D667. https://doi.org/10.1093/nar/gkx1064

Soldano, S., Pizzorni, C., Paolino, S., Trombetta, A. C., Montagna, P., Brizzolara, R., … Cutolo, M. (2016). Alternatively Activated (M2) Macrophage Phenotype Is Inducible by Endothelin-1 in Cultured Human Macrophages. *PloS One*, *11*(11), e0166433. https://doi.org/10.1371/journal.pone.0166433

Sonoda, Y., Ozawa, T., Hirose, Y., Aldape, K. D., McMahon, M., Berger, M. S., & Pieper, R. O. (2001). Formation of intracranial tumors by genetically modified human astrocytes defines four pathways critical in the development of human anaplastic astrocytoma. *Cancer Research*, *61*(13), 4956–4960. Retrieved from http://www.ncbi.nlm.nih.gov/pubmed/11431323

Sun, M.-Y., Linsenbardt, A. J., Emnett, C. M., Eisenman, L. N., Izumi, Y., Zorumski, C. F., & Mennerick, S. (2016). 24(S)-Hydroxycholesterol as a Modulator of Neuronal Signaling and Survival. *The Neuroscientist : A Review Journal Bringing Neurobiology, Neurology and Psychiatry*, *22*(2), 132–144. https://doi.org/10.1177/1073858414568122

Tarassishin, L., Casper, D., & Lee, S. C. (2014). Aberrant Expression of Interleukin-1β and Inflammasome Activation in Human Malignant Gliomas. *PLoS ONE*, *9*(7), e103432. https://doi.org/10.1371/journal.pone.0103432

Tateishi, K., & Yamamoto, T. (2019). IDH-Mutant Gliomas. In *Brain and Spinal Tumors - Primary and Secondary [Working Title]*. IntechOpen. https://doi.org/10.5772/intechopen.84543

Thomas, D. J., Reasor, M. J., & Wierda, D. (1989). Macrophage regulation of myelopoiesis is altered by exposure to the benzene metabolite hydroquinone. *Toxicology and Applied Pharmacology*, *97*(3), 440–453. https://doi.org/10.1016/0041-008X(89)90249-4

Turcan, S., Rohle, D., Goenka, A., Walsh, L. A., Fang, F., Yilmaz, E., … Chan, T. A. (2012). IDH1 mutation is sufficient to establish the glioma hypermethylator phenotype. *Nature*, *483*(7390), 479–483. https://doi.org/10.1038/nature10866

van Deventer, H. W., Burgents, J. E., Wu, Q. P., Woodford, R.-M. T., Brickey, W. J., Allen, I. C., … Ting, J. P.-Y. (2010). The inflammasome component NLRP3 impairs antitumor vaccine by enhancing the accumulation of tumor-associated myeloid-derived suppressor cells. *Cancer Research*, *70*(24), 10161–10169. https://doi.org/10.1158/0008-5472.CAN-10-1921

Vander Heiden, M. G., Cantley, L. C., & Thompson, C. B. (2009). Understanding the Warburg effect: the metabolic requirements of cell proliferation. *Science (New York, N.Y.)*, *324*(5930), 1029–1033. https://doi.org/10.1126/science.1160809

Vazquez, A., Bond, E. E., Levine, A. J., & Bond, G. L. (2008). The genetics of the p53 pathway, apoptosis and cancer therapy. *Nature Reviews Drug Discovery*, *7*(12), 979–987. https://doi.org/10.1038/nrd2656

Voet, S., Srinivasan, S., Lamkanfi, M., & van Loo, G. (2019). Inflammasomes in neuroinflammatory and neurodegenerative diseases. *EMBO Molecular Medicine*, e10248. https://doi.org/10.15252/emmm.201810248

von Deimling, A., Eibl, R. H., Ohgaki, H., Louis, D. N., von Ammon, K., Petersen, I., … Seizinger, B. R. (1992). p53 mutations are associated with 17p allelic loss in grade II and grade III astrocytoma. *Cancer Research*, *52*(10), 2987–2990. Retrieved from http://www.ncbi.nlm.nih.gov/pubmed/1349850

Waitkus, M. S., Diplas, B. H., & Yan, H. (2018). Biological Role and Therapeutic Potential of IDH Mutations in Cancer. *Cancer Cell*, *34*(2), 186–195. https://doi.org/10.1016/j.ccell.2018.04.011

Wang, F., Beck-García, K., Zorzin, C., Schamel, W. W. A., & Davis, M. M. (2016). Inhibition of T cell receptor signaling by cholesterol sulfate, a naturally occurring derivative of membrane cholesterol. *Nature Immunology*, *17*(7), 844–850. https://doi.org/10.1038/ni.3462

Wang, L., Zhang, C., Zhang, Z., Han, B., Shen, Z., Li, L., … Zhang, Y. (2018). Specific clinical and immune features of CD68 in glioma via 1,024 samples. *Cancer Management and Research*, *10*, 6409–6419. https://doi.org/10.2147/CMAR.S183293

Wang, S.-C., Hong, J.-H., Hsueh, C., & Chiang, C.-S. (2012). Tumor-secreted SDF-1 promotes glioma invasiveness and TAM tropism toward hypoxia in a murine astrocytoma model. *Laboratory Investigation*, *92*(1), 151–162. https://doi.org/10.1038/labinvest.2011.128

Watanabe, T., Nobusawa, S., Kleihues, P., & Ohgaki, H. (2009). IDH1 Mutations Are Early Events in the Development of Astrocytomas and Oligodendrogliomas. *The American Journal of Pathology*, *174*(4), 1149–1153. https://doi.org/10.2353/ajpath.2009.080958

Wei, W., Schwaid, A. G., Wang, X., Wang, X., Chen, S., Chu, Q., … Wan, Y. (2016). Ligand Activation of ERRα by Cholesterol Mediates Statin and Bisphosphonate Effects. *Cell Metabolism*, *23*(3), 479–491. https://doi.org/10.1016/J.CMET.2015.12.010

Weller, M., Wick, W., Aldape, K., Brada, M., Berger, M., Pfister, S. M., … Reifenberger, G. (2015). Glioma. *Nature Reviews Disease Primers*, *1*, 15017. https://doi.org/10.1038/nrdp.2015.17

Wesolowska, A., Kwiatkowska, A., Slomnicki, L., Dembinski, M., Master, A., Sliwa, M., …

Kaminska, B. (2008). Microglia-derived TGF-β as an important regulator of glioblastoma invasion—an inhibition of TGF-β-dependent effects by shRNA against human TGF-β type II receptor. *Oncogene*, *27*(7), 918–930. https://doi.org/10.1038/sj.onc.1210683

Wesseling, P., Kros, J. M., & Jeuken, J. W. M. (2011). The pathological diagnosis of diffuse gliomas: towards a smart synthesis of microscopic and molecular information in a multidisciplinary context. *Diagnostic Histopathology*, *17*(11), 486–494. https://doi.org/10.1016/J.MPDHP.2011.08.005

XU, G., GUO, Y., SENG, Z., CUI, G., & QU, J. (2015). Bone marrow-derived mesenchymal stem cells co-expressing interleukin-18 and interferon-β exhibit potent antitumor effect against intracranial glioma in rats. *Oncology Reports*, *34*(4), 1915–1922. https://doi.org/10.3892/or.2015.4174

Yang, W., Bai, Y., Xiong, Y., Zhang, J., Chen, S., Zheng, X., … Xu, C. (2016). Potentiating the antitumour response of CD8+ T cells by modulating cholesterol metabolism. *Nature*, *531*(7596), 651–655. https://doi.org/10.1038/nature17412

Yeung, J. T., Hamilton, R. L., Ohnishi, K., Ikeura, M., Potter, D. M., Nikiforova, M. N., … Okada, H. (2013). LOH in the HLA Class I Region at 6p21 Is Associated with Shorter Survival in Newly Diagnosed Adult Glioblastoma. *Clinical Cancer Research*, *19*(7), 1816–1826. https://doi.org/10.1158/1078-0432.CCR-12-2861

Yin, X.-F., Zhang, Q., Chen, Z.-Y., Wang, H.-F., Li, X., Wang, H.-X., … Qiu, Y.-R. (2018). NLRP3 in human glioma is correlated with increased WHO grade, and regulates cellular proliferation, apoptosis and metastasis via epithelial-mesenchymal transition and the PTEN/AKT signaling pathway. *International Journal of Oncology*, *53*(3), 973–986. https://doi.org/10.3892/ijo.2018.4480

Yuan, J., Zhang, F., & Niu, R. (2016). Multiple regulation pathways and pivotal biological functions of STAT3 in cancer. *Scientific Reports*, *5*(1), 17663. https://doi.org/10.1038/srep17663

Zhang, J., Sarkar, S., Cua, R., Zhou, Y., Hader, W., & Yong, V. W. (2012). A dialog between glioma and microglia that promotes tumor invasiveness through the CCL2/CCR2/interleukin-6 axis. *Carcinogenesis*, *33*(2), 312–319. https://doi.org/10.1093/carcin/bgr289

Zhang, L., Sorensen, M. D., Kristensen, B. W., Reifenberger, G., McIntyre, T. M., & Lin, F. (2018). D-2-Hydroxyglutarate Is an Intercellular Mediator in IDH-Mutant Gliomas Inhibiting Complement and T Cells. *Clinical Cancer Research*, *24*(21), 5381–5391. https://doi.org/10.1158/1078-0432.CCR-17-3855

Zhang, W., & Fine, H. A. (2006). Mechanisms of Gliomagenesis. In *The Cell Cycle in the Central Nervous System* (pp. 449–462). Totowa, NJ: Humana Press. https://doi.org/10.1007/978-1-59745-021-8_31

Zhang, Y., Dube, C., Gibert, M., Cruickshanks, N., Wang, B., Coughlan, M., … Abounader, R. (2018). The p53 Pathway in Glioblastoma. *Cancers*, *10*(9). https://doi.org/10.3390/cancers10090297

Zhao, Y., Hu, X., Liu, Y., Dong, S., Wen, Z., He, W., … Shi, M. (2017). ROS signaling under metabolic stress: cross-talk between AMPK and AKT pathway. *Molecular Cancer*, *16*.

https://doi.org/10.1186/S12943-017-0648-1